# EFFECT OF PRETENSION ON TRIANGULAR TENSION LEG PLATFORM (TLP) RESPONSES

MOHAMMAD BIN NOR AKMAL

CIVIL ENGINEERING
UNIVERSITI TEKNOLOGI PETRONAS

JUNE 2010

**Effect of Pretension on Triangular Tension Leg Platform (TLP) Responses**

by

Mohammad Bin Nor Akmal

Dissertation submitted in partial fulfillment of
the requirement for the
Bachelor of Engineering (Hons)
(Civil Engineering)

JUNE 2010

Universiti Teknologi PETRONAS
Bandar Seri Iskandar
31750 Tronoh
Perak Darul Ridzuan

# CERTIFICATION OF APPROVAL

## EFFECT OF PRETENSION ON TRIANGULAR TENSION LEG PLATFORM (TLP) RESPONSES

by

Mohammad Bin Nor Akmal

A project dissertation submitted to the
Civil Engineering Programme
Universiti Teknologi PETRONAS
in partial fulfilment of the requirement for the
Bachelor of Engineering (Hons)
(Civi Engineering)

Approved:

Prof. Dr. Kurian V. John
Project Supervisor

UNIVERSITI TEKNOLOGI PETRONAS

TRONOH, PERAK

June 2010

# CERTIFICATION OF ORIGINALITY

This is to certify that I am responsible for the work submitted in this project, that the original work is my own except as specified in the references and acknowledgements, and that the original work contained herein have not been undertaken or done by unspecified sources or persons.

Mohammad Bin Nor Akmal

# ABSTRACT

This report describes the research to date in the field of deepwater platform design. The economics changed of offshore petroleum production due to shortage of oil reservoir in shallow water stimulate the significant of deep water exploration. The TLP (Tension Leg Platform) is the one of the viable engineering solutions for meeting this demand. TLP is a type of column-stabilized moored platform where the buoyancy exceeds its weight and thus the vertical equilibrium of the platform requires a system of pre-tensioned tethers held in tension connecting the upper structure to a foundation on the sea bed. Due to tether tensions, the vertical responses such as heave, pitch and roll are restrained but allow horizontal responses such as sway, yaw and surge. The greatest potential for reducing costs of a TLP is to focus on design of the platform geometry, therefore triangular TLP is the one of solution for meeting this demand. The typical rectangular TLP is four-legged, while triangular TLP is three-legged. This research is necessary as the study has the objective to study the responses of a triangular TLP due to the effect of variations in tether pretension. Dynamic analysis was conducted in frequency domain using Linear Airy Wave theory to analyze the water particle of wave, Morison equation to analyze the maximum forces acting on the triangular TLP and Pierson-Moskowitz Spectrum Model to formulate the random wave. The results indicate that due to tether pretension, triangular TLP allows surge and restrained heave and pitch. Parametric study on the variation of tether pretension showed that the responses were inversely proportional to the tether pretension. Experimental study of a triangular TLP model in the offshore laboratory has been conducted in order to compare behavior of the responses obtained from dynamic analysis and laboratory model testing. The comparison showed that responses from dynamic analysis and laboratory model testing were having the same responses behavior. All project activities that have been done were explained in details further in this report.

# ACKNOWLEDGEMENT

First of all, I would like to express my utmost gratitude and appreciation to the Most Almighty God because with His Blessing and Help, I have been able to complete this FYP (Final Year Project) within the times that have been allocated. This FYP was involving many parties in order to achieve its objectives and also preparing me for the future.

I managed to get the second Runner-up place in UTP (Universiti Teknologi PETRONAS) Research Paper Contest 2010, with help of many individuals which all were extraordinary in their own way. It was an exhilarating experienced to work with them and to witness their commitment and professionalisms. It is truly a great pleasure to acknowledge their contributions.

I would like to seize this opportunity to thank to all parties who has contributed along the process in completing this project. Special acknowledgment should be given to my supervisor through out this project, Professor Dr. Kurian V. John. His tireless effort, encouragement and priceless experienced in guiding me is truly appreciated as to ensure me to complete this project and becoming an all rounder engineer in the future.

Besides that, I would like to express my gratitude to my beloved parents who always giving their supportive spirit for me to accomplish this project and my studies. Apart from that, I want to thank offshore laboratory technicians, Mr. Mior and Mr. Idris for helping me a lot during the laboratory model testing. Besides that, I would also want to give my appreciation to fellow FYP mate and friends for their guidance and warm friendship.

Lastly, thanks to UTP and everyone who has contributed directly or indirectly in completing this project.

# TABLE OF CONTENT

# LIST OF TABLES

# LIST OF FIGURES

## LIST OF APPENDICES

# LIST OF ABBREVIATIONS

1. FYP - Final Year Project
2. RAO - Response Amplitude Operator
3. TLP - Tension Leg Platform
4. UTP - Universiti Teknologi PETRONAS

# CHAPTER 1

# INTRODUCTION

## 1.1 Background Study

An offshore structure may be defined as one which has no fixed access to dry land and which is required to stay in position in all weather conditions. The offshore structure should experience minimal movement to provide a stable work station for operations such as drilling and production of oil. Offshore structures are typically built out of steel, concrete or a combination of steel and concrete, commonly referred to as hybrid construction (Chakrabarti, 2005).

Offshore structures can be classified into two major categories, fixed and compliant as shown in figure 1.1. Fixed types fully extend to the sea bed and remain in place by a combination of their weight and piles driven into the soil. Fixed platform resist the wind, current and wave effect by generating large reaction forces and small motions. Little or no motion of such structures can be observed (Demirbilek, 1989).

Compliant type platforms are on the other hand more responsive to external effects. Their movements are controlled by mooring systems which typically consist of chains, cables, ropes and anchors. Contrary to the fixed structures, compliant platforms are allowed to move a great deal more and therefore generate small resistance to environmental loadings. Thus, the compliant platforms are lighter than fixed structure in deep waters and harsh environment where dynamic effects are high (Demirbilek, 1989).

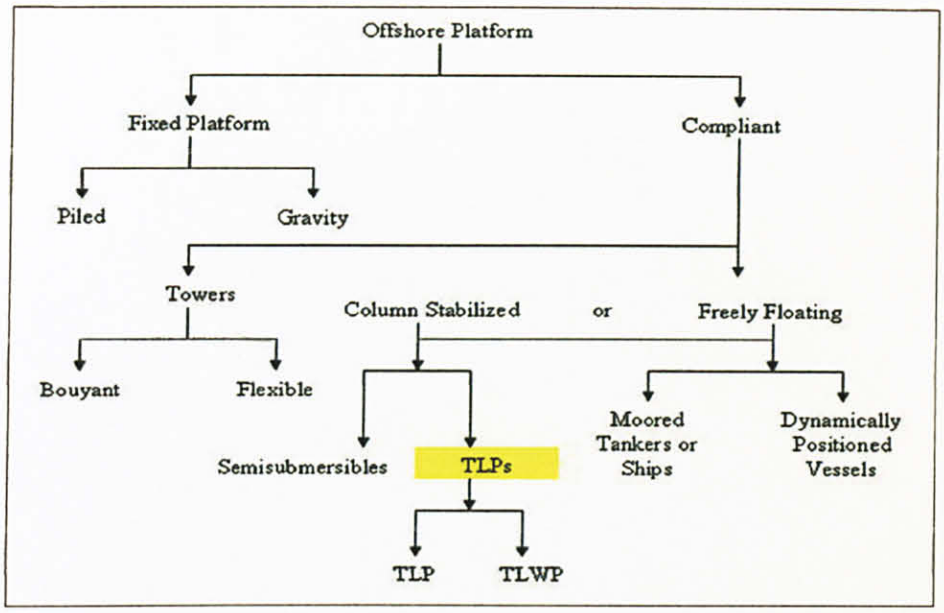


**Figure 1.1: Classes of Offshore Platform** (Demirbilek, 1989)

In the last four decades, the economics of offshore petroleum production have changed. Reserves in deep water began to offer significant financial incentives to justify their development. The Tension Leg Platform (TLP) is the one of the viable engineering solutions for meeting this demand. The saving in the weight of the steel combined with its excellent station-keeping characteristics make the TLP concept one of the most cost-effective and practical production systems for deep water developments (Demirbilek, 1989).

A triangular TLP is made of three columns structure which usually concerned as less stable. The analysis considers various nonlinearities produced due to change in tether pretension that will be conducted in order to study the responses of triangular TLP stability as shown in Figure 1.2.

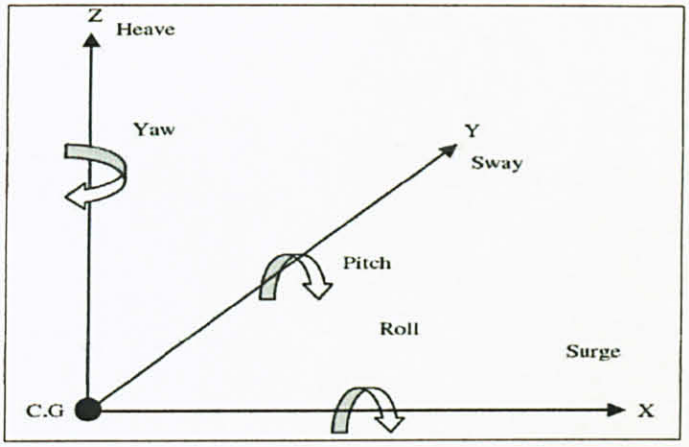


**Figure 1.2: Degree-of-Freedom of triangular TLP** (Chandrasekaran and Jain, 2001)

The TLP is the type of column-stabilized moored platform where the buoyancy of TLP exceeds its weight and thus the vertical equilibrium of the platform requires the existence of the taut moorings connecting the upper structure to a foundation on the sea bed. These taut vertical moorings are called "tension legs", "tethers", or "tendons". Based on Demirbilek (1989), the tubular pipes, cables and wire ropes of certain strength are commonly proposed as tendons (Refer Figure 1.3).

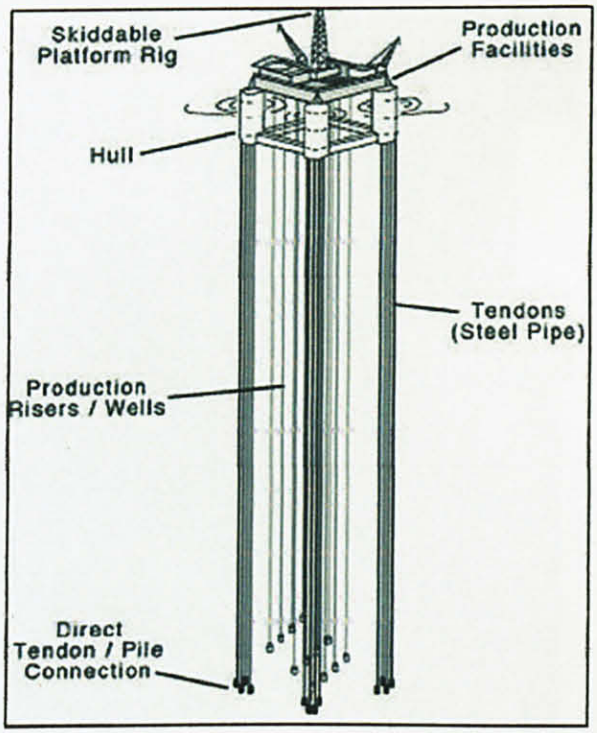


**Figure 1.3: Schematic of a TLP** (Haritos, 2007)

## 1.2 Problem Statement

A TLP can be thought of as a semi-submersible vessel with vertical mooring line (tethers). As such it is subjected to three translational degrees of freedom (surge, sway and heave) and three rotational degrees of freedom (yaw, pitch and roll). All six degrees of freedom contribute to the important of TLP responses (Heideman, 1989).

The TLP is connected by means of pretension cables tethers to the seabed and hence called tension leg. The tension cabling systems consists of three or more groups of tension legs, each leg being members of multiple parallel cables, terminated at the base of the structure. The composition of tension members terminated at the base will vary depending on the mooring requirements and the type of tension member selected. Owing to this tension the vertical motion such as heave, pitch and roll are almost restrained (Chandrasekaran, Chandak and Anupam, 2005).

As the need to get into more deepwater oil exploration, the economic viability of a project has been leading to huge platforms with high production levels. Thus, these characteristic make the necessity of reduction of the usually high values of static pretension in order to allow higher values of payload. The operation in deeper waters with reduced pretension makes the effect of tension variation along the tethers more relevant in their dynamics (Chandrasekaran, Chandak and Anupam, 2005).

The study focused on the effect of pretension of cables tethers on the triangular TLP responses. A triangular shape TLP is chosen because of as far as the TLP designed is concerned, three columns structure is less stable. In the history of the tension leg platform, triangular shape structure has been proposed, but yet not built (Chakrabarti, 2005).

Dynamics analysis of a triangular TLP to random sea wave loads will be presented in order to consider the various nonlinearities produced due to change in the tether tension. The random wave will be generated using the most suitable wave spectrum model.

Diffraction effects and second-order wave forces will not be considered. The evaluation of dynamics forces on the elements of pontoon structure will be carried out using Morison equation with water particle kinematics evaluated using Airy's linear wave theory. The effect of coupling of various structural degrees of freedom (surge, heave and pitch) on the dynamic response of the triangular TLP under random wave loads will be studied (Chandrasekaran and Jain, 2001).

## 1.3 Objectives

1. To prepare a detailed literature review survey on development of TLP and dynamic analysis for the triangular TLP.
2. To collect and finalize the dimension and required data of typical TLP.
3. To complete a dynamic analysis of typical triangular TLP using suitable wave spectrum model and random wave in order to determine the dynamic responses due to change in the tether tension.
4. To complete an experimental study of a triangular TLP model in the offshore laboratory in order to compare behavior of the responses obtained from dynamic analysis and laboratory model testing.

## 1.4 Scope of Study

1. Study on the concepts, characteristics and the responses of a functional TLP.
2. Study on the wave theories and wave parameters of Pierson-Moskowitz spectrum model
3. Conduct dynamic analysis of typical triangular TLP in frequency and time domain.
4. Determine the effect of tether pretension on the dynamic responses.

## 1.5 Assumptions and Structural Idealization

1. Related data of a triangular TLP including dimension of platform and environmental data were assumed to certain acceptable values which were based on real dimension of TLP and site condition.
2. Diffraction effects and second-order wave forces were neglected.
3. The platform is considered as a rigid body having three degree of freedom and symmetrical along the surge axis.
4. Wave force coefficients, $C_d$ and $C_m$ are the same for the pontoons and columns.
5. The wave was acting symmetrically to the cylindrical member (2-Dimension wave), thus the responses that were concerned in the dynamic analysis were surge, heave and pitch.

# CHAPTER 2

# LITERATURE REVIEW

## 2.1 Development of Offshore Structure

The design of offshore platforms for deep water drilling and production activities has presented engineers with a variety of design problems requiring innovative solutions. In the process of extrapolating from proven technology, a new class of offshore structures has evolved. These platforms are designed so that their dynamic response characteristics are detuned from wide range of environmental conditions in which they are expected to operate. In addition they are designed to allow substantial structural motion during extreme environmental loading conditions without damage to the structural integrity of the platform. This type of offshore structure is called a compliant platform (Pauling and Horton, 1970).

Drilling of oil wells in deeper sea is continuing with striking advances, reaching a water depth of more than 1000 m. These water depths are associated with larger hydrodynamic effects and total base moment, finally resulting in more material. The increase in cost of fixed offshore structures with depth of water encouraged the development of compliant- type structures (Chandrasekaran and Jain, 2001). This factor has lead to studies of the viable engineering solutions for meeting this demand. The primary consideration in selecting the concept for the deepwater application is relative insensitivity of the TLP cost to increase in water depth (Capanoglu, 1979).

## 2.2 Tension Leg Platform

The TLP is a vertically moored stable floating platform, whose buoyancy is designed to exceed its total weight. It is vertically moored to the seafloor with a bundle arrangement of tensioned tendons attached at each vertical leg. The TLP is designed to suppress heave roll and pitch motions and allow only the horizontal plane motions such as surge yaw and sway (Pauling and Horton, 1970). The Ram Powell TLP which is located in 3,214ft of water at Viosca Knoll, block 956, in the Gulf of Mexico is shown in figure 2.1 as example of typical TLP.

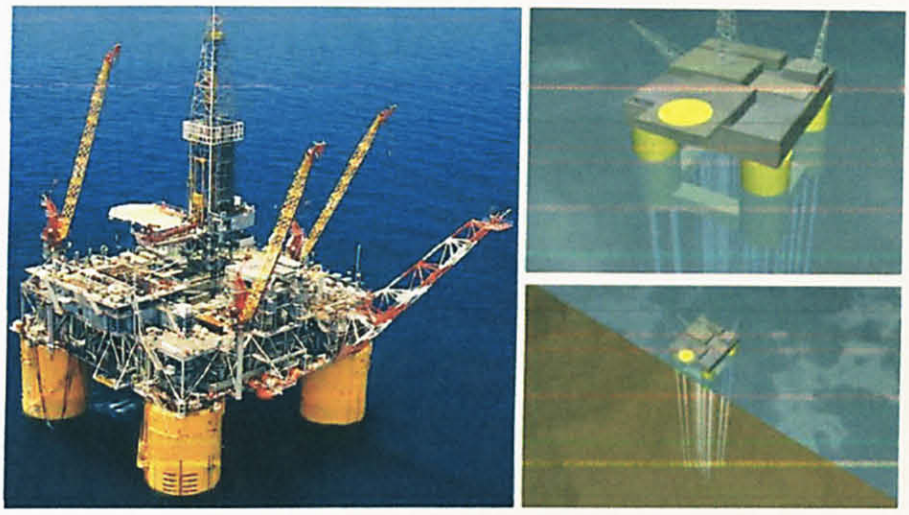

**Figure 2.1: Tension Leg Platform** (Anonymous, 2009)

Zeki Demirbilek (1989) classified the components of TLP as the combination of several parts where each part is playing the significant role and been recognized as one of the solution for deepwater production. The deck of a TLP supports the functional requirements. It provides space for accommodations, working area, processing equipment, derricks, cranes, pumps, helideck, control room, etc. Although the deck itself is similar to that of any conventional platform, but its layout and hook-ups are quite different where it is sensitive to payload increase and directly affecting its displacement requirement. The hull consists of the vertical columns, horizontal pontoons and the bracing all of which can be circular, rectangular or square in cross section. Recent and improved designs consist of larger diameter cylindrical shells for the columns and pontoons which have stiffener rings circumferentially and longitudinal

stringers for a better control of the structural stability and damage resistance. Bilge and ballast systems are fitted into the space within the hull in addition to the drilling, equipment for storing, installing and monitoring the tendons. The basic mooring system for TLP includes tendons and connectors. Risers and their relevant structural components as vertical tension member can contribute to the station-keeping capability of the mooring system. Both tendon and riser analyses make the proper design of the platform more difficult. Figure 2.2 shows the components of a typical TLP.

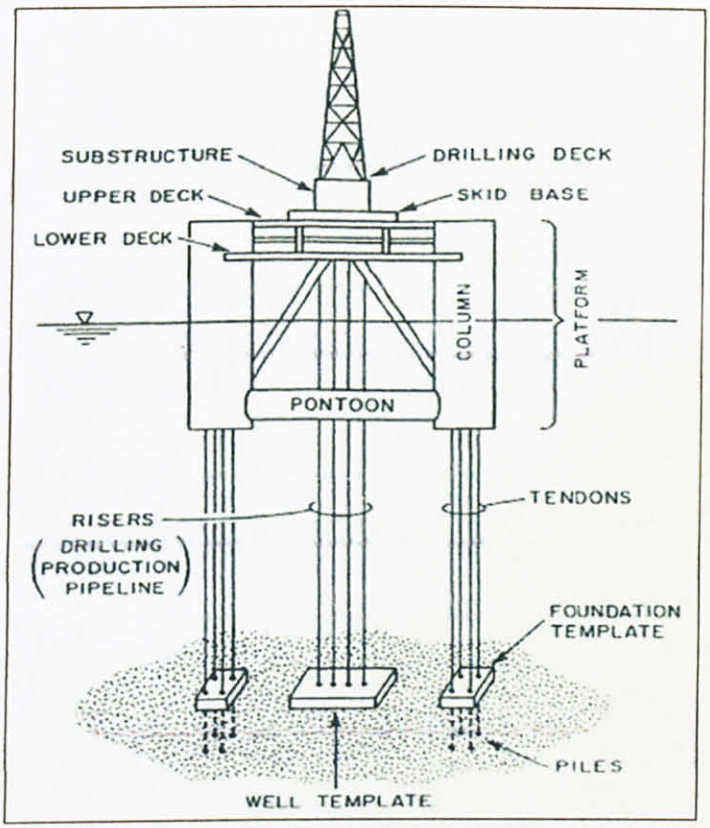


**Figure 2.2: Tension Leg Platform Components** (Chakrabarti, 2001)

During the seventies and eighties, especially 1984 when the first working TLP was successfully deployed by Conoco at the Hutton field in the United Kingdom North Sea, the concept of a TLP began attracting more attention from the offshore industry as an appropriate structure for deepwater applications (Zeki Demirbilek, 1989). The Hutton TLP consists of rectangular shaped floating platform connected to the ocean bottom by 16 vertical tendons, four per corner column. The tendons are tensioned by attaching

them to the floating structure and then deballasting the structure to provide additional buoyancy. The earliest published work on TLP performance and features is by Pauling and Horton, 1979. A one-third scale version of TLP was first designed, installed and tested in sea through a joint industry project by Deep Oil Technology Inc. (DOT) in 1970s.

Many of the TLP studies reported in the open literature can be viewed as exploratory studies, while others are more focused and address the response behaviour of realistic platform configurations. The development of TLP technology has required an interesting blend of physical model testing and numerical simulation studies. As with all studies reported in the open literature, there is a certain amount of pertinent information which is either neglected through oversight or intent. Often these omissions are not immediately noticed and only come to light when other study extending the earlier work is undertaken (Niedzwecki and Frentz, 1989).

As presented by Chandrasekaran and Jain (2001), the TLP is essentially advantageous for the following reasons:

1. It attracts a lesser impact of the wave loading due to its compliant nature and hence can operate even in rough sea.
2. The natural frequencies in the main or soft degrees of freedom (surge, sway and yaw) are well below the wave frequencies, thus avoiding the occurrence of resonance and reducing the horizontal motion and hence loading on the tether platform system.
3. It is less expensive than the bottom-supported structures, especially in deeper sea.
4. It can be easily dismantled, installed and transported according to site requirements. The change in the water depth essentially requires a change in the tether length.
5. It is much safer in a seismically active zone compared with any other fixed platform.
6. Because of the restrained vertical motion of the TLP, it is quite convenient to monitor and maintain the risers, oil wells and tethers.

7. A particularly attractive feature of the TLP is the ability to shift any resonance outside the frequency region of the active wave energy.

The greatest potential for reducing costs of a TLP in the short term is to go thoroughly through previously applied design approaches. According to Natvig and Vogel (1995), focus on design of future TLP should be on the aspects of the platform geometry that affects tether loading and on the tether system itself. Their experience with a four-legged TLP has shown that the indeterminate tether system implies some very heavy cost items. The main aspect of three-legged TLP is that all tethers share approximately the same loads despite weather directions. With the near-equal load sharing of the three-legged TLP, the maximum load level in one group is less, thus requiring less tether cross section material than that of a four-legged TLP. Studies indicate that 12 tethers are feasible for a three-legged TLP whilst 16 would be required for a four-legged equivalent TLP. This is thus an important area for savings since tethers are important cost items.

Munkejord (1996) presented a conceptual analysis of the triangular TLP behaviour and then compared the results with data from model tests. The objective was to verify maximum tether tension, maximum platform offset, minimum air gap and tether fatigue. Aker and Saga Petroleum developed the concept of a triangular TLP, which has enabled significant savings in main steel for both hull and deck due to fewer main element intersections and effective force distributions.

## 2.3 Dynamic Analysis

In order to study the effect of tethers pretension on the responses of TLP, a series of dynamic analysis with respect to triangular TLP need to be conducted. Chandrasekaran and Jain (2001) emphasized to analyze the effects of surface waves on the structures, either using a single design wave chosen to represent the extreme storm conditions in the area of interest, by use of statistical representation of the waves during extreme storm conditions in the area of interest.

As discussed by Dawson (1983), it is necessary to relate the surface wave data to water velocity, acceleration, and pressure beneath the waves, which can be achieved by using the appropriate wave theory such as Linear Airy Wave Theory.

The computation of the water wave forces on an offshore structure is one of the tasks in the design of the structure. It is also one of the most difficult tasks since it involves the complexity of the interaction of waves with the structure. Wave forces on offshore structures are calculated in three different ways which are using Morison equation, Froude-Krylov theory and Diffraction theory (Chakrabarti, 2001). In this study, Morison equation will be used to calculate the wave force on the triangular TLP.

The Morison equation was developed by Morison, O'Brien, Johnson and Shaaf (1950) in describing the horizontal wave forces acting on a vertical pile which extends from the bottom through the free surface. The Morison equation assumes as the force to be composed of inertia and drag forces linearly added together. The components involve an inertia coefficient and drag coefficient which must be determined experimentally. The Morison equation is applicable when the drag force is significant. This is usually the case when a structure is small compared to the water wave length (Chakrabarti, 2001).

The mathematical spectrum model is generally generated based on or more parameters such as significant wave height, wave period, shape factor, etc. In this study, Pierson-Moskowitz model will be used as it is extensively used by ocean engineers as one of the most representative for waters all over the world and has found for many applications in the design of offshore structures.

Pierson and Moskowitz (1964) have proposed the P-M spectral model equation which describes a fully-developed sea determined by one parameter, namely, the wind speed. The fetch and duration are considered infinite. For the applicability of such model, the wind has to blow over a large area at a nearly constant speed for many hours prior to the time when the wave record is obtained and the wind should not change its direction more than a certain specified small amount (Chakrabarti, 2001).

# CHAPTER 3

# METHODOLOGY

## 3.1 Introduction

The studies of this thesis begin with researches of offshore platform and the significance of deep water exploration in oil exploration and production industry. The researches were then continued with the studies of functional TLP and collecting available data of TLP. Once the basic of a TLP was known, studies and analysis of a triangular TLP due to environmental condition in which they were expected to operate were presented in order to consider the responses produced due to variation in tether pretension. Besides theoretical analysis, the laboratory testing of triangular TLP model has also been conducted and presented in the next part of this report. Refer Appendix A for Project Methodology Diagram and Appendix B for Gantt chart of Final Year Project 1 and 2.

## 3.2 Dimensional, Structural and Environmental Data

Data for typical TLP have been collected and several modifications have been done for the suitability of this study.

**Table 3.1: Dimensional Data of Triangular TLP** (Mohd Khalid, 2008)

| Section | Diameter (m) | Length (m) | Amount |
|---|---|---|---|
| Column | 20 | 50 | 3 |
| Pontoon | 20 | 50 | 3 |
| Tendons | 1 | 965 | 12 (4 at each column) |

**Table 3.2: Structural Data of Triangular TLP** (Mohd Khalid, 2008)

| | |
|---|---|
| **Total mass (tonnes)** | 43000 |
| **Total weight (kN)** | 421830 |
| **Tethers stiffness (kN/m)** | 105000 |
| **Draft (m)** | 35.00 (above keel) |
| **Buoyancy Force (kN)** | 805532 |
| **Centre of gravity (m)** | 31.15 (above keel) |
| **Radius of Gyration Z-axis, $r_z$ (m)** | 40.00 |

**Table 3.3: Environmental Data of Triangular TLP for operating criteria** (PTS)

| **WAVE** | |
|---|---|
| **Significant wave height, Hs (m)** | 3.6 |
| **Zero crossing wave period, Tz (s)** | 6.6 |
| **Peak wave eperiod, Tp (s)** | 9.3 |
| **Individual maximum wave height, Hmax (m)** | 6.4 |
| **Associated wave period for Hmax, Tass (s)** | 8.6 |
| **water depth, d (m)** | 1000 |
| **OCEAN CURRENT** | |
| **At Surface, d (m/s)** | 1.4 |
| **At Mid-depth, 0.5 x d (m/s)** | 1.3 |
| **At Near seabed, 0.01 x d (m/s)** | 0.7 |

## 3.3 Coordinate System of Triangular TLP

Coordinate system shown in Figure 3.1 represents the position and dimension of hulls and pontoons of the triangular TLP. As stated earlier, direction of horizontal force is assumed to be acted symmetrically to the cylindrical member.

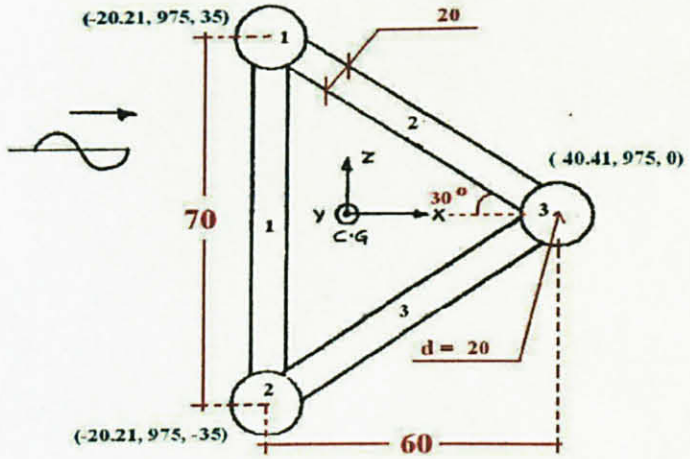


**Figure 3.1: Plan of the Triangular TLP**

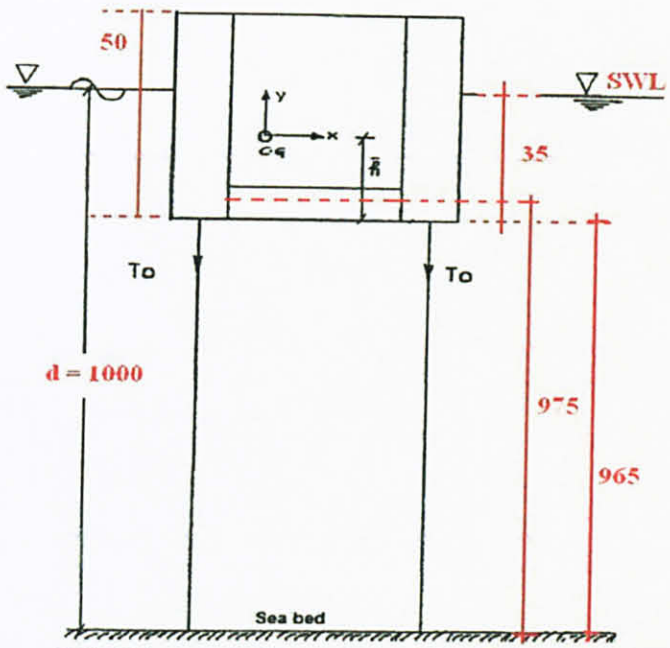


**Figure 3.2: Schematic Elevation of the Triangular TLP**

### 3.4 Wave Forces and Moment Calculation

The wave forces acting on an offshore structure is considered as the most significant of all environmental loadings, where those forces developed by the motion of water particles hitting the structure with velocities and accelerations. In this analysis, the wave forces exerted is based on unidirectional wave design to obtain highest expected wave forces. The calculation of wave forces and moment exerted on triangular TLP is based on Morison equation together with Linear Airy Wave Theory.

Morison equation expresses the wave forces as the sum of an inertia force and drag force (Chakrabarti, 2001):

$$\delta f_I = C_M p \frac{\Pi}{4} D^2 \frac{\delta u}{\delta t} \delta s \quad [1] \qquad \delta f_D = \frac{1}{2} C_D D |u| u \delta s \quad [2]$$

Where:

Force, F = Inertia force ($\delta f_I$) + Drag force ($\delta f_D$)

Moment, M = F x d

Moment Arm, d = distance between the respective forces exerted on the hull to the center of gravity of triangular TLP, m

$C_M$ = Inertia Coefficient

$C_D$ = Drag Coefficient

$\rho$ = Sea Water Density, kg/m$^3$

$D$ = Diameter of Hull, m

$\frac{\delta u}{\delta t}$ = acceleration of horizontal water particle, m/s$^2$

$u$ = velocity of horizontal water particle, m/s

$\delta s$ = Length of Segment of structure, m

The following parameters of Linear Airy Wave Theory (Chakrabarti, 2001) related to this theory as listed below will be taken in the analysis.

1. Horizontal Water Particle Velocity (m/s) $u = \frac{\Pi H}{T}\frac{\cosh ks}{\sinh kd}\cos\Theta$ [3]
2. Vertical Water Particle Velocity (m/s) $v = \frac{\Pi H}{T}\frac{\sinh ks}{\sinh kd}\sin\Theta$ [4]
3. Horizontal Water Particle Acceleration (m/s$^2$) $\frac{\delta u}{\delta t} = \frac{2\Pi^2 H}{T^2}\frac{\cosh ks}{\sinh kd}\sin\Theta$ [5]
4. Vertical Water Particle Acceleration (m/s$^2$) $\frac{\delta v}{\delta t} = \frac{2\Pi^2 H}{T^2}\frac{\sinh ks}{\sinh kd}\cos\Theta$ [6]
5. Dynamic Pressure (N/m$^2$) $\rho = pg\frac{H}{2}\frac{\cosh ks}{\cosh kd}\cos\Theta$ [7]

Where:

$\Theta = kx - \omega t$ = crest angle

$H$ = Wave height, m

$T$ = Wave period, s

$k = \frac{2\Pi}{L}$ = No. of wave, 1/m

$\omega = \frac{2\Pi}{T}$ = angular frequency, rad/s

$s$ = Distance from seabed to analyzed position, m

$d$ = Water depth, m

The various symbols to characterize the wave are given as shown in Figure 3.3 below.

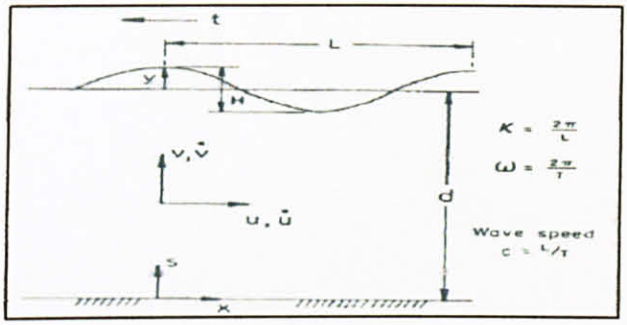


**Figure 3.3: Definition Sketch for a Wave** (Chakrabarti, 2001)

Determination of wave forces and moments exerted to the components of triangular TLP which are 3 Hulls and 3 Pontoons (refer figure 3.1) due to the wave and ocean current are analyzed at every 1m interval to obtain the maximum forces and moments acted at a particular time. The maximum forces at x, y axes and moments at z axis will be used to find the Response Amplitude Operator (RAO) of surge, heave and pitch respectively.

## 3.5 Frequency and Time Domain Analysis

Frequency domain analysis was performed using P-M wave spectrum model at the first stage of dynamic analysis to represent the density distribution of sea wave at the site. For the second stage, the motion response spectrum was constructed based on wave spectrum for the responses. For the final stage, the motion response profile in time domain was simulated from the motion response spectrum. All stages of analyses were performed for motions at 3 different axes x, y and z, which were surge, heave and pitch respectively.

### 3.5.1 Wave Spectrum

In reality, waves at sea states will occur as random instead of regular waves. In this analysis the random appearance is resulted from linear superposition of an infinite number of regular waves with varying frequency. The best way to describe a random sea state and its energy content is using the wave energy spectrum. The energy density spectrum: P-M Spectrum model was used for this analysis and may be written as:

$$S(f) = \frac{\alpha g^2}{2\Pi^4} f^{-5} \exp[-1.25(\frac{f}{f_O})^{-4}] \quad [8]$$

Where:
- $\alpha$ = 0.081
- g = 9.81 m/s$^2$
- $\prod$ = 3.142
- $f$ = Frequency of Waves, Hz
- $fo$ = Peak Frequency of Waves, Hz

Based on the range values of waves frequency, $f$ and P-M spectrum model, S($f$) related in this studies, an energy density spectrum curve can be plotted. It is necessary to calculate the height of a wave at a particular frequency from an energy density spectrum curve in order to know the responses due to the applied forces to the TLP. The wave height at this frequency was obtained as follows:

$$H(f_1) = 2\sqrt{2S(f_1)\Delta f} \quad [9]$$

Where:
- $S(f_1)$ = Wave Spectrum, m$^2$/s
- $\Delta f_1$ = Increment for each component of frequency, Hz

For a given horizontal coordinate, x, which was the location at which the wave profile was desired and time, t, the wave profile was computed using the formula:

$$\eta(x,t) = \sum_{n=1}^{N} \frac{H(n)}{2} \cos[k(n)x - 2\Pi f(n)t + \varepsilon(n)] \quad [10]$$

Where: $k(n) = \frac{2\Pi}{L(n)}$ = No. of wave, 1/m

$L(n)$ = Wave length corresponds to the $n$th frequency, $f(n)$

$x$ = Horizontal coordinate, m

$t$ = Time, s

$f(n)$ = Frequency of Waves, Hz

$\varepsilon(n)$ = $2\prod R_N$ ($R_N$ is the random number ranged from 0 to 1, thus $\varepsilon(n)$ will ranged from 0 to $2\prod$).

### 3.5.2 Response Amplitude Operator

Response Amplitude Operator (RAO) is constructed for a range of wave frequencies of interest to transfer the exciting waves into responses of the structure at 3 different axes x, y and z, which were surge, heave and pitch respectively. RAO may be written as:

$$RAO_{surge} = \frac{F_x / (\frac{H}{2})}{[(K_{surge} - m_{surge}\omega^2)^2 + (C\omega)^2]^{\frac{1}{2}}} \quad [11]$$

$$RAO_{heave} = \frac{F_y / (\frac{H}{2})}{[(K_{heave} - m_{heave}\omega^2)^2 + (C\omega)^2]^{\frac{1}{2}}} \quad [12]$$

$$RAO_{pitch} = \frac{M_z / (\frac{H}{2})}{[(K_{pitch} - m_{pitch}\omega^2)^2 + (C\omega)^2]^{\frac{1}{2}}} \quad [13]$$

Where: $F_{x, y}$ = Maximum force at x and y axis (for surge and heave respectively), N

$M_z$ = Maximum moment at z axis (for pitch), Nm

H = $H_f$ or 1m

$K_{surge, heave}$ = Stiffness of surge and heave respectively, N/m

$K_{pitch}$ = Stiffness of pitch, $Nm/rad^2$

$m_{surge,\ heave}$ = (Mass + Added Mass) at x and y axis (for surge and heave respectively), kg

$m_{pitch}$ = (Mass + Added Mass) x $r_z$, $kgm^2$

$r_z$ = radius of gyration at z axis, m

$\omega$ = $\frac{2\Pi}{T}$ = angular frequency, rad/s

C = Damping of respective axis = $2\xi\sqrt{k.m}$

### 3.5.3 Motion Response Spectrum and Profile

The responses of the triangular TLP for the motions of surge, heave and pitch were calculated to evaluate the response spectrum value at particular frequency. Equation 8 was used to generate wave spectrum. The motion response spectrum may be written as:

$$S_x(f) = [RAO(\omega)]^2 \times S(f) \quad [14]$$

Based on the response amplitude operator at different frequencies, the motion response profile can be generated. Equation 10 was used to generate wave profile in time domain. The motion response spectrum in time domain may be written as:

$$\eta_x = [RAO(\omega)] \times \eta \quad [15]$$

## 3.6 Parametric Studies

Parametric studies have been made by varying tethers pretension to study the variation in triangular TLP responses caused by changing these parameters. Total pretensions of tethers are the net of subtraction between total buoyancy and total weight. Thus, there are two ways of varying tethers pretension either by changing the draft which then will affect changing of total buoyancy, or by changing the total weight of triangular TLP itself.

For this analysis, total buoyancy was varied in order to get the variation of tether pretension. Variations of tether pretension were done for three values, which were 27.3%, 17.3%, and 7.3% of the total weight. The variation of RAO with frequencies, motion response spectrum and profile were plotted to analyze the effect of triangular TLP responses due to the variation of tether pretension.

## 3.7 Laboratory Model Testing

Laboratory model testing was started once the part of theoretical analysis has been completed. The main purpose of laboratory model testing is to compare the behavior and responses trend of triangular TLP due to the variation of tethers pretension, between the model behavior and theoretical analysis. The part of model testing can be distributed into four main activities which are model design, model fabrication, laboratory model testing and data analysis.

### 3.7.1 Model Design

The model was design and scaled down based on available water depth of wave tank in offshore laboratory. The maximum available water depth of wave tank in offshore laboratory is 1.0m and the clearance depth between model and bed of the tank should be at least 0.5m. Due to constraint of the fabrication cost, the dimension of the model was set up to be as at the optimum condition. Figures below show the dimensions and isometric view of the triangular TLP model.

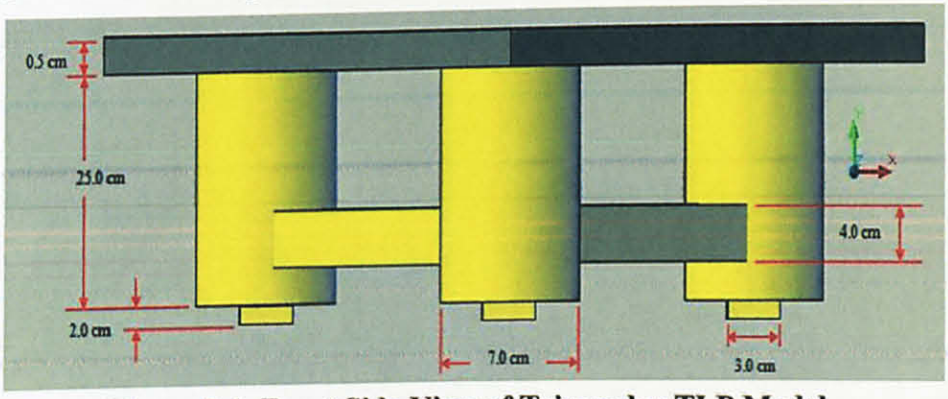


**Figure 3.4: Front Side View of Triangular TLP Model**

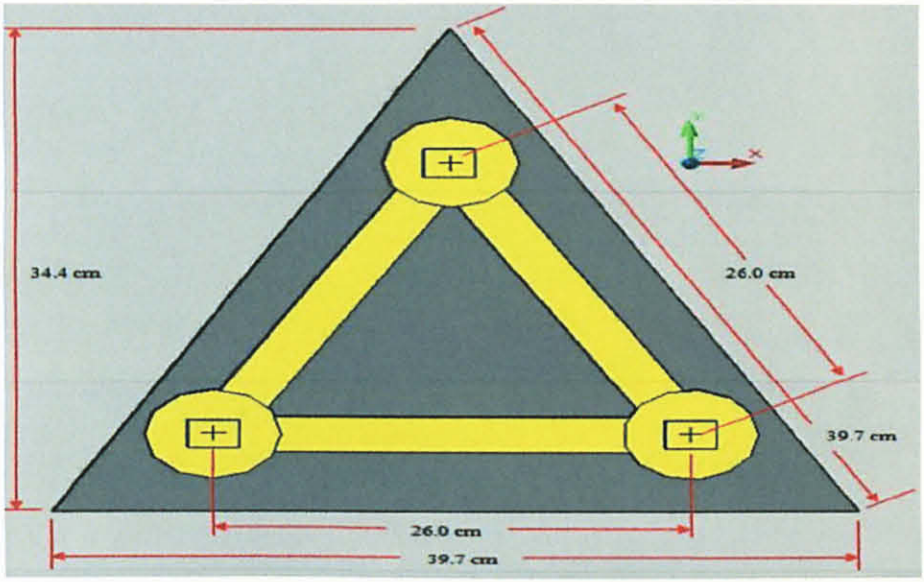


**Figure 3.5: Bottom Side View of Triangular TLP Model**

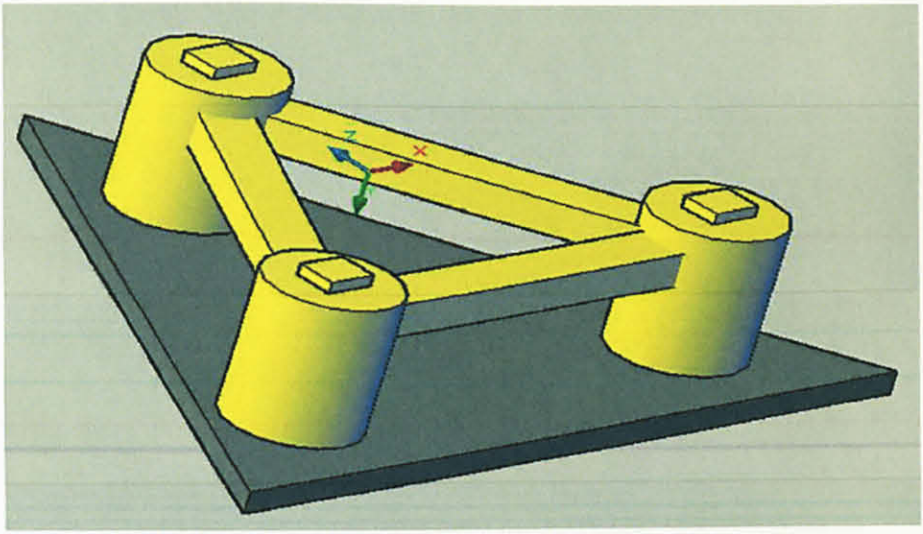

**Figure 3.6: Isometric View of Triangular TLP Model**

### 3.7.2 Model Fabrication

The model was fabricated based on the dimensions that have been set up earlier during model design phase. The material that has been used in order to fabricate this model is Perspex (transparent thermoplastic). The material has been identified as the best material to be used due to its special characteristics which are tough, light and economical. Figure 3.7 shows the picture of the triangular TLP model.

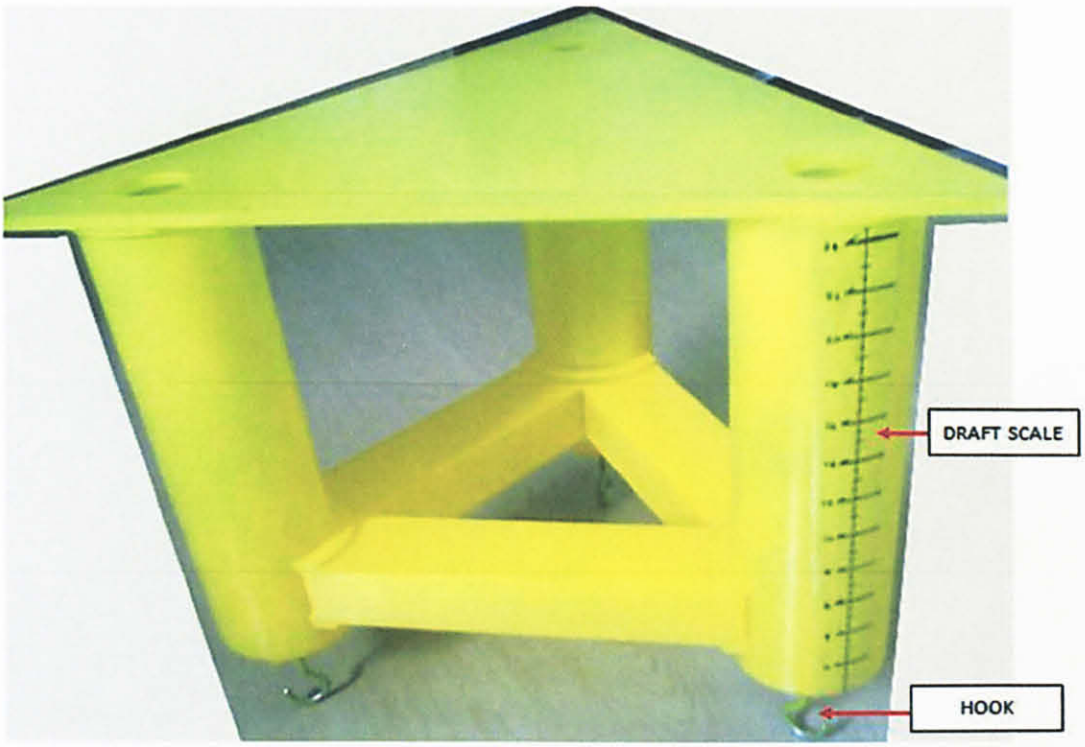


**Figure 3.7: Triangular TLP Model**

### 3.7.3 Laboratory Model Testing

The model testing was conducted in the wave tank at offshore laboratory. The details of wave properties used and procedures conducted in this testing were presented as shown below. Refer Appendix I for some of the pictures taken during laboratory model testing.

#### 3.7.3.1 Wave properties

The wave that should be used in conducting this testing is random wave in order to simulate the environmental condition in which the triangular TLP were expected to operate. Due to the constraint of the available random wave in the offshore laboratory, the Pierson-Moskowitz (P-M) wave spectrum has been chosen as the random wave that propagated to the triangular TLP model with wave period, $T_s$ of 1.2 s. The random waves have been generated for all the three series of experiments for three different triangular TLP model drafts which were 21.5 cm, 17.5 cm and 13.5 cm respectively.

### 3.7.3.2 Parametric Conditions

The variations of tether pretension have been made by varying the draft of the triangular TLP model drafts which were 21.5 cm, 17.5 cm and 13.5 cm respectively. The change of draft will affect changing of total buoyancy and thus also affecting pretension since tether pretension are the net of subtraction between total buoyancy and total weight. Draft, buoyancy and pretension are directly proportional to each other, which mean that increment of draft will increased the buoyancy and also pretension of the triangular TLP model.

### 3.7.3.3 Procedures

The procedures of laboratory model testing have been conducted as listed below. Refer Appendix I for the pictures of the model testing setup. .

1. The anchor of the triangular TLP model was setup at the bed of the wave tank.
   Note: The position of the anchors have been setup to be at the same position as the hooks of the model in to make sure the chain connecting the anchor (at the bed of the wave tank) to the model (at water surface) is straight and held in tension.
2. The triangular TLP model has been made sure to be leveled and floated with a draft of 21.5 cm.
3. A camera was setup at the observer window in order to record the video for the movement of the triangular TLP model due to the propagated wave.
4. A grid transparent paper was installed at the observer window in order to measure the response of the triangular TLP model due to the propagated wave.
   Note: The initial position of the model was marked as the datum for position of the model before its move due to the propagated wave.
5. The Pierson-Moskowitz (P-M) wave was run for a period of time so that it will propagate to the triangular TLP model.
6. Video for the movement of triangular TLP model was recorded for a period time of 100s.

7. Steps 1 to 6 were repeated for another 2 drafts which are 17.5 cm and 13.5 cm respectively.

### 3.7.4 Data Analysis

Based on measurement from recorded video for the movement of triangular TLP model, graphs of response profile for time domain of 100s were plotted for responses of the model at 2 different axes x and y which were surge and heave respectively. Due to constraint of limitation methodology in measuring the pitch response, the graph of response profile for pitch was not plotted. Three variations of triangular TLP model drafts were plotted for each of the response profile graph in order to observe the responses based on the effect of variation in tether pretension. The graphs of surge and heave response profile from this laboratory model testing were then compared with the graphs of surge and heave response profile which previously obtained form theoretical analysis. The behavior and responses trend of triangular TLP due to the variation of tethers pretension, between the model behavior and theoretical analysis can be analyzed from this analysis.

# CHAPTER 4

# RESULTS AND DISCUSSIONS

## 4.1 Conceptual Design of TLP

The concern taken in the conceptual design of TLP which reflect the studies of this project is the pretension of tether. Analysis shown below is calculation of tether pretension based on the data that have been collected.

i. Total buoyancy = $V_{(\text{hull + pontoon})} \cdot \rho . g$ = 805.532 x $10^6$ N

ii. Pretension in all tethers = Total buoyancy – Total weight = 118.832 MN

iii. Pretension in each tethers = Pretension in all tethers / total numbers of tethers

= 9.903 MN

iv. Checking:

Pretension in all tethers / Total weight = 0.173 = 17.3%

It was found that the ratio of total pretension in all the tethers was 17.3% of the total weight. Based on this value, the variation of pretension was decided for increment and decrement of 10%, which were 27.3%, 17.3%, and 7.3%.

## 4.2 Forces and Moments Exerted on Components of Triangular TLP

Analyses for random wave conducted to find maximum forces and moments exerted on components of triangular TLP were done for a range of frequencies at respective time, T (s) and wave height, H (m). At each frequency, analyses are done for every increment of

1 second up to respective time, T. The maximum force exerted at x and y axes, and moment at z axis will be used to find RAO of surge, heave and pitch respectively. Analyses shown below were forces and moments for regular wave at ($T_{ass}$ = 8.6s) and ($H_{max}$ = 6.4m).

### 4.2.1 Forces Exerted on Hulls and Pontoons

The following parameters were considered for this calculation:

i. Values of $C_M$ and $C_D$ are for clean tabular members; $C_D$= 0.65 $C_M$= 1.60

ii. Density of sea water; $\rho_{sw} = 1025 \frac{kg}{m^3}$

Due to 2-dimension wave exerted to the components of triangular TLP, resultant forces exerted will be at various axes and different equation will be applied to find forces exerted at respective axes as summarized in table 4.1 shown below:

**Table 4.1: Summary of Forces Exerted at Axes and Analyses Applied**

| | HULL | | | PONTOON | | |
|---|---|---|---|---|---|---|
| | 1 | 2 | 3 | 1 | 2 | 3 |
| $F_x$ | √ | √ | √ | √ | √ | √ |
| $F_y$ | √ | √ | √ | √ | √ | √ |
| $F_z$ | | | | | √ | √ |

**Legend:**

| | |
|---|---|
| | No forces exerted on that axis and component |
| | Dynamic pressure |
| | Morison equation on vertical members |
| | Morison equation on inclined members |

Forces were calculated at different components of the hulls and pontoons using different analyses as summarized in table 4.1 shown above. Forces on x-axis exerted at each component of hulls were calculated using Morison equation on vertical members (Equation 1 and 2), while forces on y-axis exerted at each component of hulls are calculated using dynamic pressure (Equation 7). There will be no force exerted on z-axis

of hulls due to assumption of 2-dimension wave acted symmetrical to the components of triangular TLP. Forces on x, y, and z axes exerted at each component of inclined pontoons were calculated using Morison equation on inclined members (Equation 15).

$$f_{x,y,z} = (515.221 \times 10^3 \frac{\delta u}{\delta t}_{x,y,z}) + (6.663 \times 10^3 w \mid u_{x,y,z}) \text{ [15]}$$

Where:

$$u_x = u - c_x(c_x + c_y v)$$
$$u_y = u - c_y(c_x + c_y v)$$
$$u_z = -c_z(c_x + c_y v)$$

$$\frac{\delta u}{\delta t}_x = \frac{\delta u}{\delta t} - c_x(c_x + c_y \frac{\delta v}{\delta t})$$
$$\frac{\delta u}{\delta t}_y = \frac{\delta u}{\delta t} - c_y(c_x + c_y \frac{\delta v}{\delta t})$$
$$\frac{\delta u}{\delta t}_z = -c_z(c_x + c_y \frac{\delta v}{\delta t})$$

The value of $(u_x, u_y, u_z)$ and $(\frac{\delta u}{\delta t}_x, \frac{\delta u}{\delta t}_y, \frac{\delta u}{\delta t}_z)$ have been calculated and obtained as:

**Table 4.2: Unit vector of the 3 Pontoons**

| | $u_x$ | $u_y$ | $u_z$ | $\frac{\delta u}{\delta t}_x$ | $\frac{\delta u}{\delta t}_y$ | $\frac{\delta u}{\delta t}_z$ |
|---|---|---|---|---|---|---|
| Pontoon 1 | *u* | *v* | *0* | *δu/δt* | *δv/δt* | *0* |
| Pontoon 2 | *0.25u* | *v* | *0.433u* | *0.25 δu/δt* | *δv/δt* | *0.433 δu/δt* |
| Pontoon 3 | *0.25u* | *v* | *-0.433u* | *0.25 δu/δt* | *δv/δt* | *-0.433 δu/δt* |

Forces exerted on hulls and pontoons were added up to get the total forces along the member at a particular time, t. The total forces calculation was repeated for each time step from 0 to $T_{ass}$ (0s to 9s) for every pontoon (Pontoon 1, 2 and 3) and hull (Hull 1, 2 and 3).

### 4.2.2 Moments Exerted on Hulls

Moments exerted on x, y and z axes are giving significance to response of triangular TLP such as roll, yaw and pitch respectively. Due to effect from 2-dimension wave, pitch will be the only response that is significance for this analysis. Therefore for simplicity of this analysis only pitch were calculated, where the moment will be the resultant of multiplication between forces on x-axis (surge) at each component of hulls

and moment arm, d. Whereby the moment arm was the distance between the respective forces exerted on the hull to the center of gravity of triangular TLP. Note that moment on z-axis that was contributed from forces exerted on pontoons are too small, thus has been neglected for this analysis.

Moments exerted on hulls are then added up to get the total moments along the member at a particular time, t. The total moment calculation was repeated for each time step from 0 to $T_{ass}$ (0s to 9s) for every hull (Hull 1, 2 and 3).

### 4.2.3 Summation of Forces and Moments Exerted on Hulls and Pontoons

Forces from all hulls and all pontoons were added up with respect to each of axis, while moments from all hulls were added up with respect to z-axis only (Refer Table 4.3).

$$F_{x,y,z} = \text{Hull 1} + \text{Hull 2} + \text{Hull 3} + \text{Pontoon 1} + \text{Pontoon 2} + \text{Pontoon 3}$$

$$M_z = \text{Hull 1} + \text{Hull 2} + \text{Hull 3}$$

**Table 4.3: Summation of $F_x$, $F_y$, $F_z$ and $M_z$**

| | SUMMATION OF FORCES (N) | | | SUMMATION OF MOMENTS (N.m) |
|---|---|---|---|---|
| TIME | $F_x$ | $F_y$ | $F_z$ | $M_z$ |
| 0 | -21441282.71 | 23550524.37 | 0 | -91175894.19 |
| 1 | -26729801.5 | 13791294.92 | 0 | -92063189.85 |
| 2 | -16152832.81 | -3034451.936 | 0 | -32712329.81 |
| 3 | 4047344.597 | -18428594.29 | 0 | 53172421.35 |
| 4 | 23217906.46 | -24383290.33 | 0 | 119670917.8 |
| 5 | 32158114.7 | -17765730.92 | 0 | 136039944.9 |
| 6 | 26971639.8 | -2103224.157 | 0 | 96383115.11 |
| 7 | 9687188.418 | 14528069.18 | 0 | 18559944.88 |
| 8 | -11545236.1 | 23743017.49 | 0 | -60880194.28 |
| 9 | -25497471.39 | 20918656.54 | 0 | -99562521.68 |

Based on the summation of forces for all components of this triangular TLP, it was observed that maximum $F_x$ was 32.158 MN at (t = 5s), maximum $F_y$ was 23.743 MN at (t = 8s) and maximum $M_z$ was 136.040 MN.m at (t = 5s). The summation of forces acted at z-axis has yielded zero resultant forces since no contribution of $F_z$ from Hull 1, Hull 2, Hull 3 and Pontoon 1, while summation of $F_z$ from Pontoon 2 and Pontoon 3 eliminate each other. The maximum forces of $F_x$, $F_y$ and $M_z$ will be used to calculate RAO for surge, heave and pitch respectively. Based on the analysis of RAO for regular wave, it was found that surge was 0.139, heave was 0.006 and pitch was 0.000034. Those values proved that triangular TLP allowed horizontal movements (surge), and restrained vertical movement (heave) and rotation in z-axis (pitch). Refer Appendix C for summary of forces and moments calculation.

### 4.3 Wave Spectrum

Waves at sea states occur as random which resulted from linear superposition of an infinite number of regular waves with varying frequency. Wave energy spectrum was used to describe a random sea state and its energy content. P-M Spectrum model (Equation 8) which based on single parameter was used for this analysis, since it gives accurate data which was applicable for design of offshore structure. The random wave which was propagated to hit the structure has the significant height of 3.6 m.

Wave spectrum can be obtained by means of varying frequencies (ranging from 0.035 Hz to 0.295 Hz with an interval of 0.01 Hz) in the wave train which were chosen to cover the entire range of frequencies of the wave spectrum. A graph of S(f) versus frequency, *f* was plotted as shown in Figure 4.1.

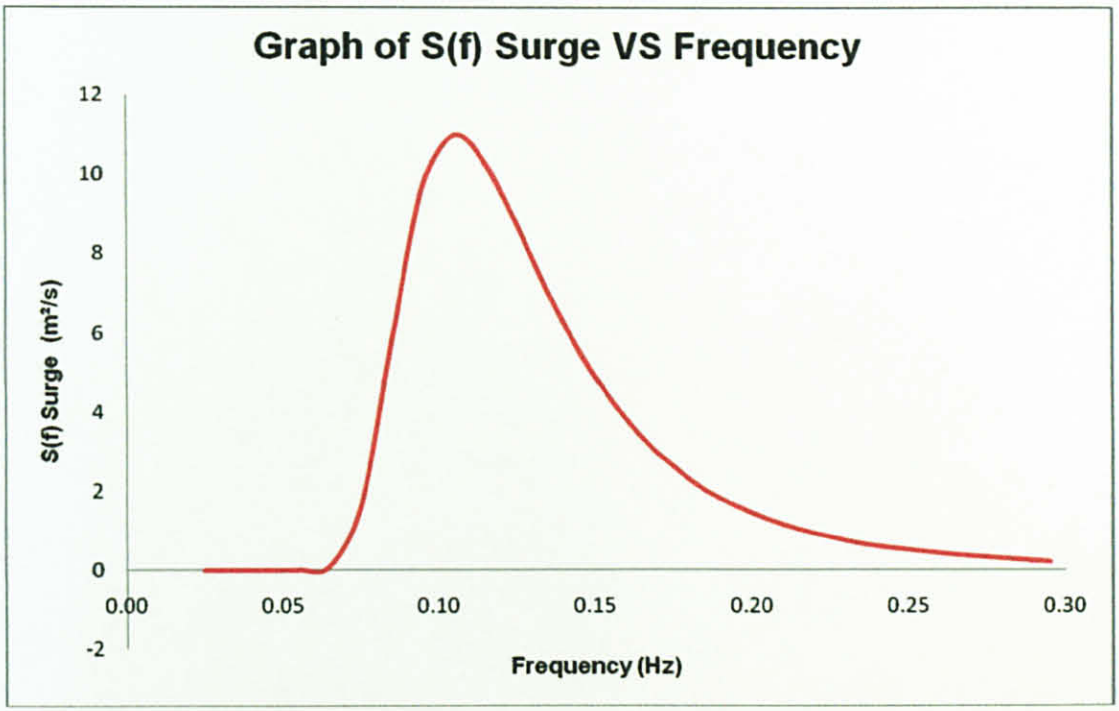


**Figure 4.1: Graph of Wave Energy Density Spectrum**

Based on figure 4.1, it was observed that maximum wave energy density which was 11.006 $m^2/s$, occur at frequency of 0.105 Hz. The area under the curve gives the total energy of wave system which was equivalent to $m_o = 0.808\ m^2$. Refer Appendix D for the summary of calculations for wave spectrum.

## 4.4 Wave Profile

The wave profile was computed based on the wave spectrum using (Equation 10). The ranges of frequencies were taken from 0.035 Hz to 0.295Hz. Values of term (n) indicate the values that vary which were random number from 0 to 1. The wave profiles were plotted for time ranging from 0s to 100s at two different locations which were Hull 1 and 2 (x coordinate = -20.21), and Hull 3 (x coordinate = 40.41) as shown in Figure 4.2 and Figure 4.3. Refer Appendix E for the summary of calculations for wave spectrum.

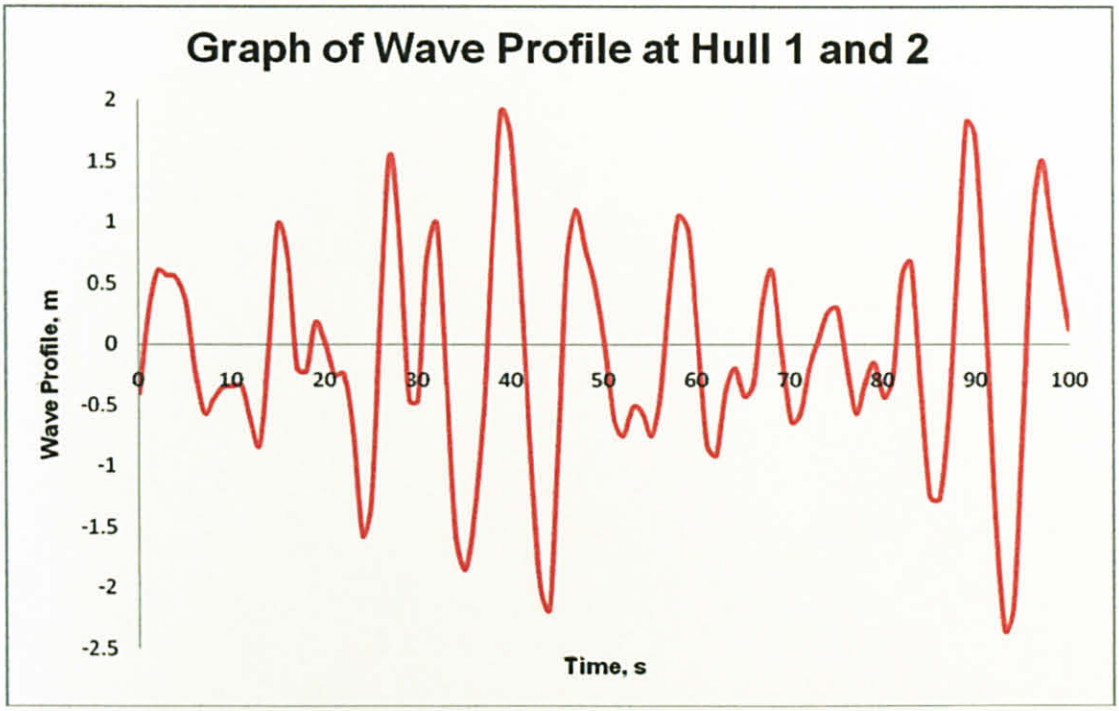


**Figure 4.2: Graph of Wave Profile at Hull 1 and Hull 2**

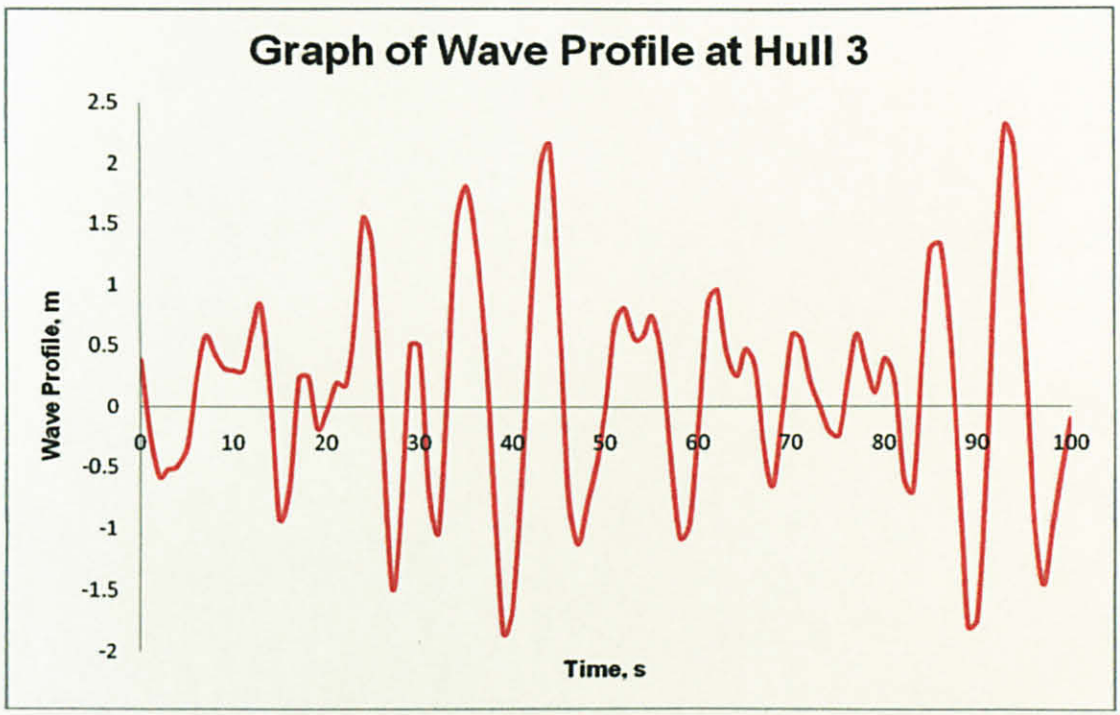


**Figure 4.3: Graph of Wave Profile at Hull 3**

Based on figure 4.1, it was observed that highest elevation of wave at Hull 1 and 2 was 1.91m at the time of 39s and lowest elevation of wave was -2.37m at the time of 93s. Based on figure 4.2, it was observed that highest elevation of wave at Hull 3 was 2.31m at the time of 93s and lowest elevation of wave was at -1.85m at the time of 39s.

## 4.5 Analysis on Surge Response

Computation of RAO surge at each frequency is obtained using (Equation 11). Variations of RAOs for a range of frequencies were plotted as shown in Figure 4.4. RAOs were then multiplied with wave energy density spectrum as in (Equation 13) to obtain the surge response spectrum as shown in Figure 4.5. The responses of triangular TLP due to effect of surge motion at two different locations as what have been discussed in section 4.4 were calculated using (Equation 14) and then plotted as shown in Figure 4.6 and Figure 4.7. Three variations of tether pretension were plotted for each of the figures in order to observe the surge responses based on the effect of variation in tether pretension. Refer Appendix F for summary for surge parameters.

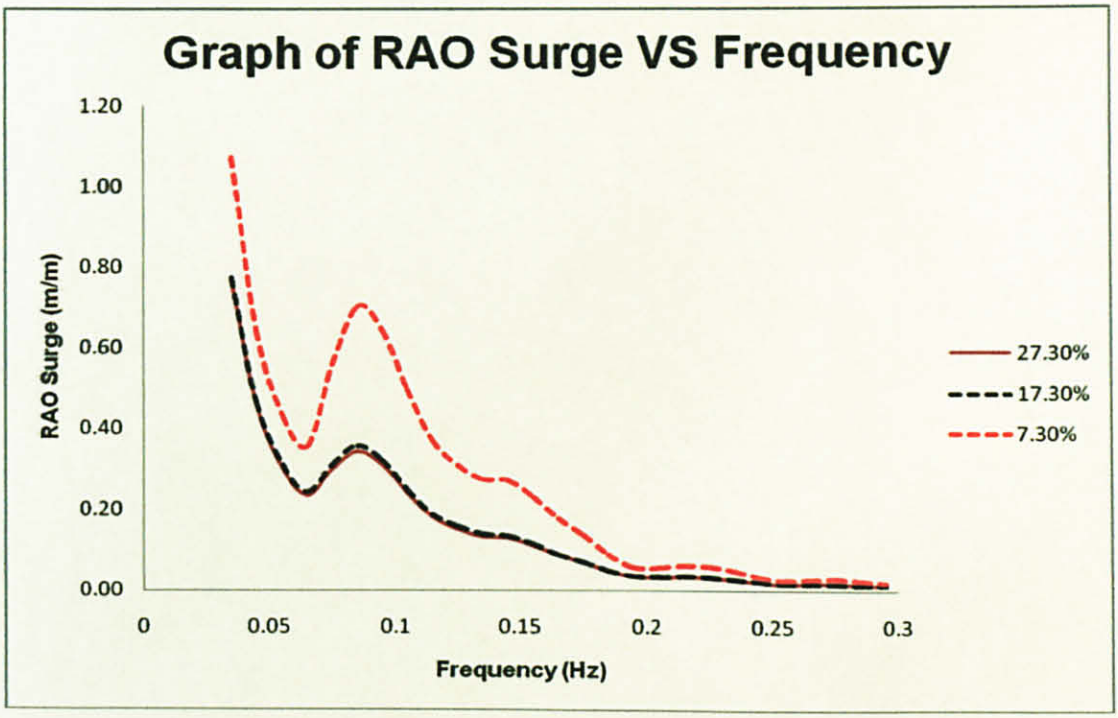


**Figure 4.4: Graph of RAO Surge**

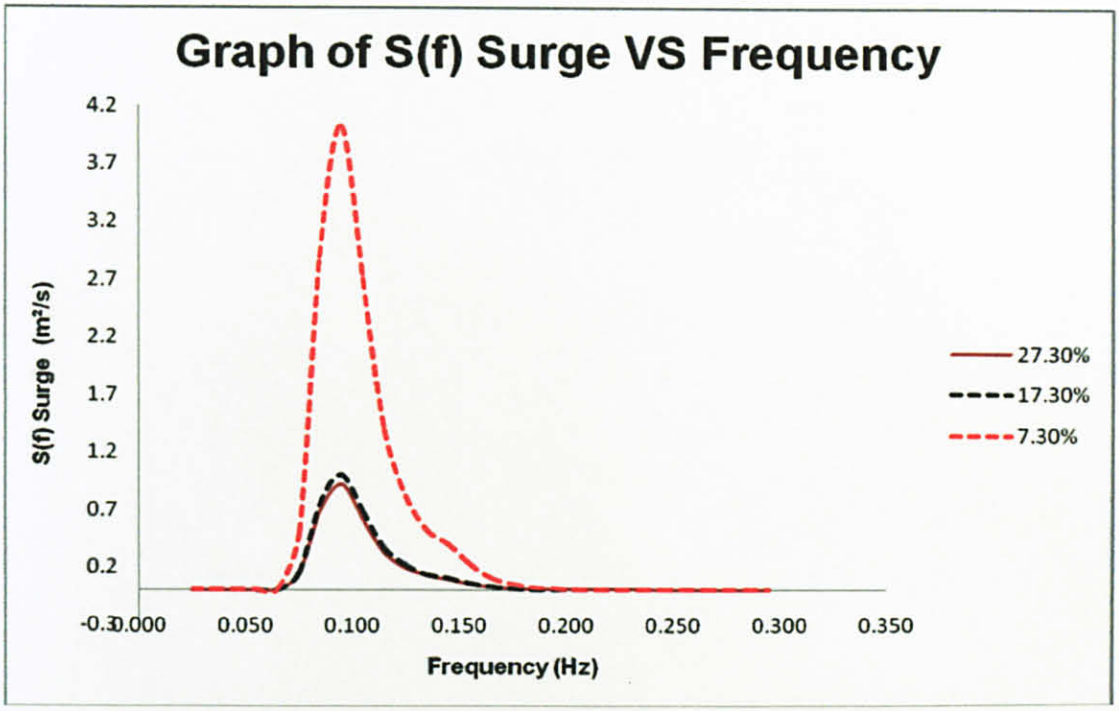


**Figure 4.5: Graph of Surge Spectrum**

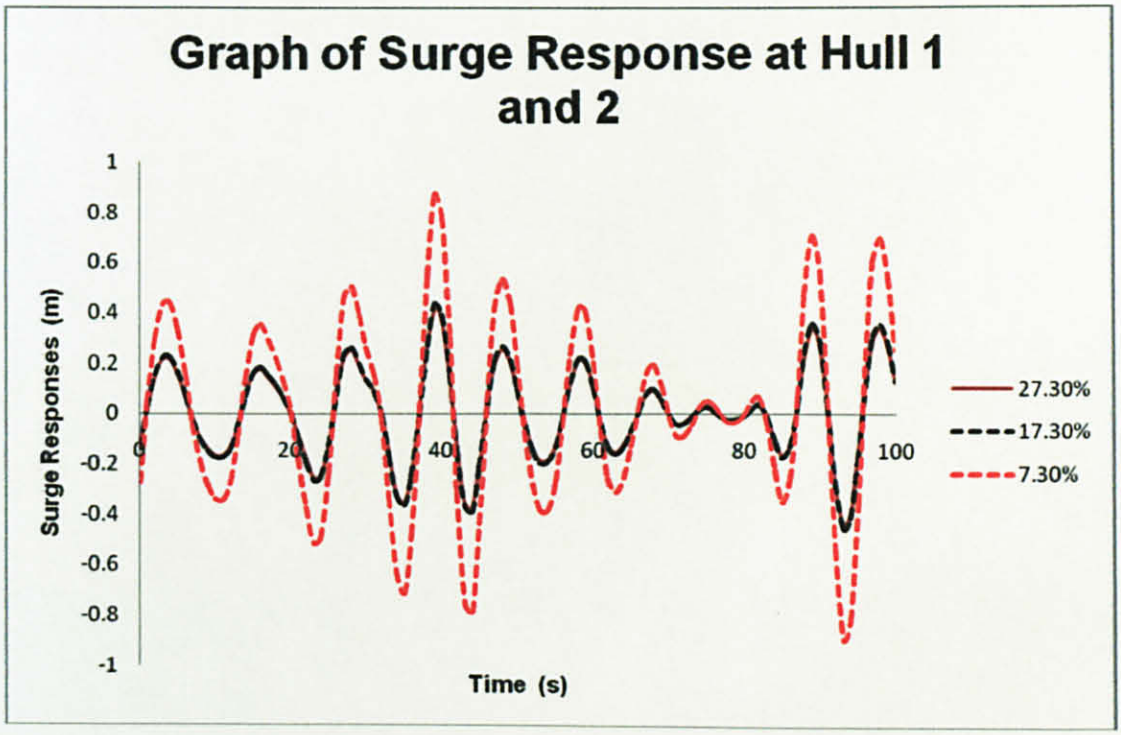


**Figure 4.6: Graph of Surge Response at Hull 1 and Hull 2**

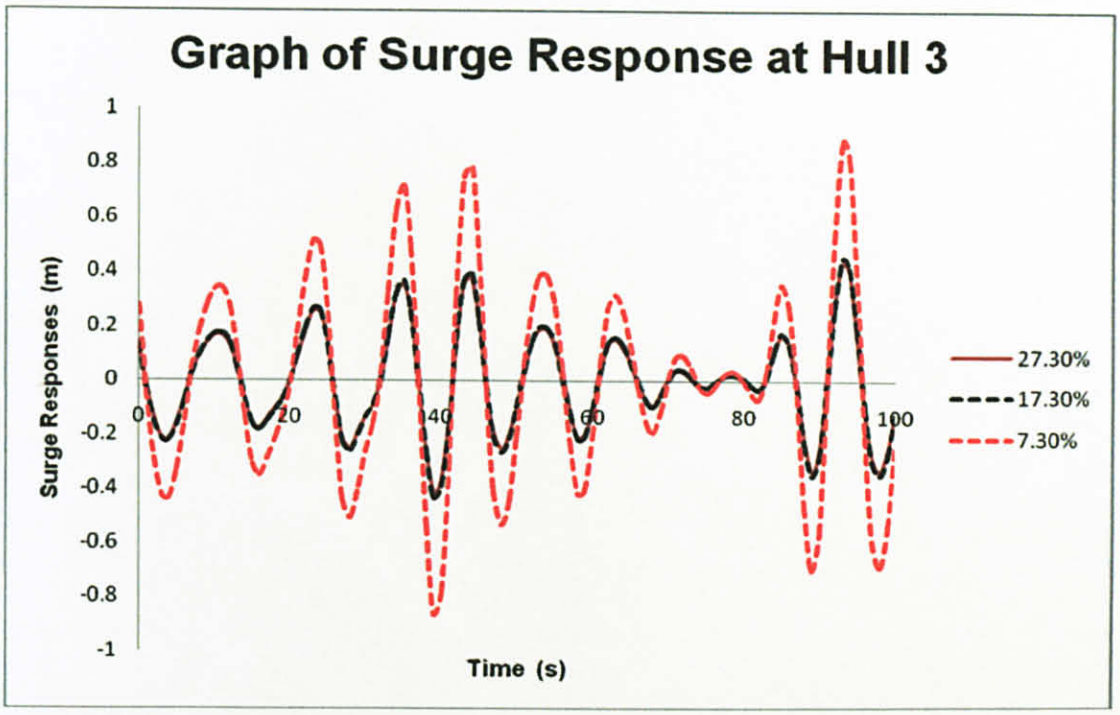


**Figure 4.7: Graph of Surge Response at Hull 3**

Based on graph of RAO surge it is observed that RAO surge is highest at lowest frequency. The area under the curve of surge spectrum gives the total energy of wave system. From the graph of surge response, the positive and negative surge response indicate the movement towards positive and negative of x axis respectively. The summary of analysis on surge response was shown as in Table 4.4.

**Table 4.4: Summary of Analysis on Surge Response**

| Pretension/Weight (%) | **RAO Surge** Behaviour | **Surge Spectrum** Max Energy Density ($m^2/s$) | Maximum **Surge Response** (m) | |
|---|---|---|---|---|
| | | | Hull 1 and 2 | Hull 3 |
| 7.3 | highest RAO at lowest frequency | 4.03 $m^2/s$ at 0.095 Hz | 0.87 | 0.87 |
| 17.3 | | 1.0 $m^2/s$ at 0.095 Hz | 0.43 | 0.45 |
| 27.3 | | 0.92 $m^2/s$ at 0.095 Hz | 0.42 | 0.43 |

## 4.6 Analysis on Heave Response

For analysis of heave response, a set of calculation as explained in section 4.5 was repeated. Variations of RAOs for a range of frequencies were plotted as shown in Figure 4.8, heave response spectrum as shown in Figure 4.9, and responses of triangular TLP due to effect of heave motion at two different locations as shown in Figure 4.10 and Figure 4.11. Three variations of tether pretension were plotted for each of the figures in order to observe the heave responses based on the effect of variation in tether pretension. Refer Appendix G for summary for heave parameters.

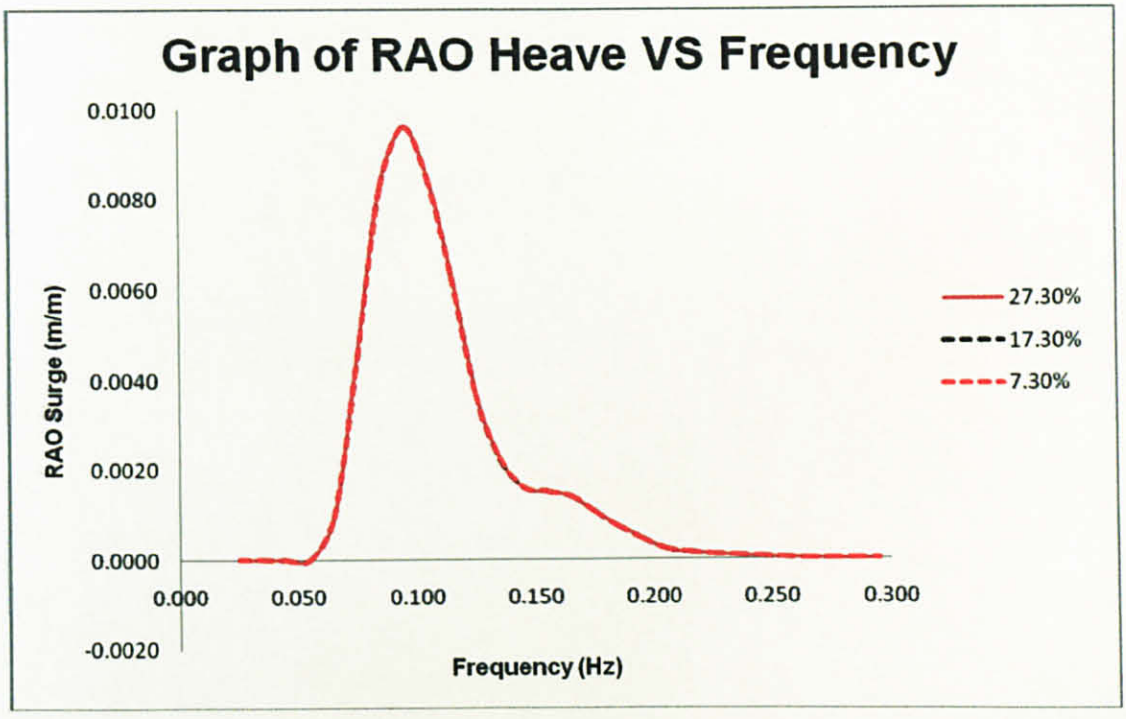


**Figure 4.8: Graph of RAO Heave**

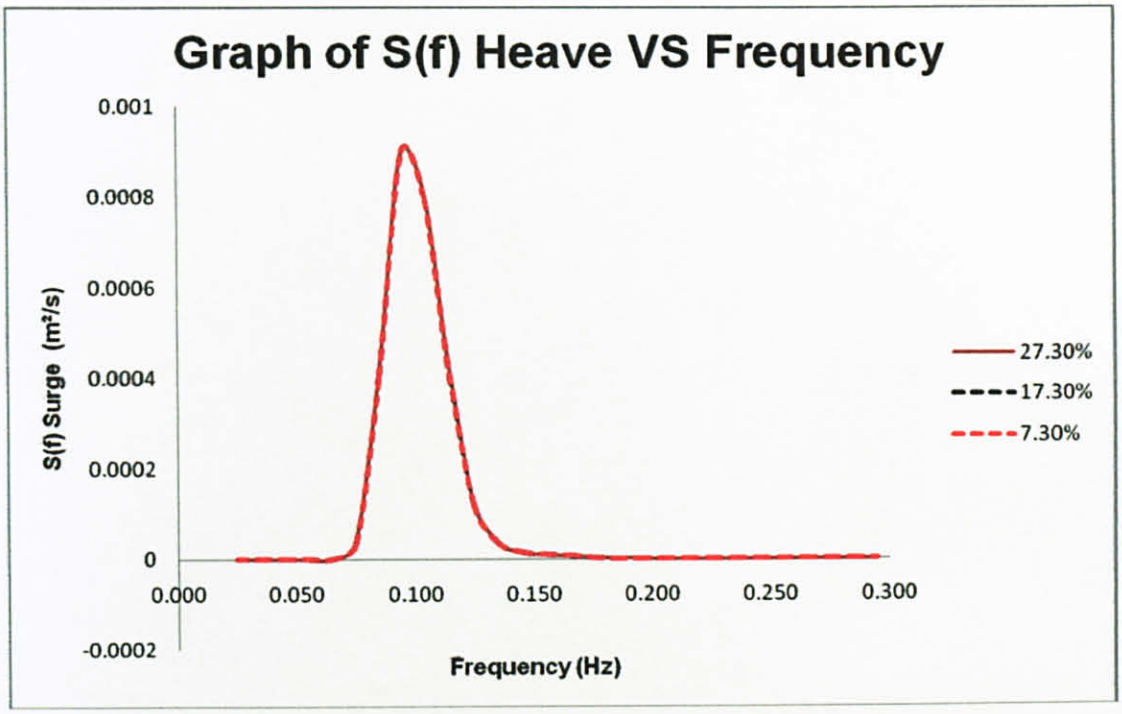


**Figure 4.9: Graph of Heave Spectrum**

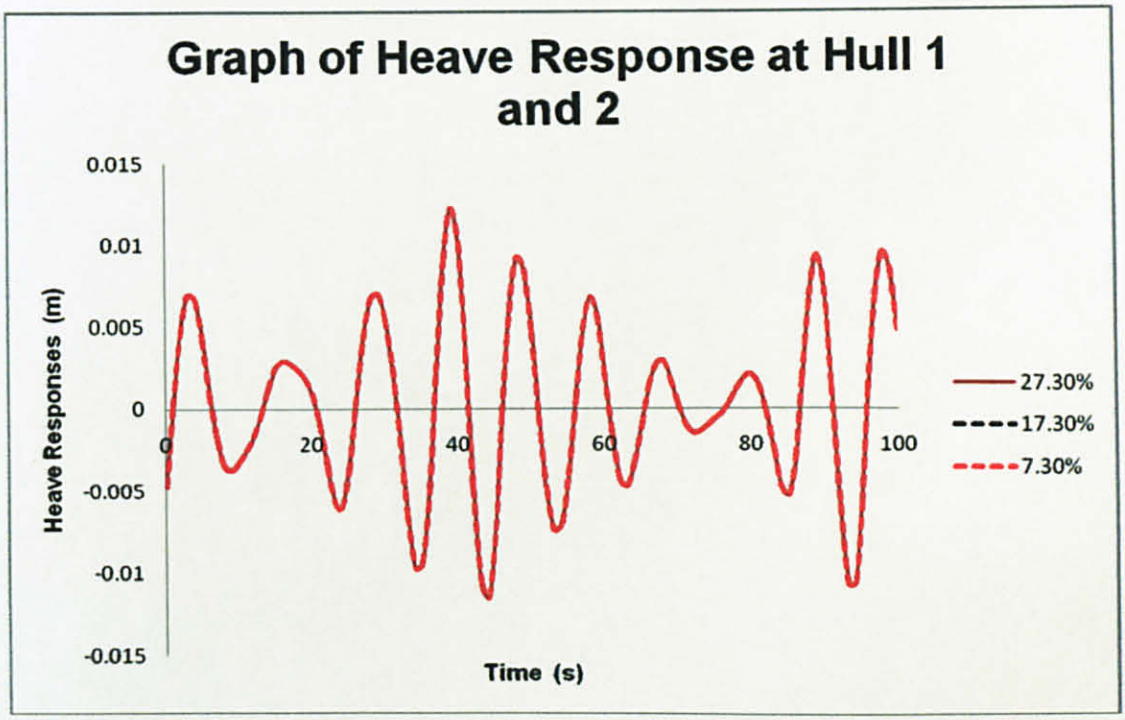


**Figure 4.10: Graph of Heave Response at Hull 1 and Hull 2**

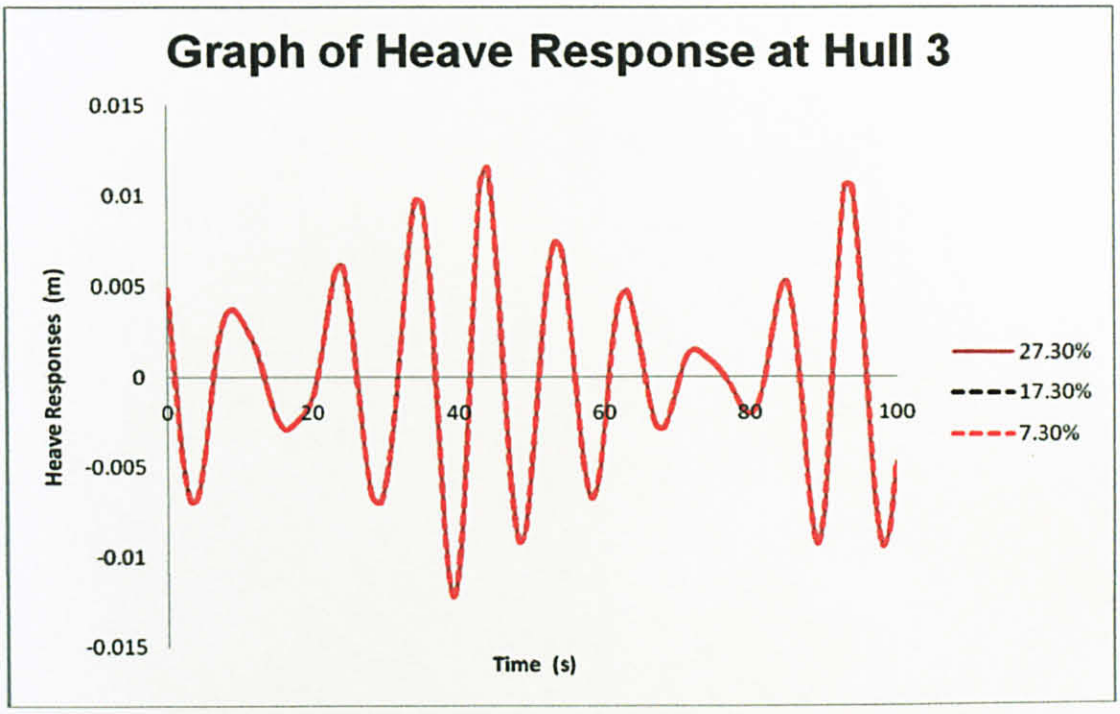


**Figure 4.11: Graph of Heave Response at Hull 3**

Based on graph of RAO heave it is observed that RAO heave is highest at frequency of 0.095 Hz. The area under the curve of heave spectrum gives the total energy of wave system. From the graph of heave response, positive and negative heave response indicate the movement towards positive and negative of y axis respectively. The summary of analysis on heave response was shown as in Table 4.5.

**Table 4.5: Summary of Analysis on Heave Response**

| Pretension/Weight (%) | **RAO Heave** Max RAO | **Heave Spectrum** Max Energy Density ($m^2/s$) | Maximum **Heave Response** (m) | |
|---|---|---|---|---|
| | | | Hull 1 and 2 | Hull 3 |
| 7.3 | 0.009623 at 0.095 Hz | 0.0008999 $m^2/s$ at 0.095 Hz | 0.012247 | 0.012255 |
| 17.3 | 0.009623 at 0.095 Hz | 0.0008997 $m^2/s$ at 0.095 Hz | 0.012245 | 0.012253 |
| 27.3 | 0.009622 at 0.095 Hz | 0.0008996 $m^2/s$ at 0.095 Hz | 0.012243 | 0.012251 |

## 4.7 Analysis on Pitch Response

For analysis of pitch response, a set of calculation as explained in section 4.5 and 4.6 was repeated. Variations of RAOs for a range of frequencies were plotted as shown in Figure 4.12, pitch response spectrum as shown in Figure 4.13, and responses of triangular TLP due to effect of pitch motion at two different locations as shown in Figure 4.14 and Figure 4.15. Three variations of tether pretension were plotted for each of the figures in order to observe the pitch responses based on the effect of variation in tether pretension. Refer Appendix H for summary for pitch parameters.

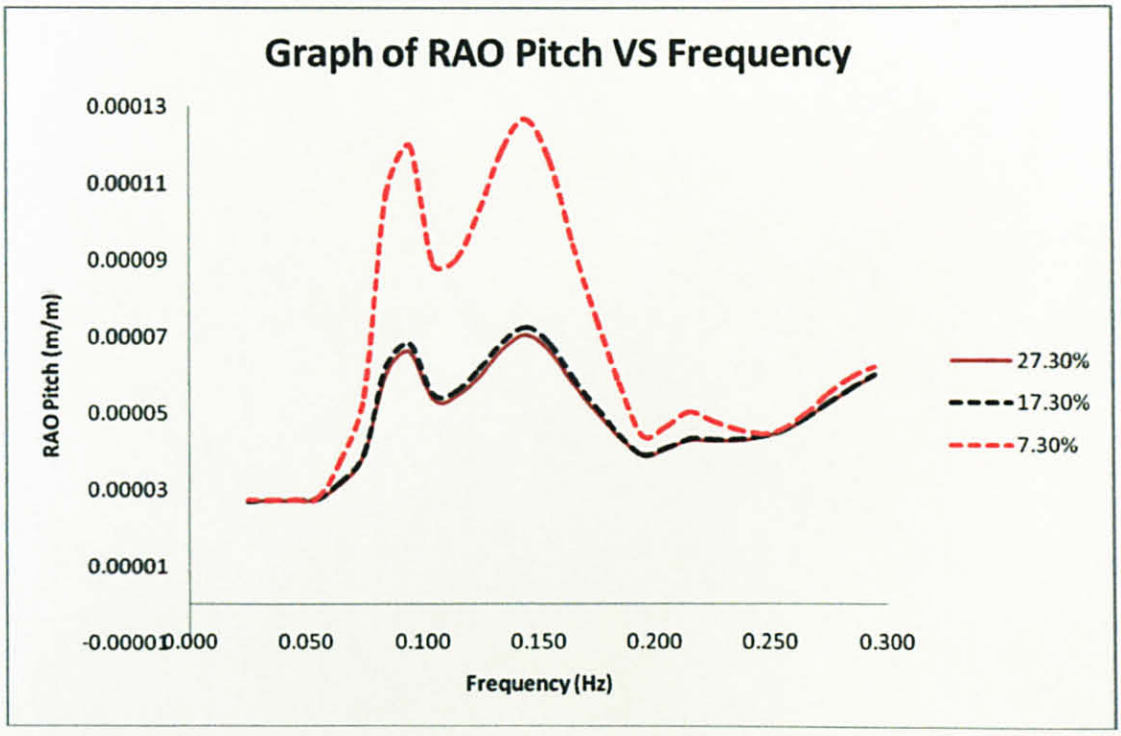


**Figure 4.12: Graph of RAO Pitch**

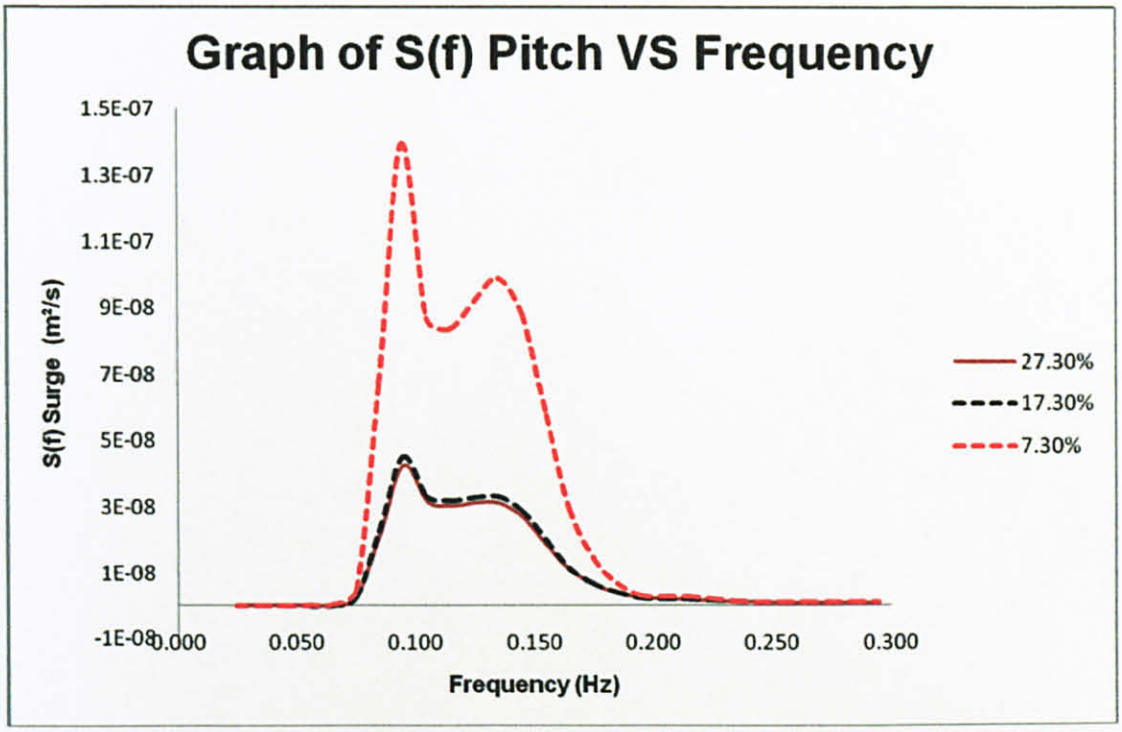


**Figure 4.13: Graph of Pitch Spectrum**

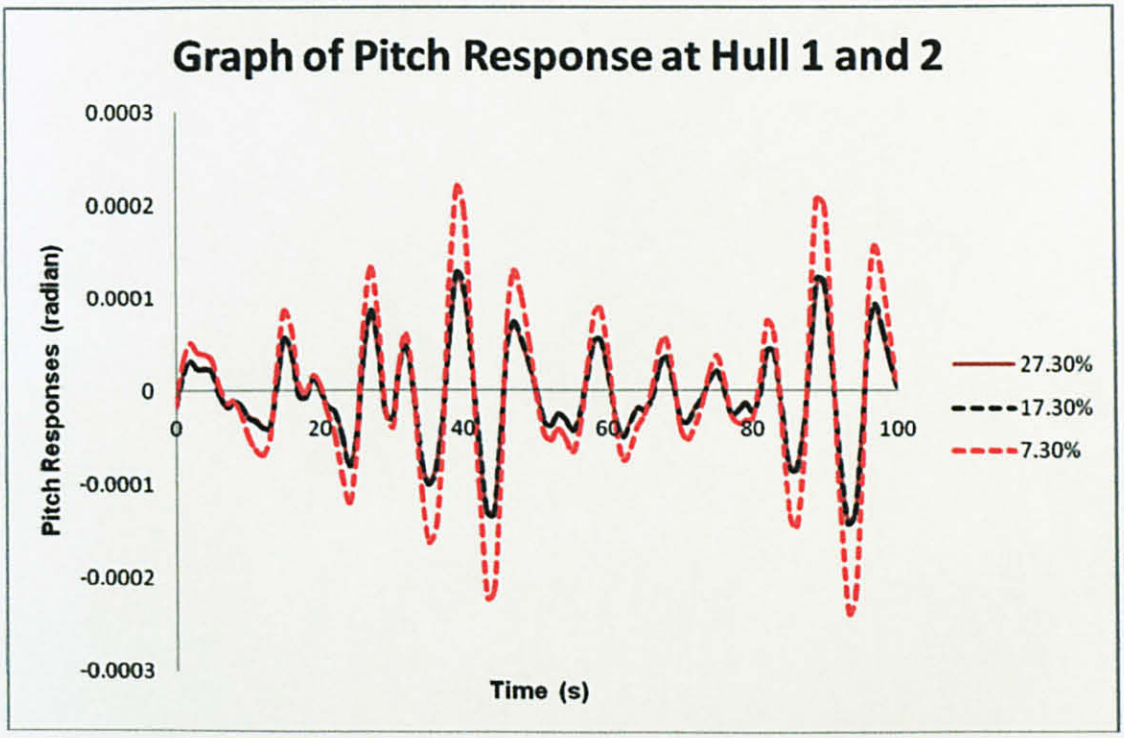


**Figure 4.14: Graph of Pitch Response at Hull 1 and Hull 2**

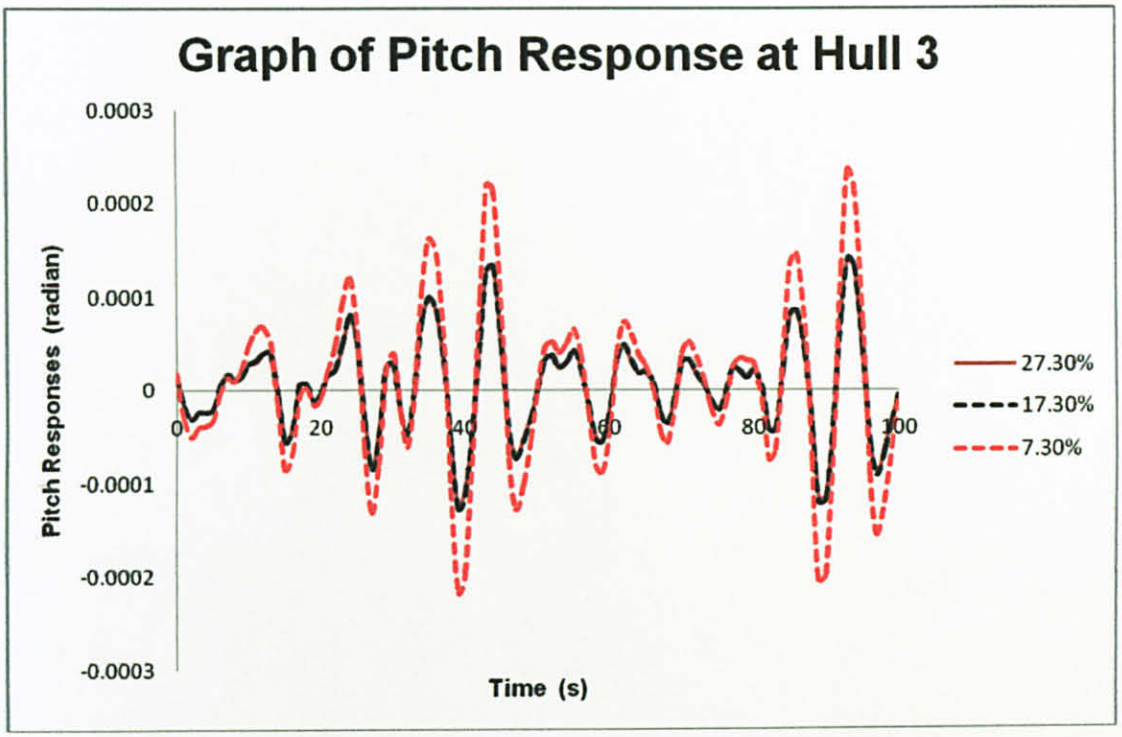


**Figure 4.15: Graph of Pitch Response at Hull 3**

Based on graph of RAO pitch it is observed that highest RAO pitch (is highest at frequency of 0.095 Hz. The area under the curve of pitch spectrum gives the total energy of wave system. From the graph of pitch response, positive and negative pitch response indicate the rotation towards positive and negative of z axis respectively. The summary of analysis on pitch response was shown as in Table 4.6.

**Table 4.6: Summary of Analysis on Pitch Response**

| Pretension/Weight (%) | **RAO Pitch** Max RAO | **Pitch Spectrum** Max Energy Density ($m^2/s$) | Maximum **Pitch Response** (degree) | |
|---|---|---|---|---|
| | | | Hull 1 and 2 | Hull 3 |
| 7.3 | 0.000127 at 0.145 Hz | $1.39542 \times 10^{-7}$ $m^2/s$ at 0.095 Hz | 0.0135 | 0.0135 |
| 17.3 | 0.000073 at 0.145 Hz | $4.51697 \times 10^{-8}$ $m^2/s$ at 0.095 Hz | 0.0081 | 0.0081 |
| 27.3 | 0.000071 at 0.145 Hz | $4.2536 \times 10^{-8}$ $m^2/s$ at 0.095 Hz | 0.0078 | 0.0079 |

## 4.8 Effect of Pretension on Triangular TLP Responses

The most concerned effect that was analyzed due to variation in tether pretension was the responses of triangular TLP produced due to the propagated wave. The responses due to effect of surge, heave and pitch responses for time ranging from 0s to 100s at two different locations (for Hull 1 and 2 at x coordinate = -20.21, and Hull 3 at x coordinate = 40.41) were plotted and summarized in Table 4.4, 4.5 and 4.6.

In order to analyze the relation between variation of tether pretension and responses in term of percentage increment and decrement, analysis for response at Hull 3 (x coordinate = 40.41) was taken as representative of triangular TLP responses. The estimated maximum amplitudes for the three motions and percentage of response differences with respect to response of 17.3% pretension are presented in Table 4.7.

**Table 4.7: Maximum amplitudes for the triangular TLP responses and percentage of responses differences with respect to response of 17.3% pretension over weight**

| Pretension/Weight (%) | | 27.3 | 17.3 | 7.3 |
|---|---|---|---|---|
| Maximum Amplitude of Responses | Surge | 0.43 | 0.45 | 0.87 |
| | | decrease 4.44% | | increase 93.33% |
| | Heave | 0.012251 | 0.012253 | 0.012255 |
| | | decrease 0.016% | | increase 0.016% |
| | Pitch | 0.0079 | 0.0081 | 0.0135 |
| | | decrease 2.50% | | increase 66.67% |

Based on the parametric analysis of tether pretension, it was observed that the responses were inversely proportional with the increment of tether pretension. The surge responses decreased by 4.4% for 10% increment of pretension and increased by 93.3% for 10% decrement of pretension. The pitch responses decreased by 2.5% for 10% increment of pretension and increased by 66.7% for 10% decrement of pretension. The heave responses decreased by 0.016% for 10% increment of pretension and increased by 0.016% for 10% decrement of pretension.

## 4.9 Laboratory Model Testing

Based from the recorded video for the movement of triangular TLP model, the measurement of responses have been done basically only for surge and heave, but not for pitch due to constraint of limitation methodology in measuring the pitch response. Figure 4.16 shows the illustrated picture of initial position of the model just after it was set up in the wave tank and response of the triangular TLP model after it was hit by the propagated wave. Figure 4.17 shows degree of freedom of the triangular TLP model.

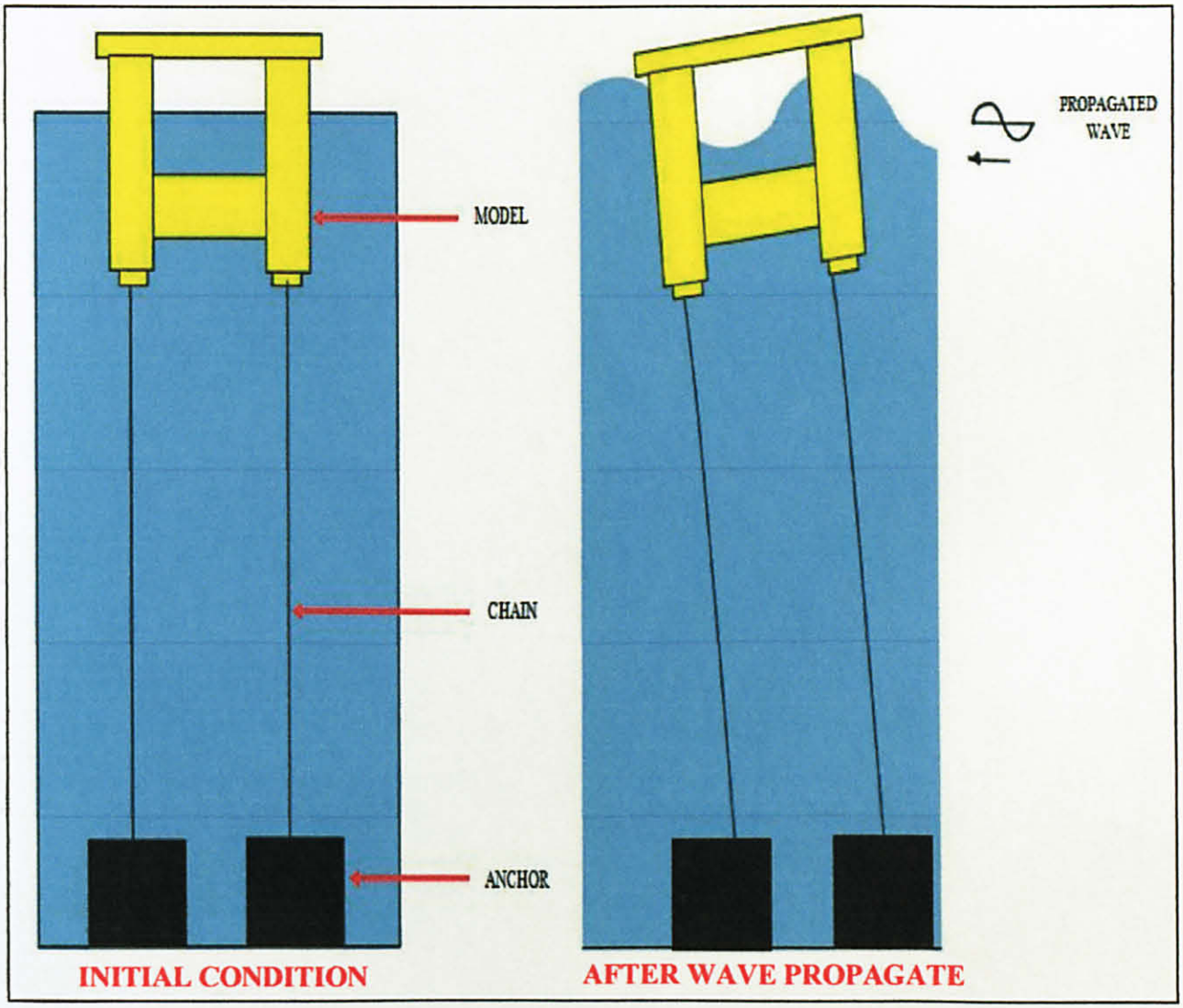


**Figure 4.16: Condition of Triangular TLP Model Due to Wave Propagated**

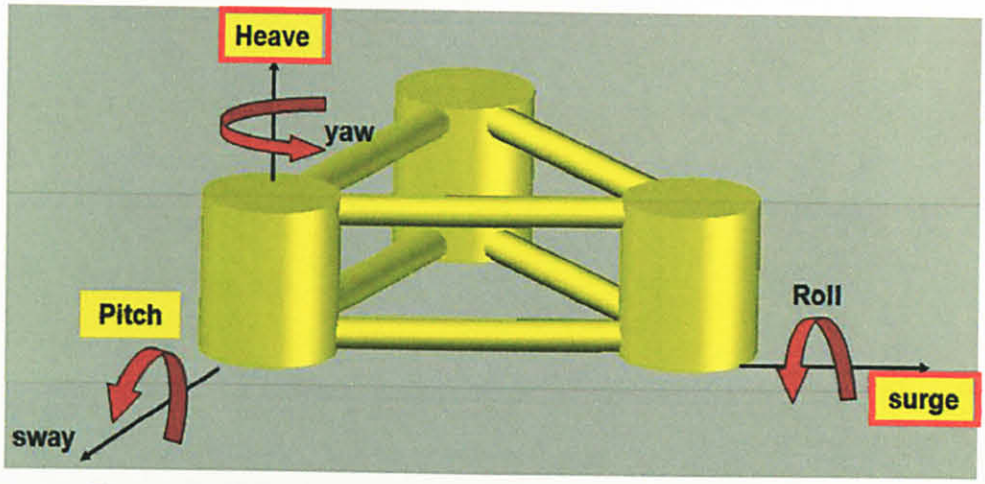


**Figure 4.17: Degree-of-Freedom of triangular TLP Model**

### 4.9.1 Surge Response

The graphs of response profile for time domain of 100s were plotted for responses of the model for x axis which was the surge as shown in Figure 4.18. In order to observe the responses based on the effect of variation in tether pretension, three variations of triangular TLP model drafts were plotted for the surge response profile graph. Refer Appendix J for data of surge response that was obtained from laboratory model testing.

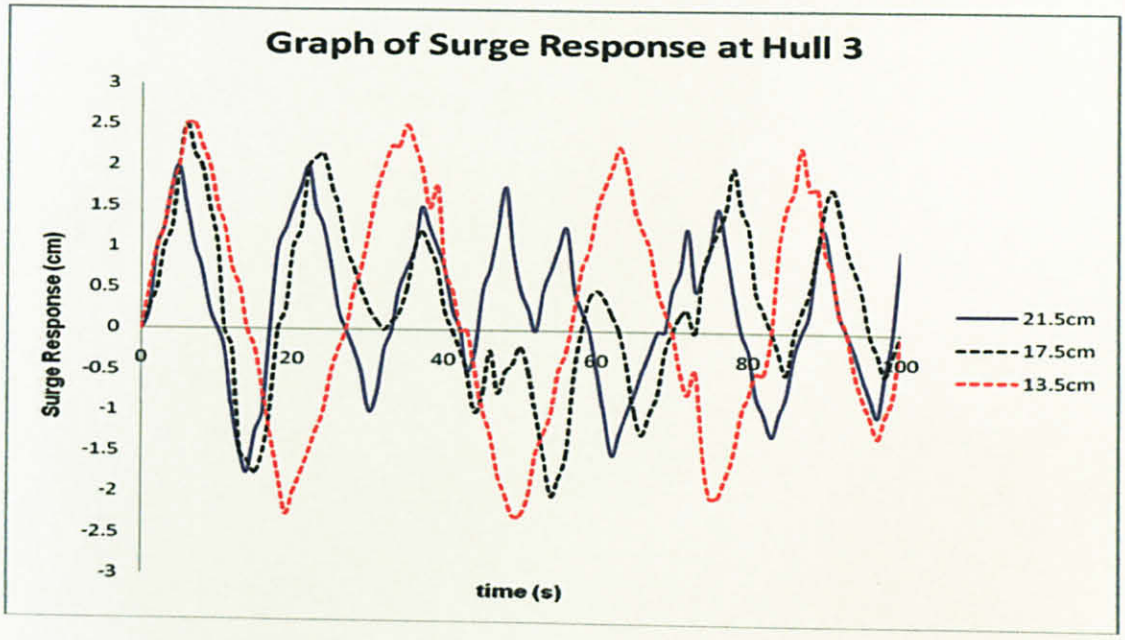


**Figure 4.18: Graph of Surge Response at Hull 3 (Model)**

### 4.9.2 Heave Response

The graphs of response profile for time domain of 100s were plotted for responses of the model for y axis which was the heave as shown in Figure 4.19. In order to observe the responses based on the effect of variation in tether pretension, three variations of triangular TLP model drafts were plotted for the heave response profile graph. Refer Appendix J for data of heave response that was obtained from laboratory model testing.

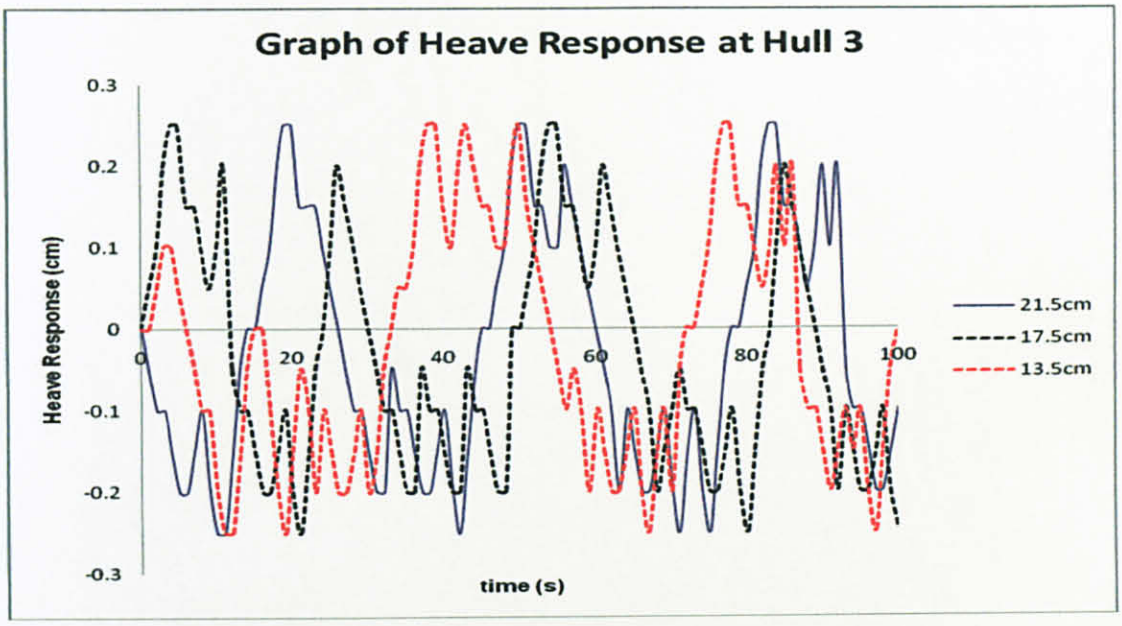


**Figure 4.19: Graph of Heave Response at Hull 3 (Model)**

### 4.9.3 Effect of Pretension on Triangular TLP Responses

In order to analyze the relation between variation of tether pretension and responses in term of percentage increment and decrement, analysis for response at Hull 3 (x coordinate = 40.41) was taken as representative of triangular TLP model responses. In this laboratory model testing, draft of triangular TLP model was changed to vary the pretension of the chain. The estimated maximum amplitudes for the two motions and percentage of response differences with respect to draft of 17.5cm are presented in Table 4.8.

**Table 4.8: Maximum amplitudes for the triangular TLP responses and percentage of responses differences with respect to response for draft of 17.5cm**

| Draft (cm) | | 21.5 | 17.5 | 13.5 |
|---|---|---|---|---|
| Maximum Amplitude of Responses | surge | 2.3 | 2.4 | 2.6 |
| | | decrease 4.17% | | increase 8.33% |
| | heave | 0.25 | 0.25 | 0.25 |
| | | constant | | constant |

Based on the parametric analysis of tether pretension, it was observed that surge responses were inversely proportional with the increment of the draft, while heave responses were not significantly affected. The surge responses decreased by 4.17% for 4cm increment of draft and increased by 8.33% for 4cm decrement of draft. The heave responses were constant both for 4cm increment and decrement of draft.

## 4.10 Comparison of Behavior between Responses from Dynamic Analysis and Laboratory Model Testing

The estimated maximum amplitudes from graphs of surge and heave responses profile obtained from the laboratory model testing were then compared with the graphs of surge and heave response profile which previously obtained from dynamic analysis. The behavior and responses trend of triangular TLP due to the variation of tethers pretension, for the model behavior and dynamic analysis can be analyzed from this analysis. The summary of behavior between responses from dynamic analysis and laboratory model testing was shown as in Table 4.9.

**Table 4.9: Summary of Responses Behavior between Responses from Dynamic Analysis and Laboratory Model Testing.**

| Pretension/Weight (%) | | 27.3 | 17.3 | 7.3 |
|---|---|---|---|---|
| Dynamic Analysis | surge | 0.43 | 0.45 | 0.87 |
| | | decrease 4.44% | | increase 93.33% |
| | heave | 0.012251 | 0.012253 | 0.012255 |
| | | decrease 0.016% | | increase 0.016% |
| Draft (cm) | | 21.5 | 17.5 | 13.5 |
| Laboratory Model Testing | surge | 2.3 | 2.4 | 2.6 |
| | | decrease 4.17% | | increase 8.33% |
| | heave | 0.25 | 0.25 | 0.25 |
| | | constant | | constant |

Based on the comparison analysis for surge responses, it was observed that surge responses were inversely proportional with the increment of tether pretension for both of dynamic analysis and laboratory model testing. From dynamic analysis, the surge responses decreased by 4.4% for 10% increment of pretension and increased by 93.3% for 10% decrement of pretension and from laboratory model testing, the surge responses decreased by 4.17% for 4cm increment of draft and increased by 8.33% for 4cm decrement of draft.

For the comparison analysis of heave responses, it was observed that heave responses were inversely proportional with the increment of tether pretension in dynamic analysis and heave responses were not significantly affected (constant both for 4cm increment and decrement of draft) in laboratory model testing. From dynamic analysis, the heave responses decreased by 0.016% for 10% increment of pretension and increased by 0.016% for 10% decrement of pretension and from laboratory model testing, the heave responses were constant both for 4cm increment and decrement of draft.

Based on the comparison, it is best to predict that both responses of surge and heave from dynamic analysis and laboratory model testing were having the same responses behavior, where surge responses were inversely proportional with tether pretension and heave responses were not significantly affected.

## 4.11 Economic Benefits

### 4.11.1 Introduction

The economic benefits of structures discussed in this thesis are discussed in terms of comparison for characteristics, functions and design considerations that relate to its cost between floating and fixed offshore structures, various types of floating offshore structures and variation in tether pretension. The cost discussed will reflect capital expenditure (CAPEX) and life cycle operating expenditure (OPEX).

### 4.11.2 Floating vs. Fixed Offshore Structures

As discussed in the literature review, the drilling of oil wells in deepwater is continuing with striking advances, reaching a water depth of more than 1000 m. Fixed structures became increasingly expensive and difficult to install as the water depths increased (Chakrabarti, 2005). This factor led to studies of the viable engineering solutions for meeting this demand, which was floating offshore structures.

Table 6.1 summarizes the main differences between floating and fixed offshore structure design. They are very different and unique in how they are constructed, transported and installed, what kind of excitation forces they are subjected to, how they respond to these excitation forces and how they are decommissioned and reused at the end of their design lives.

**Table 6.1:** Floating vs. Fixed Offshore Structures (Chakrabarti, 2005)

| Functions | Floating Structure | Fixed Structure |
|---|---|---|
| Payload Support | Buoyancy | Foundation Bearing Capacity |
| Well Access | Dynamics risers (subsea) or surface controls | Rigid conduits (conductors) surface wellheads and controls |
| Environmental loads | Resisted by vessel inertia stability, mooring strength | Resisted by strength of structure and foundation, compliant structure inertia |

| Functions | Floating Structure | Fixed Structure |
|---|---|---|
| construction | Plate and frame displacement hull: ship yards | Tubular space frame: fabrication yards |
| Installation | Wet or dry transport, towing to site and attachment to pre-installed mooring | Barge (dry) transport and launched, upended, piled foundations |
| Regulatory and design practices | Oil industry practices and government petroleum regulations and Coast Guard & International Maritime regulations | Oil industry practices and government petroleum regulations |

In term of decommissioning method, the floating structure can be decommissioned readily and moved to another site for reuse. A decommissioned fixed platform has to be removed in whole or in part, requiring the use of heavy lift equipment and the reverse of the installation procedure. Typically, such a structure has to be taken to shore for use as scrap steel or possibly modified and given a second life. Thus, the CAPEX for fixed platforms need to allocate substantial sums to cover future decommissioning costs.

### 4.11.3 Floating Offshore Structures

The process of floating facility selection and design can be a long and complicated process since selection of structures will be reflected in CAPEX and OPEX. The options for developing an oil field are innumerable, and it is not uncommon for the process of deciding which option to select to take years. Among options that should be taken into selection consideration is the factor that there are various types of floating offshore structures which varies with its functions (Refer Table 6.2).

**Table 6.2:** Functions of Floating Offshore Structures (Chakrabarti, 2005)

| | FPSO | Semi-submersible | Spar | TLP |
|---|---|---|---|---|
| Production | Yes | Yes | Yes | Yes |
| Storage | Yes | No | Yes | No |
| Drilling | No | Possible | Yes | Yes |
| Workover | No | Possible | Yes | Yes |
| Water Depth Limitation | No | No | No | Yes |

As discussed by Chakrabarti (2005), the most important fundamental decisions are:

1. How are the wells located and structured?
2. How will the drilling and completion of the wells be performed?
3. How will the well flow be delivered to the platform, processed and exported to market.

For the aspects of reducing costs of a TLP, the focus should be on the platform geometry that affects tether loading and on the tether system itself (Natvig and Vogel, 1995). The triangular TLP is chosen as it is three-legged and feasible for 12 tethers which are important for cost savings since hull, pontoon and tether are the important cost items.

### 4.11.4 Variation of Tether Pretension

Long and slender tethers with very high pretensions are susceptible to not only the high frequency dynamics but a higher probability of failure during its design life. Therefore the design pretension of TLP should be in the range of the optimum pretension, where for typical rectangular TLP it is about 15 to 20% of its total weight. From this study, out of the three variation of tether pretension, it was found that the optimum pretension of triangular TLP was about 17.3% of its total weight, which is still in the permissible range. The significance of optimum tether pretension is important as overdesign may lead to increase of CAPEX and underdesign may cause excessive responses of TLP.

# CHAPTER 5

## CONCLUSION AND RECOMMENDATIONS

### 5.1 Conclusion

As the conclusion of this study, the details of literature review about development of TLP and dynamic analysis for the triangular TLP have been presented. The problem statement for this study has been properly identified and suitable data of a triangular TLP has been collected and analyzed. In completing the dynamic analysis on responses of triangular TLP due to regular wave for one constant tethers pretension and random waves for three variation of tether pretension, some mathematical methods have been used as presented in methodology part. Theoretical models and some assumption which serve as the basic for the numerical models have been properly developed for meeting practical goals. Relations of Response Amplitude Operator at different axes of motion responses which were surge, heave and pitch, for three variation of tether pretension have been observed.

Experimental study of a triangular TLP model in the offshore laboratory has been done. The effect of responses due to variation of tether pretension by varying the draft of the triangular TLP model has been observed. The relation of motion responses trend of triangular TLP due to the variation of tethers pretension, for the model behavior and dynamic analysis have be compared.

Based on the discussion in the previous section, the conclusions on details of dynamic analysis are summarized as follow:

i. A frequency domain dynamic analysis approach methodology was presented as a tool of motion estimate for triangular TLP using Microsoft excels spread sheets. The developed frequency domain dynamic analysis of a typical triangular TLP was able to predict the responses for surge heave and pitch degrees of freedom when the triangular TLP was subjected to a random wave developed from Pierson-Moskowitz (P-M) spectrum.

ii. RAO due to regular wave at ($T_{ass}$ = 8.6s) and ($H_{max}$ = 6.4m) has been obtained as 0.139 for surge, 0.006 for heave and 0.000034 for pitch.

iii. Due to the effect of tether pretension, triangular TLP allowed horizontal movement (surge), and restrained vertical movement (heave) and rotation in z-axis (pitch) to a certain extent.

iv. Based on the parametric analysis of tether pretension for random wave , it was observed that the responses were inversely proportional to the tether pretension. The surge responses decreased by 4.4% for 10% increment of pretension and increased by 93.3% for 10% decrement of pretension. The pitch responses decreased by 2.5% for 10% increment of pretension and increased by 66.7% for 10% decrement of pretension. The heave responses were not significantly affected.

v. The optimum pretension of triangular TLP was approximately about 20% of its total weight.

The conclusions of experimental study of a triangular TLP model in the offshore laboratory are summarized as follow: s

i. The surge responses were inversely proportional with the increment of the draft, while heave responses were not significantly affected.

ii. The surge responses decreased by 4.17% for 4cm increment of draft and increased by 8.33% for 4cm decrement of draft. The heave responses were constant both for 4cm increment and decrement of draft.

Based on the comparison of motion responses trend of triangular TLP due to the variation of tethers pretension, for the model behavior and dynamic analysis, it is best to relate that both responses of surge and heave from dynamic analysis and laboratory

model testing were having the same responses behavior, where surge responses were inversely proportional with tether pretension and heave responses were not significantly affected.

## 5.2 Recommendations

Based on the present study, the following recommendations can be made for further study in order to improve the dynamic analysis and future works.

i. The result obtained from this triangular TLP can be used to compare with the result of the typical four legged TLP, basically in order to compare the performance of triangular TLP and typical four legged TLP.

ii. As stated earlier in assumptions and structural idealization part, the diffraction effects and second-order wave forces were neglected in this study. Therefore this assumption can be included in future study, in order to perform more accurate dynamic analysis.

iii. The wave that was consider in this study, was assumed to act symmetrically to the cylindrical member (2-Dimension wave), thus for future study 3-Dimension wave can be considered in order to simulate the real wave at sea.

iv. The Experimental study of a triangular TLP on more accurate approach (accurate scaled down model) can be done in order to obtain accurate scaled down model data that is reliable to industry for development of triangular TLP and field of deepwater platform design.

# REFERENCES


1. PETRONAS Technical Standard *Design of Fixed Offshore Structures – Supplementary to PTS 20.073 – Rev. 4-August 2005.* PETRONAS Carigali Sdn. Bhd.

2. Capanoglu, M. C., 1979, *Tension Leg Platform Design: Interaction of Naval Architectural and Structural Design Considerations.* Marine Technology, Vol 16, No 4, 343-352.

3. Chakrabarti S.K., 2005, *Handbook of Offshore Engineering.* ELSEVIER Ltd.

4. Chakrabarti S.K., 2001, *Hydronamics of Offshore Structures.* WIT Press.

5. Chandrasekaran S., Chandak N. R., Anupam G., 2005, *Stability Analysis of TLP Tethers.* Department of Civil Engineering, Institute of Technology, Baramas Hindu University, Varanasi-05, India.

6. Chandrasekaran S, Jain A.K., 2001, *Triangular Configuration Tension Leg Platform behaviour under random sea wave loads.* Department of Civil Engineering, I.I.T. Delhi, Haus Khan, New Delhi, 1106, India.

7. Chandrasekaran S, Jain A.K., 2001, *Dynamic Behaviour of Square and Triangular Offshore Tension Leg Platform Under Regular Wave Loads.* Department of Civil Engineering, I.I.T. Delhi, Haus Khan, New Delhi, 1106, India.

8. Dawson T. H., 1983, *Offshore Structural Engineering.* Prentice-Hall, Englewood Cliffs. N.J.

9. Demirbilek Z., 1989, *Tension Leg Platform: An Overview of the Concept, Analysis and Design.* American Society of Civil Engineers, ASCE.

10. Haritos N., 2007, *Introduction to the Analysis and Design of Offshore Structures – An Overview.* The University of Melbourne, Australia.

11. Heideman J.C, 1989, *Tension Leg Platform: Environmental Design Criteria.* American Society of Civil Engineers, ASCE.

12. Mohd Khalid M. A., 2008, *Effect of Water Depth on the Behaviour of Triangular Tension Leg Platform.* Final Year Project, Universiti Teknologi PETRONAS.

13. Munkejord, T., 1996, *The Heidrun TLP and concept development for deep water.* ISOPE, Los Angeles, 1-11.

14. Natvig B.J, Vogel H., 1995, *TLP Design Philosophy – Past, Present, Future.* ISOPE, The Hague, 64-69.

15. Niedzwecki J.M., Frentz G. T., 1989, *An Overview of Tension Leg Platform Model Studies.* Civil Engineering Department, Ocean Engineering Program, Texas A&M University, College Station, Texas 77843.

16. Pauling J.R., 1970, *Analysis of the Tension Leg Stable Platform.* Second Offshore Technology Conference, OTC 1263, Vol. II, 379-389.

17. Anonymous, 2009, *The Ram Powell TLP* [Online] Available from: URL http://www.offshore-technology.com/projects/rampowell/rampowell

# APPENDICES

## APPENDIX A

## PROJECT METHODOLOGY DIAGRAM

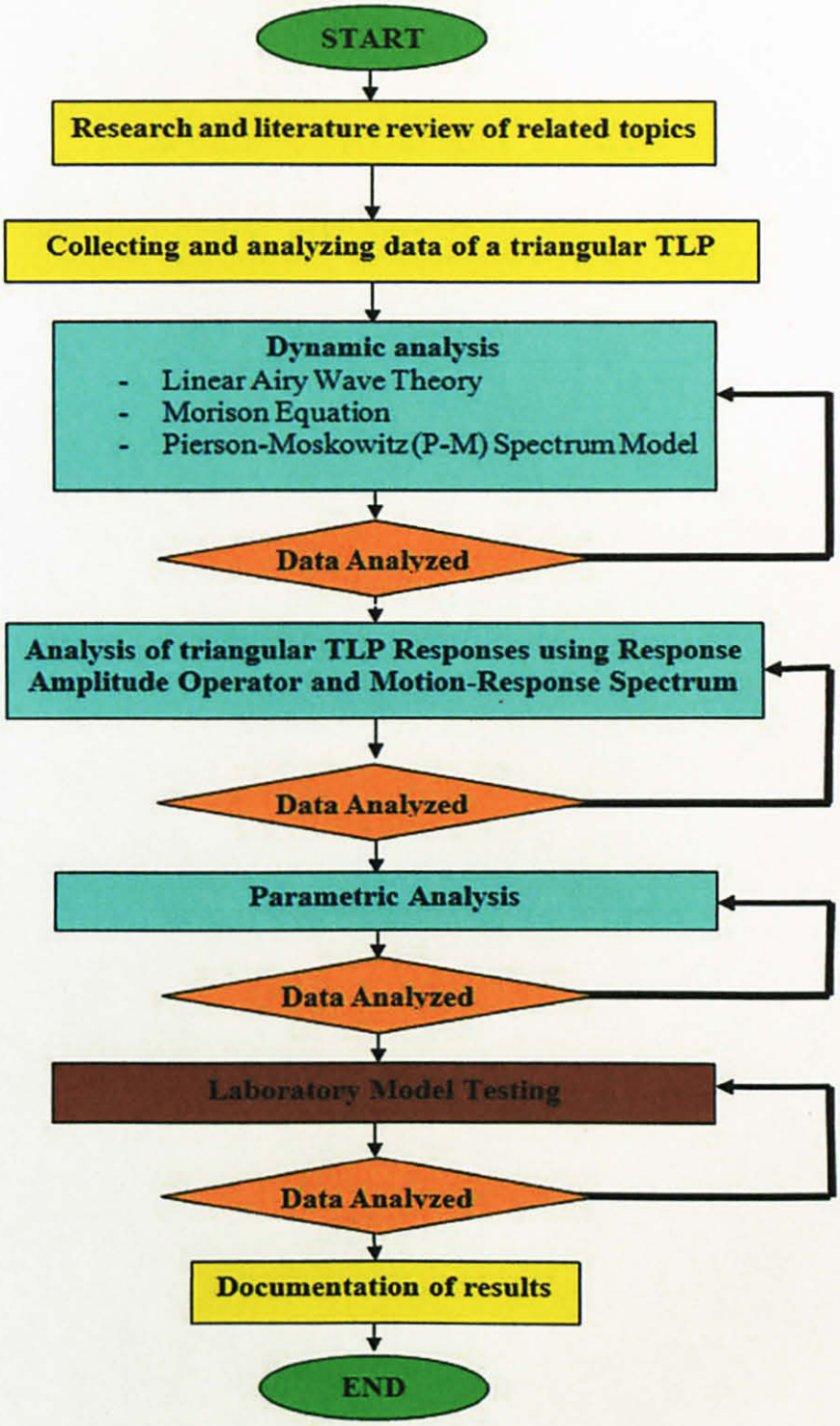

## APPENDIX B

## GANTT CHART

**FINAL YEAR PROJECT I**

| No. | Detail | 1 | 2 | 3 | 4 | 5 | 6 | 7 | 8 | 9 | 10 | 11 | 12 | 13 | 14 | 15 | 16 | 30-nov to 3-dec |
|---|---|---|---|---|---|---|---|---|---|---|---|---|---|---|---|---|---|---|
| 1 | Selection of Project Topic | | | | | | | | | | | | | | | | | |
| 2 | Preliminary Research Work | | | | | | | | | | | | | | | | | |
| 3 | Submission of Progress Report | | | | | | | | | | | | | | | | | |
| 4 | Project work continues | | | | | | | | | | | | | | | | | |
| 5 | Submission of Interim Report Final Draft | | | | | | | | | | | | | | | | | |
| 6 | Oral Presentation | | | | | | | | | | | | | | | | | |
| 7 | FYP SEMINAR 1 (EIM TALK) | | | | 12-Aug | | | | | | | | | | | | | |
| 8 | FYP WORKSHOP 1 (IRC) | | | | | 17-Aug | | | | | | | | | | | | |
| 9 | FYP WORKSHOP 2 (TECHNICAL WRITING) | | | | | 17-Aug | | | | | | | | | | | | |
| 10 | FYP WORKSHOP 3 (LAB BRIEFING) | | | | | | 24-Aug | | | | | | | | | | | |
| 10 | FYP WORKSHOP 4 (REFERENCING) | | | | | | | | | 14-Sep | | | | | | | | |
| 10 | FYP WORKSHOP 5 (HSE BRIEFING) | | | | | | | | | | | | | | 19-Oct | | | |

| | |
|---|---|
| | MILESTONE OF FYP 1 |
| | SEMINAR / WORKSHOP |

**FINAL YEAR PROJECT II**

| No. | Detail | 1 | 2 | 3 | 4 | 5 | 6 | 7 | 8 | 9 | 10 | 11 | 12 | 13 | 14 | 15 |
|---|---|---|---|---|---|---|---|---|---|---|---|---|---|---|---|---|
| 1 | Pitch Response, Parametric Analysis | | | | | | | | | | | | | | | |
| 2 | Collecting Required Information for Model | | | | | | | | | | | | | | | |
| 3 | Finish up Report Documentation | | | | | | | | | | | | | | | |
| 4 | Construction of the Model | | | | | | | | | | | | | | | |
| 5 | Submission of Progress Report | | | | | | | 12 March | | | | | | | | |
| 6 | Model Testing | | | | | | | | | | | | | | | |
| 7 | Documentation from Model Testing | | | | | | | | | | | | | | | |
| 8 | Preparation for Poster Presentation | | | | | | | | | | | | | | | |
| 9 | Poster Exhibition | | | | | | | | | | | 14 April | | | | |
| 10 | Final Report Documentation for Dissertation and Oral Presentation | | | | | | | | | | | | | | | |
| 11 | Submission of Dissertation (soft bound) | | | | | | | | | | | | | 6 May | | |
| 12 | Submission of Dissertation (hard bound) | | | | | | | | | | | | | | | |
| 13 | Oral Presentation | | | | | | | | | | | | | | | 7 - 10 June |

## APPENDIX C

## SUMMARY OF ENTIRE FORCES AND MOMENTS EXERTED ON COMPONENTS OF TRIANGULAR TLP

### FORCES EXERTED ON HULLS

Spread sheet for summary of forces ($F_x$) exerted on Hull 1, 2 and 3 from (t = 0) to (t = 9);

HULL 1 and 2:

| t (s) | Fd (N/m) | Fi (N/m) | Fx (N/m) |
|---|---|---|---|
| 0 | 830638.4435 | -12266636.91 | -11435998 |
| 1 | 301298.5469 | -13298856.93 | -12997558 |
| 2 | 106422.9972 | -7540918.999 | -7434496 |
| 3 | 71503.84088 | 2067276.992 | 2138780.83 |
| 4 | 154049.4538 | 10619958.41 | 10774007.9 |
| 5 | 483527.0457 | 13750279.44 | 14233806.5 |
| 6 | 1088890.745 | 9859954.279 | 10948845 |
| 7 | 1459512.166 | 935313.216 | 2394825.38 |
| 8 | 1194729.626 | -8466882.008 | -7272152.4 |
| 9 | 585137.8276 | -13546039.06 | -12960901 |

HULL 3

| t (s) | Fd (N/m) | Fi (N/m) | Fx (N/m) |
|---|---|---|---|
| 0 | 167392.6613 | 11126355.27 | 11293748 |
| 1 | 527115.0265 | 13691280.8 | 14218396 |
| 2 | 1136945.099 | 9265683.789 | 10402629 |
| 3 | 1462554.668 | 109194.735 | 1571749 |
| 4 | 1149313.203 | -9103047.193 | -7953734 |
| 5 | 538980.3192 | -13667436.41 | -1.3E+07 |
| 6 | 171265.3341 | -11253477.6 | -1.1E+07 |
| 7 | 74904.71896 | -3093694.862 | -3018790 |
| 8 | 97635.52526 | 6645673.014 | 6743309 |
| 9 | 265819.3844 | 12991879.38 | 13257699 |

Spread sheet for summary of forces ($F_y$) exerted on Hull 1, 2 and 3 from (t = 0) to (t = 9);

HULL 1 and 2:

| t (s) | Fy (N) |
|---|---|
| 0 | 505749.4 |
| 1 | -287002 |
| 2 | -933216 |
| 3 | -1102946 |
| 4 | -709532 |
| 5 | 46156.55 |
| 6 | 778278.1 |
| 7 | 1113025 |
| 8 | 879481 |
| 9 | 196890 |

HULL 3

| t (s) | Fy (N) |
|---|---|
| 0 | -656559 |
| 1 | 113002.2 |
| 2 | 824866.8 |
| 3 | 1115569 |
| 4 | 836681.9 |
| 5 | 130599.9 |
| 6 | -642164 |
| 7 | -1087051 |
| 8 | -976909 |
| 9 | -367975 |

## FORCES EXERTED ON PONTOONS

Spread sheet for summary of forces ($F_x$, Fy and $F_z$) exerted on Pontoon 1, 2 and 3 from (t = 0) to (t = 9);

PONTOON 1:

| t (s) | Fd (N/m) | Fi (N/m) | Fx (N/m) | Fd (N/m) | Fi (N/m) | Fy (N/m) |
|---|---|---|---|---|---|---|
| 0 | 1360710.408 | -14081710.08 | -12721000 | -436229.304 | 7162071.318 | 6725842 |
| 1 | 792456.5254 | -15266665.92 | -14474209 | -369996.6802 | -4064324.796 | -4434321 |
| 2 | 396736.4596 | 2373168.413 | -8259999 | -145855.8868 | -13215549.53 | -13361405 |
| 3 | 302113.4865 | 2373168.413 | 2675282 | 33909.97959 | -15619151.58 | -15585242 |
| 4 | 526845.5426 | 12191375.39 | 12718221 | 240430.3729 | -10047894.82 | -9807464 |
| 5 | 1020452.624 | 15784884.64 | 16805337 | 430503.6078 | 653636.9055 | 1084141 |
| 6 | 1575888.43 | 11318914.76 | 12894803 | 373292.7204 | 11021433.35 | 11394726 |
| 7 | 1853189.151 | 1073709.904 | 2926899 | 37883.21253 | 15761883.49 | 15799767 |
| 8 | 1658238.438 | -9719711.977 | -8061474 | -327480.5366 | 12454598.48 | 12127118 |
| 9 | 1128830.841 | -15550423.16 | -14421592 | -443831.4773 | 2788218.749 | 2344387 |

PONTOON 2:

| t (s) | Fd (N/m) | Fi (N/m) | Fx (N/m) | Fd (N/m) | Fi (N/m) | Fy (N/m) | Fd (N/m) | Fi (N/m) | Fz (N/m) |
|---|---|---|---|---|---|---|---|---|---|
| 0 | 168188.0112 | 1069348.129 | 1428983 | 66944.05006 | 7064667.1 | 8234871 | 291301.6 | 1852111 | 2474999 |
| 1 | 175010.3839 | -382367.7803 | -239436 | -24260.25188 | 8115807.173 | 9343309 | 303118 | -662261 | -414702.4 |
| 2 | 155147.6845 | -1638853.556 | -1713235 | -100446.6911 | 5023161.59 | 5684259 | 268715.8 | -2838494 | -2967323 |
| 3 | 119863.7659 | -2058570.084 | -2238624 | -124864.4455 | -634220.2551 | -876515 | 207604 | -3565443 | -3877297 |
| 4 | 87217.54145 | -1427217.63 | -1547298 | -91561.35768 | -5967780.607 | -6996722 | 151060.8 | -2471941 | -2679920 |
| 5 | 73051.31435 | -67153.4388 | 6810.277 | -4462.596864 | -8254299.161 | -9536392 | 126524.9 | -116310 | 11795.4 |
| 6 | 85012.36453 | 1327198.094 | 1630679 | 85590.32335 | -6326320.532 | -7206171 | 147241.4 | 2298707 | 2824337 |
| 7 | 116580.9559 | 2043906.072 | 2494714 | 124373.3248 | -1168236.047 | -1205348 | 201918.2 | 3540045 | 4320845 |
| 8 | 152385.6338 | 1717032.249 | 2158617 | 104866.3217 | 4586328.821 | 5416923 | 263931.9 | 2973900 | 3738724 |
| 9 | 174249.2188 | 513472.5399 | 794112.3 | 32527.78236 | 7999196.409 | 9274232 | 301799.6 | 889334.4 | 1375403 |

PONTOON 3:

| t (s) | Fd (N/m) | Fi (N/m) | Fx (N/m) | Fd (N/m) | Fi (N/m) | Fy (N/m) | Fd (N/m) | Fi (N/m) | Fz (N/m) |
|---|---|---|---|---|---|---|---|---|---|
| 0 | 168188.0112 | 1069348.129 | 1428983 | 66944.05006 | 7064667.1 | 8234871 | -291302 | -1852111 | -2474999 |
| 1 | 175010.3839 | -382367.7803 | -239436 | -24260.25188 | 8115807.173 | 9343309 | -303118 | 662261 | 414702.4 |
| 2 | 155147.6845 | -1638853.556 | -1713235 | -100446.6911 | 5023161.59 | 5684259 | -268716 | 2838494 | 2967323 |
| 3 | 119863.7659 | -2058570.084 | -2238624 | -124864.4455 | -634220.2551 | -876515 | -207604 | 3565443 | 3877297 |
| 4 | 87217.54145 | -1427217.63 | -1547298 | -91561.35768 | -5967780.607 | -6996722 | -151061 | 2471941 | 2679920 |
| 5 | 73051.31435 | -67153.4388 | 6810.277 | -4462.596864 | -8254299.161 | -9536392 | -126525 | 116309.8 | -11795.4 |
| 6 | 85012.36453 | 1327198.094 | 1630679 | 85590.32335 | -6326320.532 | -7206171 | -147241 | -2298707 | -2824337 |
| 7 | 116580.9559 | 2043906.072 | 2494714 | 124373.3248 | -1168236.047 | -1205348 | -201918 | -3540045 | -4320845 |
| 8 | 152385.6338 | 1717032.249 | 2158617 | 104866.3217 | 4586328.821 | 5416923 | -263932 | -2973900 | -3738724 |
| 9 | 174249.2188 | 513472.5399 | 794112.3 | 32527.78236 | 7999196.409 | 9274232 | -301800 | -889334 | -1375403 |

## SUMMARY OF ENTIRE FORCES EXERTED ON COMPONENTS OF TRIANGULAR TLP

summation (Fx)

| TIME | HULL 1 | HULL 2 | HULL 3 | PONTOON 1 | PONTOON 2 | PONTOON 3 | SUMMATION |
|---|---|---|---|---|---|---|---|
| 0 | -11435998.47 | -11435998.47 | 11293747.93 | -12720999.67 | 1428982.981 | 1428982.981 | -2.1E+07 |
| 1 | -12997558.38 | -12997558.38 | 14218395.83 | -14474209.39 | -239435.5857 | -239435.5857 | -2.7E+07 |
| 2 | -7434496.002 | -7434496.002 | 10402628.89 | -8259999.354 | -1713235.169 | -1713235.169 | -1.6E+07 |
| 3 | 2138780.833 | 2138780.833 | 1571749.403 | 2675281.899 | -2238624.185 | -2238624.185 | 4047345 |
| 4 | 10774007.86 | 10774007.86 | -7953733.99 | 12718220.93 | -1547298.102 | -1547298.102 | 2.3E+07 |
| 5 | 14233806.48 | 14233806.48 | -13128456.09 | 16805337.26 | 6810.276899 | 6810.276899 | 3.2E+07 |
| 6 | 10948845.02 | 10948845.02 | -11082212.27 | 12894803.18 | 1630679.417 | 1630679.417 | 2.7E+07 |
| 7 | 2394825.382 | 2394825.382 | -3018790.143 | 2926899.055 | 2494714.372 | 2494714.372 | 9687188 |
| 8 | -7272152.382 | -7272152.382 | 6743308.539 | -8061473.539 | 2158616.83 | 2158616.83 | -1.2E+07 |
| 9 | -12960901.23 | -12960901.23 | 13257698.77 | -14421592.32 | 794112.3148 | 794112.3148 | -2.5E+07 |

summation (Fy)

| TIME | HULL 1 | HULL 2 | HULL 3 | PONTOON 1 | PONTOON 2 | PONTOON 3 | SUMMATION |
|---|---|---|---|---|---|---|---|
| 0 | 505749.4165 | 505749.4165 | -656559.2643 | 6725842.013 | 8234871.395 | 8234871.395 | 2.4E+07 |
| 1 | -287002.1539 | -287002.1539 | 113002.2426 | -4434321.476 | 9343309.23 | 9343309.23 | 1.4E+07 |
| 2 | -933215.5694 | -933215.5694 | 824866.8302 | -13361405.41 | 5684258.893 | 5684258.893 | -3034452 |
| 3 | -1102945.844 | -1102945.844 | 1115569.201 | -15585241.6 | -876515.1038 | -876515.1038 | -1.8E+07 |
| 4 | -709531.7427 | -709531.7427 | 836681.9359 | -9807464.449 | -6996722.166 | -6996722.166 | -2.4E+07 |
| 5 | 46156.54731 | 46156.54731 | 130599.8728 | 1084140.513 | -9536392.201 | -9536392.201 | -1.8E+07 |
| 6 | 778278.1317 | 778278.1317 | -642164.1441 | 11394726.07 | -7206171.172 | -7206171.172 | -2103224 |
| 7 | 1113024.854 | 1113024.854 | -1087050.661 | 15799766.71 | -1205348.285 | -1205348.285 | 1.5E+07 |
| 8 | 879481.0378 | 879481.0378 | -976908.5967 | 12127117.95 | 5416923.032 | 5416923.032 | 2.4E+07 |
| 9 | 196889.9698 | 196889.9698 | -367974.5156 | 2344387.272 | 9274231.924 | 9274231.924 | 2.1E+07 |

summation (Fz)

| TIME | HULL 1 | HULL 2 | HULL 3 | PONTOON 1 | PONTOON 2 | PONTOON 3 | SUMMATION |
|---|---|---|---|---|---|---|---|
| 0 | 0 | 0 | 0 | 0 | 2474998.524 | -2474998.524 | 0 |
| 1 | 0 | 0 | 0 | 0 | -414702.4344 | 414702.4344 | 0 |
| 2 | 0 | 0 | 0 | 0 | -2967323.313 | 2967323.313 | 0 |
| 3 | 0 | 0 | 0 | 0 | -3877297.089 | 3877297.089 | 0 |
| 4 | 0 | 0 | 0 | 0 | -2679920.313 | 2679920.313 | 0 |
| 5 | 0 | 0 | 0 | 0 | 11795.39959 | -11795.39959 | 0 |
| 6 | 0 | 0 | 0 | 0 | 2824336.75 | -2824336.75 | 0 |
| 7 | 0 | 0 | 0 | 0 | 4320845.291 | -4320845.291 | 0 |
| 8 | 0 | 0 | 0 | 0 | 3738724.349 | -3738724.349 | 0 |
| 9 | 0 | 0 | 0 | 0 | 1375402.529 | -1375402.529 | 0 |

## MOMENTS IN Z AXIS EXERTED ON HULLS

Spread sheet for summary of moments ($M_x$) exerted on Hull 1, 2 and 3 from (t = 0) to (t = 9);

HULL 1 and 2:

| t (s) | $M_z$ (N.m) |
|---|---|
| 0 | -94028336 |
| 1 | -106974011 |
| 2 | -60919115 |
| 3 | 19428514 |
| 4 | 92439019.6 |
| 5 | 122025659 |
| 6 | 93793680 |
| 7 | 21240357.1 |
| 8 | -59552118 |
| 9 | -106625309 |

HULL 3:

| t (s) | $M_z$ (N.m) |
|---|---|
| 0 | 96880778.4 |
| 1 | 121884831.3 |
| 2 | 89125899.65 |
| 3 | 14315393.35 |
| 4 | -65207121.37 |
| 5 | -108011373.8 |
| 6 | -91204244.97 |
| 7 | -23920769.35 |
| 8 | 58224042.71 |
| 9 | 113688096.3 |

## SUMMARY OF MOMENTS IN Z AXIS EXERTED ON HULLS OF TRIANGULAR TLP

SUMMATION Mz

| TIME | HULL 1 | HULL 2 | HULL 3 | SUMMATION |
|---|---|---|---|---|
| 0 | -94028336.29 | -94028336.29 | 96880778.4 | -91175894.19 |
| 1 | -106974010.6 | -106974010.6 | 121884831.3 | -92063189.85 |
| 2 | -60919114.73 | -60919114.73 | 89125899.65 | -32712329.81 |
| 3 | 19428514 | 19428514 | 14315393.35 | 53172421.35 |
| 4 | 92439019.59 | 92439019.59 | -65207121.37 | 119670917.8 |
| 5 | 122025659.3 | 122025659.3 | -108011373.8 | 136039944.9 |
| 6 | 93793680.04 | 93793680.04 | -91204244.97 | 96383115.11 |
| 7 | 21240357.12 | 21240357.12 | -23920769.35 | 18559944.88 |
| 8 | -59552118.5 | -59552118.5 | 58224042.71 | -60880194.28 |
| 9 | -106625309 | -106625309 | 113688096.3 | -99562521.68 |

## APPENDIX D

## SUMMARY OF CALCULATIONS FOR WAVE SPECTRUM

| component | delta f | f | omega | omega (peak) | s(omega) | s(f) | H(f) |
|---|---|---|---|---|---|---|---|
| 1 | 0.01 | 0.025 | 0.1571 | 0.662363193 | 2.3E-168 | 1.5E-167 | 1.08E-84 |
| 2 | 0.01 | 0.035 | 0.21994 | 0.662363193 | 3.36E-42 | 2.11E-41 | 1.3E-21 |
| 3 | 0.01 | 0.045 | 0.28278 | 0.662363193 | 1.97E-14 | 1.23E-13 | 9.94E-08 |
| 4 | 0.01 | 0.055 | 0.34562 | 0.662363193 | 7.51E-06 | 4.72E-05 | 0.001944 |
| 5 | 0.01 | 0.065 | 0.40846 | 0.662363193 | 0.012083 | 0.075932 | 0.07794 |
| 6 | 0.01 | 0.075 | 0.4713 | 0.662363193 | 0.255573 | 1.606019 | 0.358443 |
| 7 | 0.01 | 0.085 | 0.53414 | 0.662363193 | 0.932958 | 5.862705 | 0.684848 |
| 8 | 0.01 | 0.095 | 0.59698 | 0.662363193 | 1.546418 | 9.717694 | 0.881712 |
| 9 | 0.01 | 0.105 | 0.65982 | 0.662363193 | 1.751497 | 11.00641 | 0.938356 |
| 10 | 0.01 | 0.115 | 0.72266 | 0.662363193 | 1.636913 | 10.28636 | 0.907143 |
| 11 | 0.01 | 0.125 | 0.7855 | 0.662363193 | 1.385551 | 8.706801 | 0.834592 |
| 12 | 0.01 | 0.135 | 0.84834 | 0.662363193 | 1.114885 | 7.005935 | 0.748649 |
| 13 | 0.01 | 0.145 | 0.91118 | 0.662363193 | 0.875417 | 5.501121 | 0.663393 |
| 14 | 0.01 | 0.155 | 0.97402 | 0.662363193 | 0.680597 | 4.276874 | 0.584936 |
| 15 | 0.01 | 0.165 | 1.03686 | 0.662363193 | 0.528222 | 3.319344 | 0.515313 |
| 16 | 0.01 | 0.175 | 1.0997 | 0.662363193 | 0.411155 | 2.583696 | 0.454638 |
| 17 | 0.01 | 0.185 | 1.16254 | 0.662363193 | 0.321793 | 2.022148 | 0.402209 |
| 18 | 0.01 | 0.195 | 1.22538 | 0.662363193 | 0.253586 | 1.593533 | 0.357047 |
| 19 | 0.01 | 0.205 | 1.28822 | 0.662363193 | 0.20134 | 1.265223 | 0.318148 |
| 20 | 0.01 | 0.215 | 1.35106 | 0.662363193 | 0.161098 | 1.012338 | 0.284582 |
| 21 | 0.01 | 0.225 | 1.4139 | 0.662363193 | 0.129892 | 0.816244 | 0.255538 |
| 22 | 0.01 | 0.235 | 1.47674 | 0.662363193 | 0.105519 | 0.663082 | 0.230318 |
| 23 | 0.01 | 0.245 | 1.53958 | 0.662363193 | 0.08634 | 0.542562 | 0.208339 |
| 24 | 0.01 | 0.255 | 1.60242 | 0.662363193 | 0.071137 | 0.447023 | 0.189108 |
| 25 | 0.01 | 0.265 | 1.66526 | 0.662363193 | 0.058996 | 0.370733 | 0.172217 |
| 26 | 0.01 | 0.275 | 1.7281 | 0.662363193 | 0.049234 | 0.309384 | 0.157324 |
| 27 | 0.01 | 0.285 | 1.79094 | 0.662363193 | 0.04133 | 0.259715 | 0.144143 |
| 28 | 0.01 | 0.295 | 1.85378 | 0.662363193 | 0.034889 | 0.21924 | 0.132436 |

## APPENDIX E

## SUMMARY OF CALCULATIONS FOR WAVE PROFILE

The calculation for wave profile is calculated for 28 components of frequencies for time ranging from 0s to 100s. Table below shows the summary of raw data for the graph of wave profile.

HULL 1 and 2:

| f | 0.025 | 0.035 | 0.045 | 0.055 | 0.065 | 0.075 | 0.085 | 0.095 | 0.105 | 0.115 | 0.125 | 0.135 | 0.145 | | 0.255 | 0.265 | 0.275 | 0.285 | 0.295 | |
|---|---|---|---|---|---|---|---|---|---|---|---|---|---|---|---|---|---|---|---|---|
| component | 3 | 4 | 5 | 6 | 7 | 8 | 9 | 10 | 11 | 12 | 13 | 14 | 15 | | 26 | 27 | 28 | 29 | 30 | |
| H(f) | 0.000 | 0.000 | 0.000 | 0.002 | 0.078 | 0.358 | 0.685 | 0.882 | 0.938 | 0.907 | 0.835 | 0.749 | 0.663 | | 0.189 | 0.172 | 0.157 | 0.144 | 0.132 | |
| t | η1 | η2 | η3 | η4 | η5 | η6 | η7 | η8 | η9 | η 10 | η 11 | η 12 | η 13 | ..... | η 24 | η 25 | η 26 | η 27 | η 28 | total η |
| 0 | 0.00 | 0.00 | 0.00 | 0.00 | 0.02 | -0.04 | -0.22 | -0.41 | 0.23 | -0.41 | 0.28 | 0.17 | 0.24 | | 0.09 | 0.07 | -0.07 | -0.05 | -0.06 | -0.40 |
| 1 | 0.00 | 0.00 | 0.00 | 0.00 | 0.00 | 0.04 | -0.06 | -0.43 | 0.43 | -0.17 | 0.42 | 0.36 | -0.04 | | -0.03 | 0.04 | -0.02 | 0.06 | 0.03 | 0.24 |
| 2 | 0.00 | 0.00 | 0.00 | 0.00 | -0.02 | 0.12 | 0.12 | -0.29 | 0.45 | 0.15 | 0.31 | 0.31 | -0.28 | | -0.09 | -0.08 | 0.08 | 0.02 | 0.04 | 0.60 |
| 3 | 0.00 | 0.00 | 0.00 | 0.00 | -0.03 | 0.17 | 0.27 | -0.06 | 0.29 | 0.39 | 0.02 | 0.05 | -0.31 | | 0.04 | -0.03 | 0.00 | -0.07 | -0.06 | 0.56 |
| 4 | 0.00 | 0.00 | 0.00 | 0.00 | -0.04 | 0.18 | 0.34 | 0.20 | 0.00 | 0.44 | -0.28 | -0.25 | -0.10 | | 0.08 | 0.08 | -0.08 | 0.01 | -0.01 | 0.55 |
| 5 | 0.00 | 0.00 | 0.00 | 0.00 | -0.04 | 0.15 | 0.32 | 0.38 | -0.29 | 0.27 | -0.42 | -0.37 | 0.19 | | -0.05 | 0.01 | 0.03 | 0.07 | 0.07 | 0.36 |
| 6 | 0.00 | 0.00 | 0.00 | 0.00 | -0.03 | 0.09 | 0.21 | 0.44 | -0.45 | -0.03 | -0.31 | -0.25 | 0.33 | | -0.08 | -0.09 | 0.07 | -0.04 | -0.03 | -0.21 |
| 7 | 0.00 | 0.00 | 0.00 | 0.00 | -0.02 | 0.01 | 0.04 | 0.34 | -0.43 | -0.32 | -0.02 | 0.05 | 0.22 | | 0.05 | 0.01 | -0.05 | -0.05 | -0.05 | -0.57 |
| 8 | 0.00 | 0.00 | 0.00 | 0.00 | -0.01 | -0.07 | -0.14 | 0.13 | -0.23 | -0.45 | 0.28 | 0.31 | -0.07 | | 0.08 | 0.08 | -0.05 | 0.06 | 0.05 | -0.46 |
| 9 | 0.00 | 0.00 | 0.00 | 0.00 | 0.01 | -0.14 | -0.28 | -0.13 | 0.07 | -0.35 | 0.42 | 0.36 | -0.30 | | -0.06 | -0.02 | 0.07 | 0.02 | 0.02 | -0.36 |
| 10 | 0.00 | 0.00 | 0.00 | 0.00 | 0.02 | -0.17 | -0.34 | -0.35 | 0.34 | -0.08 | 0.31 | 0.17 | -0.30 | | -0.08 | -0.08 | 0.03 | -0.07 | -0.07 | -0.35 |
| 11 | 0.00 | 0.00 | 0.00 | 0.00 | 0.03 | -0.17 | -0.31 | -0.44 | 0.47 | 0.24 | 0.02 | -0.14 | -0.07 | | 0.06 | 0.04 | -0.08 | 0.01 | 0.02 | -0.35 |
| 12 | 0.00 | 0.00 | 0.00 | 0.00 | 0.04 | -0.14 | -0.19 | -0.38 | 0.40 | 0.43 | -0.28 | -0.35 | 0.21 | | 0.07 | 0.07 | -0.01 | 0.07 | 0.06 | -0.65 |
| ..... | | | | | | | | | | | | | | | | | | | | |
| 100 | 0.00 | 0.00 | 0.00 | 0.00 | -0.02 | 0.04 | 0.22 | 0.41 | -0.23 | 0.41 | -0.29 | -0.18 | -0.24 | | -0.09 | -0.07 | 0.07 | 0.05 | 0.06 | 0.12 |

HULL 3:

| f | 0.025 | 0.035 | 0.045 | 0.055 | 0.065 | 0.075 | 0.085 | 0.095 | 0.105 | 0.115 | 0.125 | 0.135 | 0.145 | | 0.255 | 0.265 | 0.275 | 0.285 | 0.295 | |
|---|---|---|---|---|---|---|---|---|---|---|---|---|---|---|---|---|---|---|---|---|
| component | 3 | 4 | 5 | 6 | 7 | 8 | 9 | 10 | 11 | 12 | 13 | 14 | 15 | | 26 | 27 | 28 | 29 | 30 | |
| H(f) | 0.000 | 0.000 | 0.000 | 0.002 | 0.078 | 0.358 | 0.685 | 0.882 | 0.938 | 0.907 | 0.835 | 0.749 | 0.663 | | 0.189 | 0.172 | 0.157 | 0.144 | 0.132 | |
| t | η1 | η2 | η3 | η4 | η5 | η6 | η7 | η8 | η9 | η10 | η11 | η12 | η13 | ..... | η24 | η25 | η26 | η27 | η28 | total η |
| 0 | 0.00 | 0.00 | 0.00 | 0.00 | -0.02 | 0.04 | 0.23 | 0.41 | -0.22 | 0.41 | -0.28 | -0.17 | -0.24 | | -0.09 | -0.07 | 0.07 | 0.05 | 0.06 | 0.38 |
| 1 | 0.00 | 0.00 | 0.00 | 0.00 | 0.00 | -0.04 | 0.07 | 0.43 | -0.43 | 0.18 | -0.42 | -0.36 | 0.03 | | 0.03 | -0.04 | 0.02 | -0.06 | -0.03 | -0.24 |
| 2 | 0.00 | 0.00 | 0.00 | 0.00 | 0.02 | -0.11 | -0.11 | 0.30 | -0.46 | -0.14 | -0.31 | -0.31 | 0.28 | | 0.09 | 0.08 | -0.08 | -0.02 | -0.04 | -0.57 |
| 3 | 0.00 | 0.00 | 0.00 | 0.00 | 0.03 | -0.16 | -0.26 | 0.06 | -0.29 | -0.39 | -0.02 | -0.05 | 0.31 | | -0.04 | 0.03 | 0.00 | 0.07 | 0.06 | -0.52 |
| 4 | 0.00 | 0.00 | 0.00 | 0.00 | 0.04 | -0.18 | -0.34 | -0.19 | 0.00 | -0.45 | 0.28 | 0.25 | 0.10 | | -0.08 | -0.08 | 0.08 | -0.01 | 0.01 | -0.49 |
| 5 | 0.00 | 0.00 | 0.00 | 0.00 | 0.04 | -0.15 | -0.32 | -0.38 | 0.28 | -0.28 | 0.42 | 0.37 | -0.19 | | 0.04 | -0.01 | -0.03 | -0.07 | -0.07 | -0.32 |
| 6 | 0.00 | 0.00 | 0.00 | 0.00 | 0.03 | -0.10 | -0.21 | -0.44 | 0.45 | 0.03 | 0.31 | 0.25 | -0.33 | | 0.08 | 0.09 | -0.07 | 0.04 | 0.03 | 0.23 |
| 7 | 0.00 | 0.00 | 0.00 | 0.00 | 0.02 | -0.02 | -0.04 | -0.35 | 0.43 | 0.32 | 0.02 | -0.04 | -0.22 | | -0.05 | -0.01 | 0.05 | 0.05 | 0.05 | 0.57 |
| 8 | 0.00 | 0.00 | 0.00 | 0.00 | 0.01 | 0.07 | 0.13 | -0.13 | 0.23 | 0.45 | -0.28 | -0.31 | 0.06 | | -0.08 | -0.08 | 0.05 | -0.06 | -0.05 | 0.44 |
| 9 | 0.00 | 0.00 | 0.00 | 0.00 | 0.00 | 0.14 | 0.28 | 0.13 | -0.07 | 0.36 | -0.42 | -0.36 | 0.30 | | 0.05 | 0.02 | -0.06 | -0.02 | -0.02 | 0.32 |
| 10 | 0.00 | 0.00 | 0.00 | 0.00 | -0.02 | 0.17 | 0.34 | 0.34 | -0.34 | 0.08 | -0.31 | -0.17 | 0.30 | | 0.08 | 0.08 | -0.03 | 0.07 | 0.07 | 0.29 |
| 11 | 0.00 | 0.00 | 0.00 | 0.00 | -0.03 | 0.17 | 0.31 | 0.44 | -0.47 | -0.23 | -0.02 | 0.14 | 0.07 | | -0.06 | -0.04 | 0.08 | -0.01 | -0.02 | 0.30 |
| 12 | 0.00 | 0.00 | 0.00 | 0.00 | -0.04 | 0.14 | 0.19 | 0.38 | -0.40 | -0.43 | 0.28 | 0.35 | -0.21 | | -0.07 | -0.07 | 0.01 | -0.07 | -0.06 | 0.62 |
| ..... | | | | | | | | | | | | | | | | | | | | |
| 100 | 0.00 | 0.00 | 0.00 | 0.00 | 0.02 | -0.04 | -0.23 | -0.41 | 0.23 | -0.41 | 0.28 | 0.17 | 0.24 | | 0.09 | 0.07 | -0.07 | -0.05 | -0.06 | -0.09 |

## APPENDIX F

## SURGE PARAMETERS

| | | |
|---|---|---|
| Pretension / Weight (%) | = | 27.3% |
| K surge | = | 195772.621 N/m |
| M surge | = | 143012691kg |
| C | = | 529131.0743 kg/s |
| Draft | = | 42.25 m |

| F (Hz) | T (s) | omega | Fx (N) | RAO Surge |
|---|---|---|---|---|
| 0.025 | 40.000 | 0.157 | 2550368.078 | 1.530 |
| 0.035 | 28.571 | 0.220 | 2550368.078 | 0.759 |
| 0.045 | 22.222 | 0.283 | 2550367.855 | 0.454 |
| 0.055 | 18.182 | 0.346 | 2550668.776 | 0.302 |
| 0.065 | 15.385 | 0.408 | 2787860.737 | 0.236 |
| 0.075 | 13.333 | 0.471 | 4691003.719 | 0.297 |
| 0.085 | 11.765 | 0.534 | 6945744.745 | 0.342 |
| 0.095 | 10.526 | 0.597 | 7805598.232 | 0.307 |
| 0.105 | 9.524 | 0.660 | 7401346.393 | 0.238 |
| 0.115 | 8.696 | 0.723 | 6699896.333 | 0.180 |
| 0.125 | 8.000 | 0.786 | 6630132.952 | 0.151 |
| 0.135 | 7.407 | 0.848 | 6844416.324 | 0.133 |
| 0.145 | 6.897 | 0.911 | 7664563.915 | 0.129 |
| 0.155 | 6.452 | 0.974 | 7510163.116 | 0.111 |

| F (Hz) | T (s) | omega | Fx (N) | RAO Surge |
|---|---|---|---|---|
| 0.165 | 6.061 | 1.037 | 6604689.736 | 0.086 |
| 0.175 | 5.714 | 1.100 | 5890671.748 | 0.068 |
| 0.185 | 5.405 | 1.163 | 4617711.649 | 0.048 |
| 0.195 | 5.128 | 1.225 | 3535598.325 | 0.033 |
| 0.205 | 4.878 | 1.288 | 3766235.110 | 0.032 |
| 0.215 | 4.651 | 1.351 | 4390515.601 | 0.034 |
| 0.225 | 4.444 | 1.414 | 4474846.127 | 0.031 |
| 0.235 | 4.255 | 1.477 | 4139262.709 | 0.027 |
| 0.245 | 4.082 | 1.540 | 3423321.458 | 0.020 |
| 0.255 | 3.922 | 1.602 | 2953399.246 | 0.016 |
| 0.265 | 3.774 | 1.665 | 3333216.828 | 0.017 |
| 0.275 | 3.636 | 1.728 | 3605547.161 | 0.017 |
| 0.285 | 3.509 | 1.791 | 3326405.060 | 0.015 |
| 0.295 | 3.390 | 1.854 | 3008256.889 | 0.012 |

| | | |
|---|---|---|
| Pretension / Weight (%) | = | 17.3% |
| K surge | = | 123141.969 N/m |
| M surge | = | 136013000 kg |
| C | = | 409254.305 kg/s |
| Draft | = | 35 m |

| F (Hz) | T (s) | Omega | Fx (N) | RAO surge |
|---|---|---|---|---|
| 0.025 | 40.000 | 0.1571 | 2500368.078 | 1.546 |
| 0.035 | 28.571 | 0.21994 | 2500368.078 | 0.774 |
| 0.045 | 22.222 | 0.28278 | 2500367.855 | 0.465 |
| 0.055 | 18.182 | 0.34562 | 2500668.776 | 0.310 |
| 0.065 | 15.385 | 0.40846 | 2737860.737 | 0.243 |
| 0.075 | 13.333 | 0.4713 | 4641003.719 | 0.308 |
| 0.085 | 11.765 | 0.53414 | 6895744.745 | 0.357 |
| 0.095 | 10.526 | 0.59698 | 7755598.232 | 0.321 |
| 0.105 | 9.524 | 0.65982 | 7351346.393 | 0.249 |
| 0.115 | 8.696 | 0.72266 | 6649896.333 | 0.188 |
| 0.125 | 8.000 | 0.7855 | 6580132.952 | 0.157 |
| 0.135 | 7.407 | 0.84834 | 6794416.324 | 0.139 |
| 0.145 | 6.897 | 0.91118 | 7614563.915 | 0.135 |
| 0.155 | 6.452 | 0.97402 | 7460163.116 | 0.116 |

| F (Hz) | T (s) | Omega | Fx (N) | RAO surge |
|---|---|---|---|---|
| 0.165 | 6.061 | 1.03686 | 6554689.736 | 0.090 |
| 0.175 | 5.714 | 1.0997 | 5840671.748 | 0.071 |
| 0.185 | 5.405 | 1.16254 | 4567711.649 | 0.050 |
| 0.195 | 5.128 | 1.22538 | 3485598.325 | 0.034 |
| 0.205 | 4.878 | 1.28822 | 3716235.110 | 0.033 |
| 0.215 | 4.651 | 1.35106 | 4340515.601 | 0.035 |
| 0.225 | 4.444 | 1.4139 | 4424846.127 | 0.033 |
| 0.235 | 4.255 | 1.47674 | 4089262.709 | 0.028 |
| 0.245 | 4.082 | 1.53958 | 3373321.458 | 0.021 |
| 0.255 | 3.922 | 1.60242 | 2903399.246 | 0.017 |
| 0.265 | 3.774 | 1.66526 | 3283216.828 | 0.017 |
| 0.275 | 3.636 | 1.7281 | 3555547.161 | 0.018 |
| 0.285 | 3.509 | 1.79094 | 3276405.060 | 0.015 |
| 0.295 | 3.390 | 1.85378 | 2958256.889 | 0.013 |

| | | |
|---|---|---|
| Pretension / Weight (%) | = | 7.3% |
| K surge | = | 51593.93265 N/m |
| M surge | = | 59012691 kg |
| C | = | 174490.5964 kg/s |
| Draft | = | 27.75 m |

| F (Hz) | T (s) | omega | Fx (N) | RAO Surge |
|---|---|---|---|---|
| 0.025 | 40.000 | 0.157 | 1501145.563 | 2.136 |
| 0.035 | 28.571 | 0.220 | 1500756.815 | 1.070 |
| 0.045 | 22.222 | 0.283 | 1500756.592 | 0.643 |
| 0.055 | 18.182 | 0.346 | 1501057.513 | 0.429 |
| 0.065 | 15.385 | 0.408 | 1738249.474 | 0.355 |
| 0.075 | 13.333 | 0.471 | 3641392.456 | 0.558 |
| 0.085 | 11.765 | 0.534 | 5896133.482 | 0.702 |
| 0.095 | 10.526 | 0.597 | 6755986.969 | 0.644 |
| 0.105 | 9.524 | 0.660 | 6351735.131 | 0.495 |
| 0.115 | 8.696 | 0.723 | 5650285.071 | 0.367 |
| 0.125 | 8.000 | 0.786 | 5580521.690 | 0.307 |
| 0.135 | 7.407 | 0.848 | 5794805.061 | 0.273 |
| 0.145 | 6.897 | 0.911 | 6614952.652 | 0.270 |
| 0.155 | 6.452 | 0.974 | 6460551.854 | 0.231 |

| F (Hz) | T (s) | omega | Fx (N) | RAO Surge |
|---|---|---|---|---|
| 0.165 | 6.061 | 1.037 | 5555078.474 | 0.175 |
| 0.175 | 5.714 | 1.100 | 4841060.486 | 0.136 |
| 0.185 | 5.405 | 1.163 | 3568100.386 | 0.090 |
| 0.195 | 5.128 | 1.225 | 2485987.062 | 0.056 |
| 0.205 | 4.878 | 1.288 | 2716623.847 | 0.056 |
| 0.215 | 4.651 | 1.351 | 3340904.338 | 0.062 |
| 0.225 | 4.444 | 1.414 | 3425234.865 | 0.058 |
| 0.235 | 4.255 | 1.477 | 3089651.446 | 0.048 |
| 0.245 | 4.082 | 1.540 | 2373710.196 | 0.034 |
| 0.255 | 3.922 | 1.602 | 1903787.983 | 0.025 |
| 0.265 | 3.774 | 1.665 | 2283605.566 | 0.028 |
| 0.275 | 3.636 | 1.728 | 2555935.899 | 0.029 |
| 0.285 | 3.509 | 1.791 | 2276793.798 | 0.024 |
| 0.295 | 3.390 | 1.854 | 1958645.627 | 0.019 |

## APPENDIX G

## HEAVE PARAMETERS

| | | |
|---|---|---|
| Pretension / Weight (%) | = | 27.3% |
| K heave | = | 1209000000 N/m |
| M heave | = | 124742000 kg |
| C | = | 38834659.5 kg/s |
| Draft | = | 42.25 m |

| F (Hz) | T (s) | omega | Fy (N) | RAO Heave |
|---|---|---|---|---|
| 0.025 | 40.000 | 0.157 | 0.000 | 0.0000000 |
| 0.035 | 28.571 | 0.220 | 0.000 | 0.0000000 |
| 0.045 | 22.222 | 0.283 | 0.610 | 0.0000000 |
| 0.055 | 18.182 | 0.346 | 12819.519 | 0.0000215 |
| 0.065 | 15.385 | 0.408 | 570418.109 | 0.0009601 |
| 0.075 | 13.333 | 0.471 | 2665438.511 | 0.0045122 |
| 0.085 | 11.765 | 0.534 | 4872739.748 | 0.0083040 |
| 0.095 | 10.526 | 0.597 | 5603556.792 | 0.0096217 |
| 0.105 | 9.524 | 0.660 | 4905387.993 | 0.0084944 |
| 0.115 | 8.696 | 0.723 | 3595546.941 | 0.0062848 |
| 0.125 | 8.000 | 0.786 | 2084513.996 | 0.0036814 |
| 0.135 | 7.407 | 0.848 | 1250503.363 | 0.0022336 |
| 0.145 | 6.897 | 0.911 | 878514.724 | 0.0015886 |
| 0.155 | 6.452 | 0.974 | 822478.501 | 0.0015073 |

| F (Hz) | T (s) | omega | Fy (N) | RAO Heave |
|---|---|---|---|---|
| 0.165 | 6.061 | 1.037 | 753977.370 | 0.0014019 |
| 0.175 | 5.714 | 1.100 | 561480.856 | 0.0010604 |
| 0.185 | 5.405 | 1.163 | 385058.077 | 0.0007395 |
| 0.195 | 5.128 | 1.225 | 236433.613 | 0.0004623 |
| 0.205 | 4.878 | 1.288 | 113902.406 | 0.0002271 |
| 0.215 | 4.651 | 1.351 | 75900.577 | 0.0001545 |
| 0.225 | 4.444 | 1.414 | 55104.281 | 0.0001147 |
| 0.235 | 4.255 | 1.477 | 36648.619 | 0.0000781 |
| 0.245 | 4.082 | 1.540 | 23760.725 | 0.0000519 |
| 0.255 | 3.922 | 1.602 | 10721.106 | 0.0000241 |
| 0.265 | 3.774 | 1.665 | 6106.828 | 0.0000141 |
| 0.275 | 3.636 | 1.728 | 3537.801 | 0.0000084 |
| 0.285 | 3.509 | 1.791 | 2030.943 | 0.0000050 |
| 0.295 | 3.390 | 1.854 | 892.126 | 0.0000023 |

| | | |
|---|---|---|
| Pretension / Weight (%) | = | 17.3% |
| K heave | = | 1209000000 N/m |
| M heave | = | 124742000 kg |
| C | = | 38834659.5 kg/s |
| Draft | = | 35 m |

| F (Hz) | T (s) | Omega | Fy (N) | RAO heave |
|---|---|---|---|---|
| 0.025 | 40.000 | 0.1571 | 0.000 | 0.0000000 |
| 0.035 | 28.571 | 0.21994 | 0.000 | 0.0000000 |
| 0.045 | 22.222 | 0.28278 | 0.610 | 0.0000000 |
| 0.055 | 18.182 | 0.34562 | 13319.519 | 0.0000223 |
| 0.065 | 15.385 | 0.40846 | 570918.109 | 0.0009609 |
| 0.075 | 13.333 | 0.4713 | 2665938.511 | 0.0045131 |
| 0.085 | 11.765 | 0.53414 | 4873239.748 | 0.0083048 |
| 0.095 | 10.526 | 0.59698 | 5604056.792 | 0.0096226 |
| 0.105 | 9.524 | 0.65982 | 4905887.993 | 0.0084952 |
| 0.115 | 8.696 | 0.72266 | 3596046.941 | 0.0062857 |
| 0.125 | 8.000 | 0.7855 | 2085013.996 | 0.0036823 |
| 0.135 | 7.407 | 0.84834 | 1251003.363 | 0.0022345 |
| 0.145 | 6.897 | 0.91118 | 879014.724 | 0.0015895 |
| 0.155 | 6.452 | 0.97402 | 822978.501 | 0.0015082 |

| F (Hz) | T (s) | Omega | Fy (N) | RAO heave |
|---|---|---|---|---|
| 0.165 | 6.061 | 1.03686 | 754477.370 | 0.0014028 |
| 0.175 | 5.714 | 1.0997 | 561980.856 | 0.0010613 |
| 0.185 | 5.405 | 1.16254 | 385558.077 | 0.0007405 |
| 0.195 | 5.128 | 1.22538 | 236933.613 | 0.0004633 |
| 0.205 | 4.878 | 1.28822 | 114402.406 | 0.0002281 |
| 0.215 | 4.651 | 1.35106 | 76400.577 | 0.0001555 |
| 0.225 | 4.444 | 1.4139 | 55604.281 | 0.0001157 |
| 0.235 | 4.255 | 1.47674 | 37148.619 | 0.0000791 |
| 0.245 | 4.082 | 1.53958 | 24260.725 | 0.0000530 |
| 0.255 | 3.922 | 1.60242 | 11221.106 | 0.0000252 |
| 0.265 | 3.774 | 1.66526 | 6606.828 | 0.0000153 |
| 0.275 | 3.636 | 1.7281 | 4037.801 | 0.0000096 |
| 0.285 | 3.509 | 1.79094 | 2530.943 | 0.0000062 |
| 0.295 | 3.390 | 1.85378 | 1392.126 | 0.0000036 |

| | | |
|---|---|---|
| Pretension / Weight (%) | = | 7.3% |
| K heave | = | 1209000000 N/m |
| M heave | = | 124742000 kg |
| C | = | 38834659.5 kg/s |
| Draft | = | 27.75 m |

| F (Hz) | T (s) | omega | Fy (N) | RAO Heave |
|---|---|---|---|---|
| 0.025 | 40.000 | 0.157 | 0.000 | 0.0000000 |
| 0.035 | 28.571 | 0.220 | 0.000 | 0.0000000 |
| 0.045 | 22.222 | 0.283 | 0.610 | 0.0000000 |
| 0.055 | 18.182 | 0.346 | 13819.519 | 0.0000231 |
| 0.065 | 15.385 | 0.408 | 571418.109 | 0.0009617 |
| 0.075 | 13.333 | 0.471 | 2666438.511 | 0.0045139 |
| 0.085 | 11.765 | 0.534 | 4873739.748 | 0.0083057 |
| 0.095 | 10.526 | 0.597 | 5604556.792 | 0.0096234 |
| 0.105 | 9.524 | 0.660 | 4906387.993 | 0.0084961 |
| 0.115 | 8.696 | 0.723 | 3596546.941 | 0.0062866 |
| 0.125 | 8.000 | 0.786 | 2085513.996 | 0.0036832 |
| 0.135 | 7.407 | 0.848 | 1251503.363 | 0.0022354 |
| 0.145 | 6.897 | 0.911 | 879514.724 | 0.0015904 |
| 0.155 | 6.452 | 0.974 | 823478.501 | 0.0015092 |

| F (Hz) | T (s) | omega | Fy (N) | RAO Heave |
|---|---|---|---|---|
| 0.165 | 6.061 | 1.037 | 754977.3702 | 0.0014038 |
| 0.175 | 5.714 | 1.100 | 562480.8561 | 0.0010623 |
| 0.185 | 5.405 | 1.163 | 386058.0774 | 0.0007414 |
| 0.195 | 5.128 | 1.225 | 237433.6133 | 0.0004643 |
| 0.205 | 4.878 | 1.288 | 114902.4061 | 0.0002291 |
| 0.215 | 4.651 | 1.351 | 76900.57689 | 0.0001565 |
| 0.225 | 4.444 | 1.414 | 56104.28142 | 0.0001167 |
| 0.235 | 4.255 | 1.477 | 37648.61926 | 0.0000802 |
| 0.245 | 4.082 | 1.540 | 24760.72479 | 0.0000541 |
| 0.255 | 3.922 | 1.602 | 11721.10613 | 0.0000263 |
| 0.265 | 3.774 | 1.665 | 7106.828405 | 0.0000164 |
| 0.275 | 3.636 | 1.728 | 4537.801383 | 0.0000108 |
| 0.285 | 3.509 | 1.791 | 3030.942826 | 0.0000075 |
| 0.295 | 3.390 | 1.854 | 1892.125708 | 0.0000048 |

## APPENDIX H

## PITCH PARAMETERS

| | | |
|---|---|---|
| Pretension / Weight (%) | = | 27.3% |
| K pitch | = | 1445360936507 N.m/rad |
| M pitch | = | 2.2882E+11 kg.m$^2$ |
| C | = | 5.75E+10 N/rad$^{0.5}$ |
| Draft | = | 42.25 m |

| F (Hz) | T (s) | omega | Mz (N.m) | RAO Pitch |
|---|---|---|---|---|
| 0.025 | 40.000 | 0.157 | 19484206.055 | 0.000027 |
| 0.035 | 28.571 | 0.220 | 19484206.055 | 0.000027 |
| 0.045 | 22.222 | 0.283 | 19484207.556 | 0.000027 |
| 0.055 | 18.182 | 0.346 | 19544182.214 | 0.000028 |
| 0.065 | 15.385 | 0.408 | 22274751.885 | 0.000032 |
| 0.075 | 13.333 | 0.471 | 27058158.018 | 0.000039 |
| 0.085 | 11.765 | 0.534 | 41886990.153 | 0.000061 |
| 0.095 | 10.526 | 0.597 | 45129094.700 | 0.000066 |
| 0.105 | 9.524 | 0.660 | 36101581.352 | 0.000054 |
| 0.115 | 8.696 | 0.723 | 36101581.352 | 0.000054 |
| 0.125 | 8.000 | 0.786 | 39102573.773 | 0.000060 |
| 0.135 | 7.407 | 0.848 | 42835864.895 | 0.000067 |
| 0.145 | 6.897 | 0.911 | 44274358.151 | 0.000070 |
| 0.155 | 6.452 | 0.974 | 40841608.835 | 0.000066 |

| F (Hz) | T (s) | omega | Mz (N.m) | RAO Pitch |
|---|---|---|---|---|
| 0.165 | 6.061 | 1.037 | 34715137.5 | 0.000058 |
| 0.175 | 5.714 | 1.100 | 29448619.2 | 0.000050 |
| 0.185 | 5.405 | 1.163 | 24960476.6 | 0.000044 |
| 0.195 | 5.128 | 1.225 | 21442226.2 | 0.000039 |
| 0.205 | 4.878 | 1.288 | 21625514.5 | 0.000040 |
| 0.215 | 4.651 | 1.351 | 22107876.8 | 0.000043 |
| 0.225 | 4.444 | 1.414 | 21198019.3 | 0.000043 |
| 0.235 | 4.255 | 1.477 | 20369570 | 0.000043 |
| 0.245 | 4.082 | 1.540 | 19739023.2 | 0.000044 |
| 0.255 | 3.922 | 1.602 | 19488086.9 | 0.000045 |
| 0.265 | 3.774 | 1.665 | 19750545.8 | 0.000048 |
| 0.275 | 3.636 | 1.728 | 20110747.7 | 0.000052 |
| 0.285 | 3.509 | 1.791 | 20213924.9 | 0.000056 |
| 0.295 | 3.390 | 1.854 | 19941887.9 | 0.000060 |

| | | |
|---|---|---|
| Pretension / Weight (%) | = | 7.3% |
| K pitch | = | 596413073938 N.m/rad |
| M pitch | = | 9.44E+10 $kg.m^2$ |
| C | = | 2.37E+10 $N/rad^{0.5}$ |
| Draft | = | 27.75 m |

| F (Hz) | T (s) | omega | Mz (N.m) | RAO Pitch |
|---|---|---|---|---|
| 0.025 | 40.000 | 0.157 | 8084206.055 | 0.000027 |
| 0.035 | 28.571 | 0.220 | 8084206.055 | 0.000027 |
| 0.045 | 22.222 | 0.283 | 8084207.556 | 0.000027 |
| 0.055 | 18.182 | 0.346 | 8144182.214 | 0.000028 |
| 0.065 | 15.385 | 0.408 | 10874751.885 | 0.000037 |
| 0.075 | 13.333 | 0.471 | 15658158.018 | 0.000054 |
| 0.085 | 11.765 | 0.534 | 30486990.153 | 0.000107 |
| 0.095 | 10.526 | 0.597 | 33729094.700 | 0.000120 |
| 0.105 | 9.524 | 0.660 | 24701581.352 | 0.000089 |
| 0.115 | 8.696 | 0.723 | 24701581.352 | 0.000090 |
| 0.125 | 8.000 | 0.786 | 27702573.773 | 0.000103 |
| 0.135 | 7.407 | 0.848 | 31435864.895 | 0.000119 |
| 0.145 | 6.897 | 0.911 | 32874358.151 | 0.000127 |
| 0.155 | 6.452 | 0.974 | 29441608.835 | 0.000116 |

| F (Hz) | T (s) | omega | Mz (N.m) | RAO Pitch |
|---|---|---|---|---|
| 0.165 | 6.061 | 1.037 | 23315137.462 | 0.000094 |
| 0.175 | 5.714 | 1.100 | 18048619.152 | 0.000075 |
| 0.185 | 5.405 | 1.163 | 13560476.550 | 0.000058 |
| 0.195 | 5.128 | 1.225 | 10042226.228 | 0.000044 |
| 0.205 | 4.878 | 1.288 | 10225514.530 | 0.000046 |
| 0.215 | 4.651 | 1.351 | 10707876.777 | 0.000050 |
| 0.225 | 4.444 | 1.414 | 9798019.289 | 0.000048 |
| 0.235 | 4.255 | 1.477 | 8969570.016 | 0.000046 |
| 0.245 | 4.082 | 1.540 | 8339023.243 | 0.000045 |
| 0.255 | 3.922 | 1.602 | 8088086.856 | 0.000045 |
| 0.265 | 3.774 | 1.665 | 8350545.805 | 0.000050 |
| 0.275 | 3.636 | 1.728 | 8710747.717 | 0.000055 |
| 0.285 | 3.509 | 1.791 | 8813924.856 | 0.000059 |
| 0.295 | 3.390 | 1.854 | 8541887.888 | 0.000062 |

## APPENDIX I

## RANDOM PICTURES TAKEN DURING LABORATORY MODEL TESTING

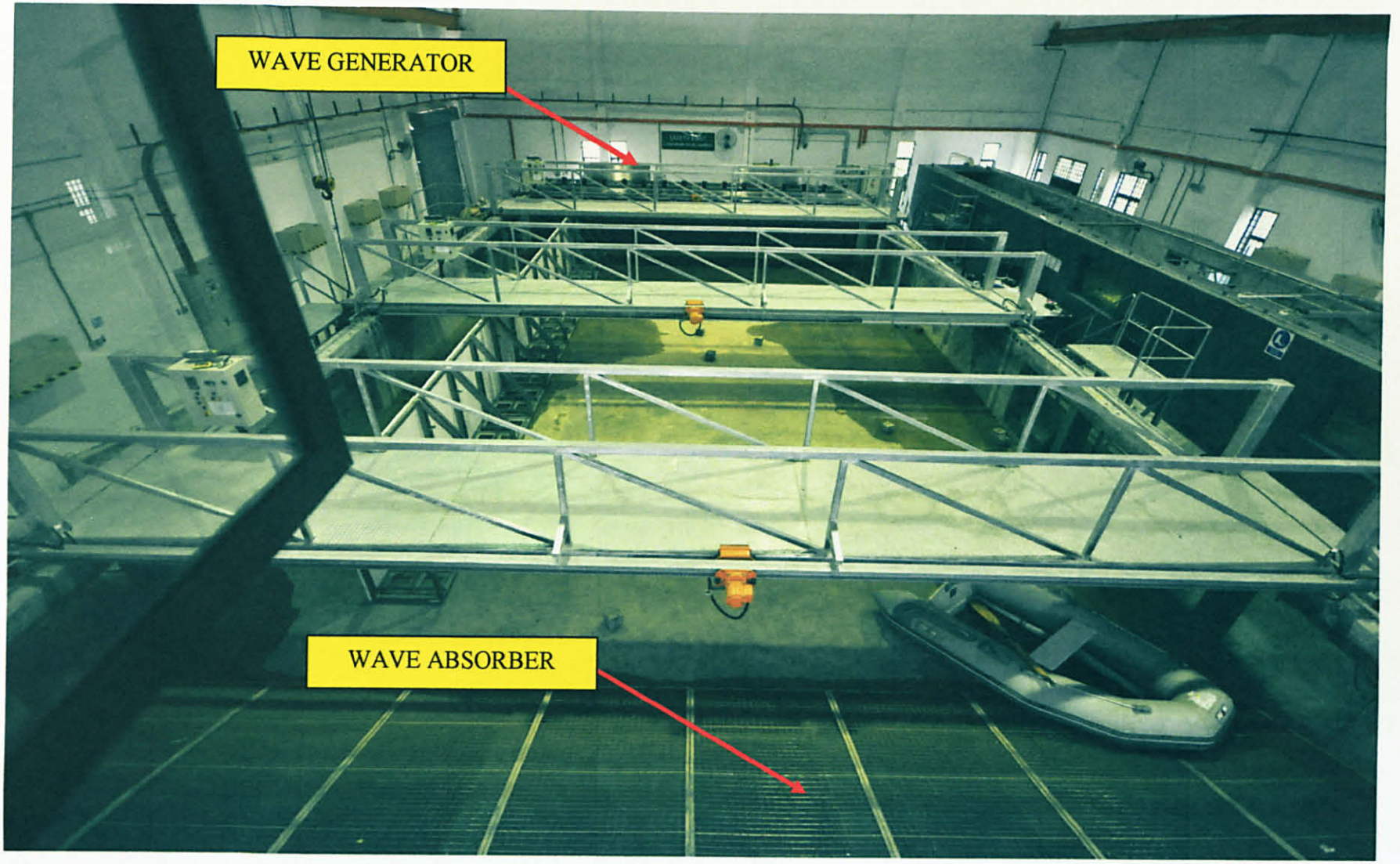


THE WAVE TANK

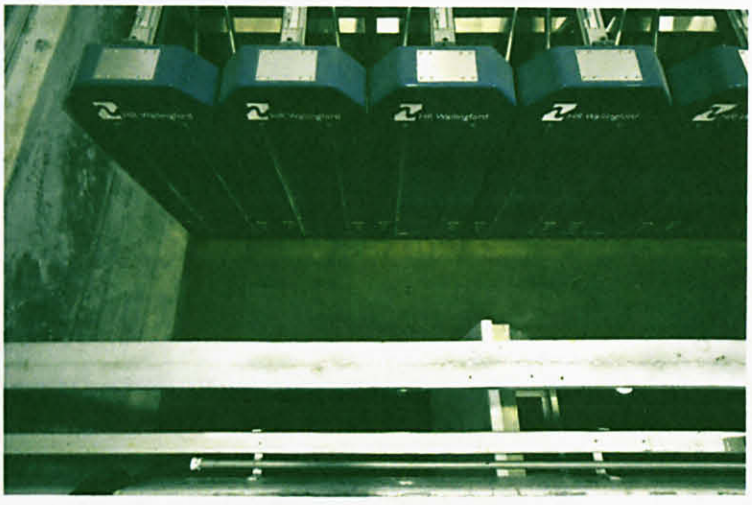

WAVE GENERATOR

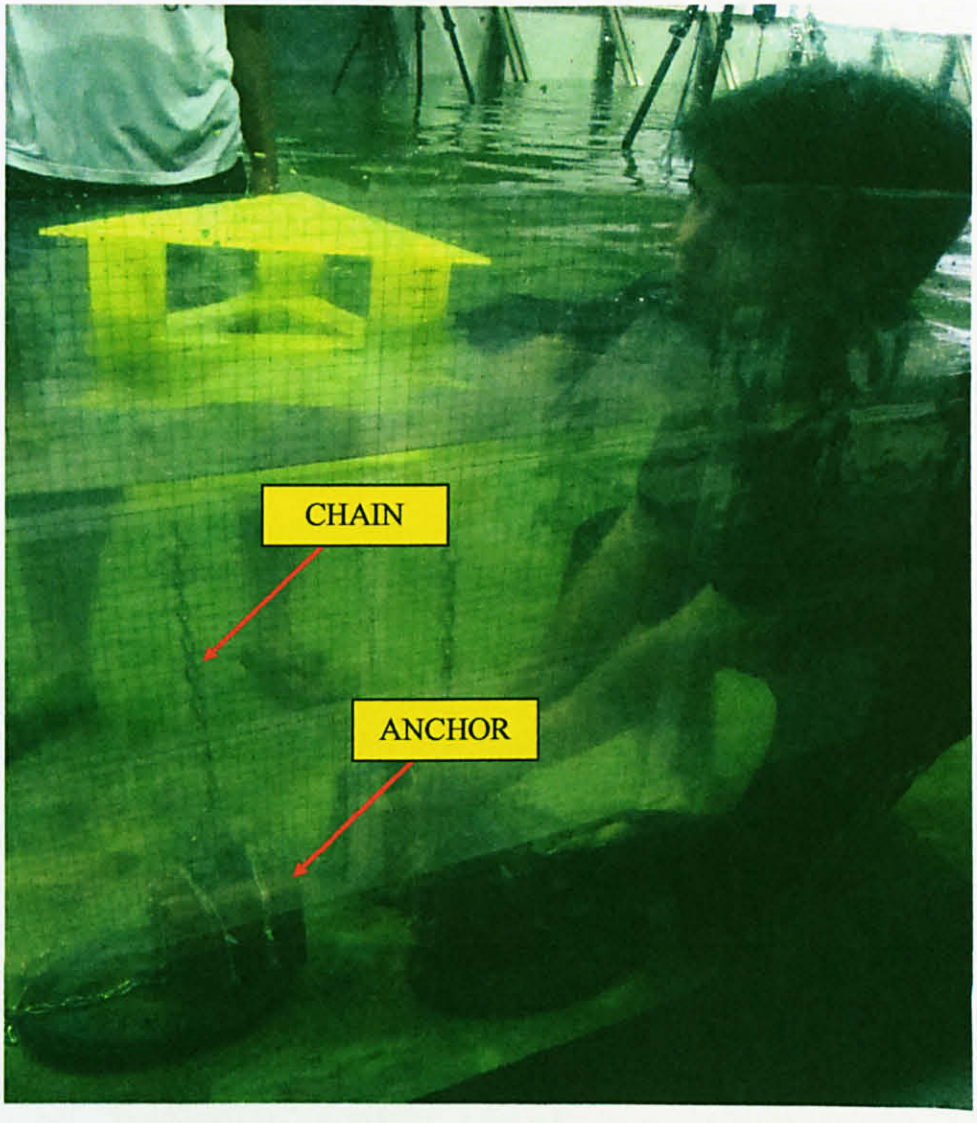


INSTALLATION OF THE CHAIN AND ANCHOR

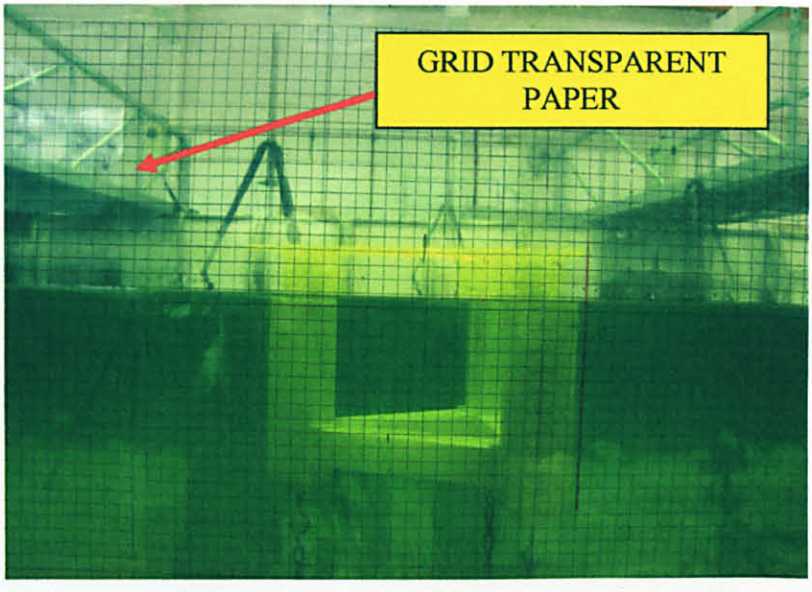


THE MODEL AT DRAFT POSITION OF 21.5cm

THE MODEL VIEWED FROM THE OBSERVER WINDOW

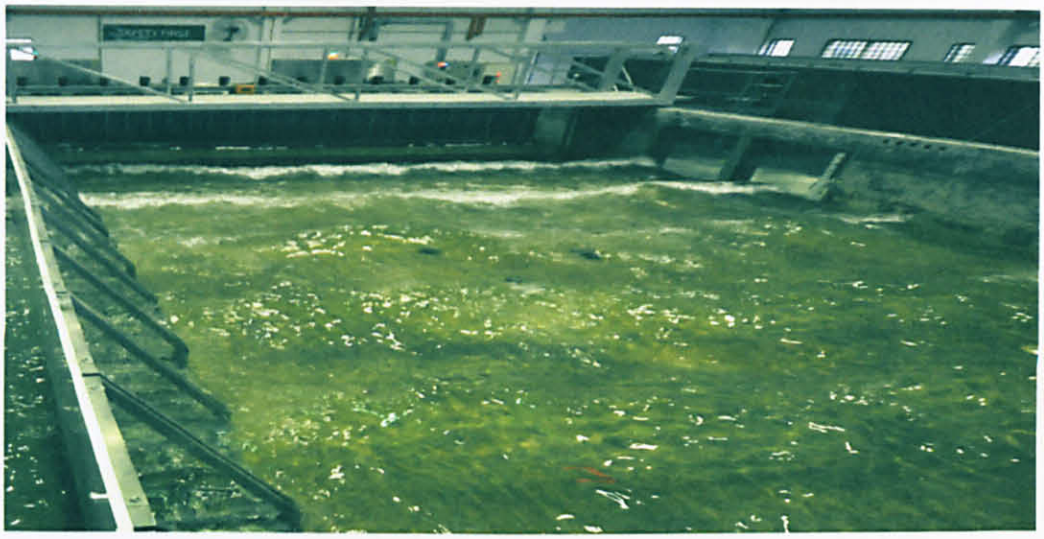

PROPAGATED WAVE GENERATED BY THE WAVE GENERATOR

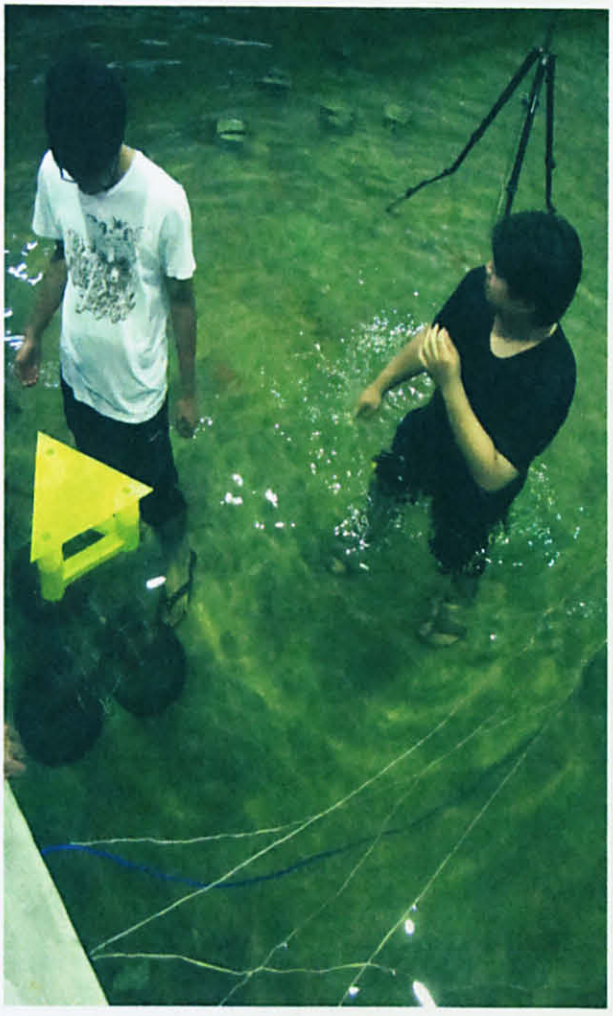

MODEL SETUP

# APPENDIX J

# DATA FROM LABORATORY MODEL TESTING

## SURGE RESPONSE

| DRAFT (cm) | 21.5 | 17.5 | 13.5 |
|---|---|---|---|
| t (s) | η (cm) | η (cm) | η (cm) |
| 0 | 0 | 0 | 0 |
| 1 | 0.2 | 0.25 | 0.5 |
| 2 | 1 | 0.5 | 1 |
| 3 | 1.25 | 1 | 1.25 |
| 4 | 1.75 | 1.25 | 1.75 |
| 5 | 2 | 2 | 2 |
| 6 | 1.5 | 2.5 | 2.5 |
| 7 | 1 | 2.15 | 2.5 |
| 8 | 0.75 | 2 | 2.25 |
| 9 | 0.25 | 1.5 | 2 |
| 10 | 0 | 1 | 1.5 |
| 11 | -0.25 | 0 | 1.25 |
| 12 | -1 | -0.25 | 0.75 |
| 13 | -1.5 | -1.5 | 0.5 |
| 14 | -1.75 | -1.6 | 0 |
| 15 | -1.25 | -1.75 | -0.25 |
| 16 | -1 | -1.5 | -0.75 |
| 17 | 0 | -1 | -1.25 |
| 18 | 1 | 0 | -1.75 |
| 19 | 1.25 | 0.25 | -2.25 |
| 20 | 1.5 | 1 | -2 |
| 21 | 1.75 | 1.25 | -1.75 |
| 22 | 2 | 2 | -1.5 |
| 23 | 1.5 | 2.1 | -1.25 |
| 24 | 1.25 | 2.15 | -1 |
| 25 | 0.75 | 1.75 | -0.5 |

| DRAFT (cm) | 21.5 | 17.5 | 13.5 |
|---|---|---|---|
| t (s) | η (cm) | η (cm) | η (cm) |
| 26 | 0.25 | 1.5 | -0.25 |
| 27 | 0 | 1 | 0 |
| 28 | -0.25 | 0.75 | 0.5 |
| 29 | -0.5 | 0.5 | 0.75 |
| 30 | -1 | 0.25 | 1.25 |
| 31 | -0.75 | 0.1 | 1.75 |
| 32 | -0.25 | 0 | 2 |
| 33 | 0 | 0.1 | 2.25 |
| 34 | 0.5 | 0.2 | 2.25 |
| 35 | 0.75 | 0.5 | 2.5 |
| 36 | 1 | 1 | 2.25 |
| 37 | 1.5 | 1.2 | 2 |
| 38 | 1.25 | 1 | 1.5 |
| 39 | 1 | 0.75 | 1.75 |
| 40 | 0.75 | 0.25 | 0.75 |
| 41 | 0.25 | 0 | 0.5 |
| 42 | 0 | -0.25 | 0 |
| 43 | -0.5 | -0.5 | 0 |
| 44 | -0.25 | -1 | -0.5 |
| 45 | 0.5 | -0.75 | -1 |
| 46 | 0.75 | -0.25 | -1.25 |
| 47 | 1.25 | -0.75 | -1.75 |
| 48 | 1.75 | -0.5 | -2 |
| 49 | 1 | -0.4 | -2.25 |
| 50 | 0.5 | -0.2 | -2.25 |
| 51 | 0.25 | -0.5 | -2 |

| DRAFT (cm) | 21.5 | 17.5 | 13.5 |
|---|---|---|---|
| t (s) | η (cm) | η (cm) | η (cm) |
| 52 | 0 | -1 | -1.5 |
| 53 | 0.5 | -1.5 | -1.25 |
| 54 | 0.75 | -2 | -1 |
| 55 | 1 | -1.8 | -0.5 |
| 56 | 1.25 | -1.5 | -0.25 |
| 57 | 0.5 | -0.5 | 0.25 |
| 58 | 0.25 | 0 | 0.75 |
| 59 | 0 | 0.4 | 1 |
| 60 | -0.5 | 0.5 | 1.5 |
| 61 | -1 | 0.4 | 1.75 |
| 62 | -1.5 | 0.2 | 2 |
| 63 | -1.25 | 0 | 2.25 |
| 64 | -1 | -0.4 | 2 |
| 65 | -0.75 | -1 | 1.5 |
| 66 | -0.5 | -1.25 | 1.25 |
| 67 | -0.25 | -1 | 1 |
| 68 | 0 | -0.75 | 0.5 |
| 69 | 0 | -0.25 | 0.25 |
| 70 | 0.5 | 0 | 0 |
| 71 | 0.75 | 0.2 | -0.5 |
| 72 | 1.25 | 0.25 | -0.75 |
| 73 | 0.5 | 0 | -0.5 |
| 74 | 0.75 | 0.75 | -1.5 |
| 75 | 1 | 1 | -2 |
| 76 | 1.5 | 1.25 | -2 |
| 77 | 1 | 1.5 | -1.75 |

| DRAFT (cm) | 21.5 | 17.5 | 13.5 |
|---|---|---|---|
| t (s) | η (cm) | η (cm) | η (cm) |
| 78 | 0.5 | 2 | -1.5 |
| 79 | 0 | 1.5 | -1 |
| 80 | -0.25 | 1.25 | -0.75 |
| 81 | -0.75 | 0.5 | -0.5 |
| 82 | -1 | 0.25 | -0.5 |
| 83 | -1.25 | 0 | 0 |
| 84 | -1 | -0.25 | 1 |
| 85 | -0.75 | -0.5 | 1.5 |
| 86 | -0.25 | 0 | 1.75 |
| 87 | 0 | 0.25 | 2.25 |
| 88 | 0.25 | 0.5 | 1.75 |
| 89 | 1 | 1 | 1.75 |
| 90 | 1.25 | 1.5 | 1 |
| 91 | 0.75 | 1.75 | 0.75 |
| 92 | 0.25 | 1.5 | 0.25 |
| 93 | 0 | 1 | 0 |
| 94 | -0.25 | 0.75 | -0.5 |
| 95 | -0.5 | 0.5 | -0.75 |
| 96 | -0.75 | 0 | -1 |
| 97 | -1 | -0.25 | -1.25 |
| 98 | -0.5 | -0.5 | -1 |
| 99 | 0 | -0.25 | -0.75 |
| 100 | 1 | 0 | 0 |

## HEAVE RESPONSE

| DRAFT (cm) | 21.5 | 17.5 | 13.5 |
|---|---|---|---|
| t (s) | η (cm) | η (cm) | η (cm) |
| 0 | 0 | 0 | 0 |
| 1 | -0.05 | 0.05 | 0 |
| 2 | -0.1 | 0.1 | 0.05 |
| 3 | -0.1 | 0.2 | 0.1 |
| 4 | -0.15 | 0.25 | 0.1 |
| 5 | -0.2 | 0.25 | 0.05 |
| 6 | -0.2 | 0.15 | 0 |
| 7 | -0.15 | 0.15 | -0.05 |
| 8 | -0.1 | 0.1 | -0.1 |
| 9 | -0.2 | 0.05 | -0.1 |
| 10 | -0.25 | 0.1 | -0.2 |
| 11 | -0.25 | 0.2 | -0.25 |
| 12 | -0.15 | -0.05 | -0.25 |
| 13 | -0.05 | -0.1 | -0.15 |
| 14 | 0 | -0.1 | -0.05 |
| 15 | 0 | -0.15 | 0 |
| 16 | 0.05 | -0.2 | 0 |
| 17 | 0.1 | -0.2 | -0.1 |
| 18 | 0.2 | -0.15 | -0.2 |
| 19 | 0.25 | -0.1 | -0.25 |
| 20 | 0.25 | -0.2 | -0.15 |
| 21 | 0.15 | -0.25 | -0.05 |
| 22 | 0.15 | -0.15 | -0.1 |
| 23 | 0.15 | -0.05 | -0.2 |
| 24 | 0.1 | 0 | -0.1 |
| 25 | 0.05 | 0.1 | -0.15 |

| DRAFT (cm) | 21.5 | 17.5 | 13.5 |
|---|---|---|---|
| t (s) | η (cm) | η (cm) | η (cm) |
| 26 | 0 | 0.2 | -0.2 |
| 27 | -0.05 | 0.15 | -0.2 |
| 28 | -0.1 | 0.1 | -0.15 |
| 29 | -0.1 | 0.05 | -0.1 |
| 30 | -0.15 | 0 | -0.2 |
| 31 | -0.2 | -0.05 | -0.15 |
| 32 | -0.2 | -0.1 | -0.05 |
| 33 | -0.05 | -0.1 | 0 |
| 34 | -0.1 | -0.15 | 0.05 |
| 35 | -0.1 | -0.2 | 0.05 |
| 36 | -0.15 | -0.2 | 0.1 |
| 37 | -0.2 | -0.05 | 0.2 |
| 38 | -0.2 | -0.1 | 0.25 |
| 39 | -0.15 | -0.1 | 0.25 |
| 40 | -0.1 | -0.15 | 0.15 |
| 41 | -0.2 | -0.2 | 0.1 |
| 42 | -0.25 | -0.2 | 0.2 |
| 43 | -0.15 | -0.05 | 0.25 |
| 44 | -0.05 | -0.1 | 0.2 |
| 45 | 0 | -0.1 | 0.15 |
| 46 | 0 | -0.15 | 0.15 |
| 47 | 0.05 | -0.2 | 0.1 |
| 48 | 0.1 | -0.2 | 0.1 |
| 49 | 0.2 | 0 | 0.2 |
| 50 | 0.25 | 0 | 0.25 |
| 51 | 0.25 | 0.05 | 0.15 |

| DRAFT (cm) | 21.5 | 17.5 | 13.5 |
|---|---|---|---|
| t (s) | η (cm) | η (cm) | η (cm) |
| 52 | 0.15 | 0.1 | 0.1 |
| 53 | 0.15 | 0.2 | 0.05 |
| 54 | 0.1 | 0.25 | 0 |
| 55 | 0.1 | 0.25 | -0.05 |
| 56 | 0.2 | 0.15 | -0.1 |
| 57 | 0.15 | 0.15 | -0.05 |
| 58 | 0.1 | 0.1 | -0.1 |
| 59 | 0.05 | 0.05 | -0.2 |
| 60 | 0 | 0.1 | -0.1 |
| 61 | -0.05 | 0.2 | -0.15 |
| 62 | -0.1 | 0.15 | -0.2 |
| 63 | -0.2 | 0.1 | -0.2 |
| 64 | -0.1 | 0.05 | -0.15 |
| 65 | -0.15 | 0 | -0.1 |
| 66 | -0.2 | -0.05 | -0.2 |
| 67 | -0.2 | -0.1 | -0.25 |
| 68 | -0.15 | -0.2 | -0.15 |
| 69 | -0.1 | -0.15 | -0.1 |
| 70 | -0.2 | -0.1 | -0.2 |
| 71 | -0.25 | -0.05 | -0.05 |
| 72 | -0.15 | -0.1 | 0 |
| 73 | -0.1 | -0.1 | 0 |
| 74 | -0.2 | -0.15 | 0.05 |
| 75 | -0.25 | -0.2 | 0.1 |
| 76 | -0.15 | -0.2 | 0.2 |
| 77 | -0.05 | -0.15 | 0.25 |

| DRAFT (cm) | 21.5 | 17.5 | 13.5 |
|---|---|---|---|
| t (s) | η (cm) | η (cm) | η (cm) |
| 78 | 0 | -0.1 | 0.25 |
| 79 | 0 | -0.2 | 0.15 |
| 80 | 0.05 | -0.25 | 0.15 |
| 81 | 0.1 | -0.15 | 0.1 |
| 82 | 0.2 | -0.05 | 0.05 |
| 83 | 0.25 | 0 | 0.1 |
| 84 | 0.25 | 0.1 | 0.2 |
| 85 | 0.15 | 0.2 | 0.1 |
| 86 | 0.15 | 0.15 | 0.2 |
| 87 | 0.1 | 0.1 | -0.05 |
| 88 | 0.05 | 0.05 | -0.1 |
| 89 | 0.1 | 0 | -0.1 |
| 90 | 0.2 | -0.05 | -0.15 |
| 91 | 0.1 | -0.1 | -0.2 |
| 92 | 0.2 | -0.2 | -0.15 |
| 93 | -0.05 | -0.1 | -0.1 |
| 94 | -0.1 | -0.15 | -0.15 |
| 95 | -0.1 | -0.2 | -0.1 |
| 96 | -0.15 | -0.2 | -0.2 |
| 97 | -0.2 | -0.15 | -0.25 |
| 98 | -0.2 | -0.1 | -0.15 |
| 99 | -0.15 | -0.2 | -0.05 |
| 100 | -0.1 | -0.25 | 0 |